

1-1-2015

Chemoselective Formation of Unsymmetrically Substituted Ethers from Catalytic Reductive Coupling of Aldehydes and Ketones with Alcohols in Aqueous Solution

Nishantha Kumara Kalutharage

Marquette University

Chae S. Yi

Marquette University, chae.yi@marquette.edu

Chemoselective Formation of Unsymmetrically Substituted Ethers from Catalytic Reductive Coupling of Aldehydes and Ketones with Alcohols in Aqueous Solution

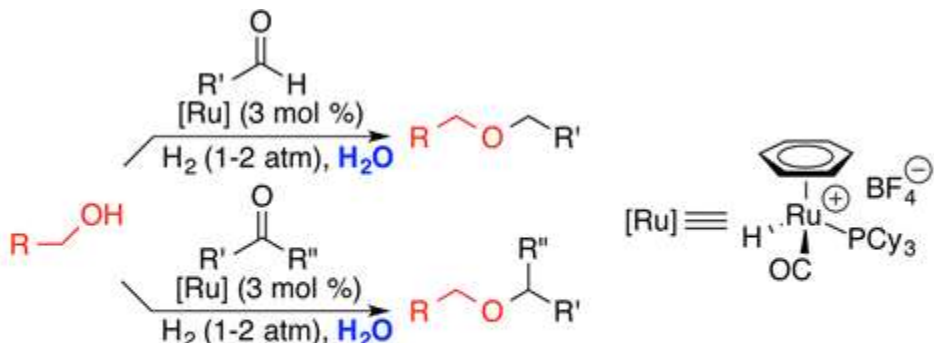
Nishantha Kalutharage

*Department of Chemistry, Marquette University,
Milwaukee, WI*

Chae S. Yi

*Department of Chemistry, Marquette University,
Milwaukee, WI*

Abstract



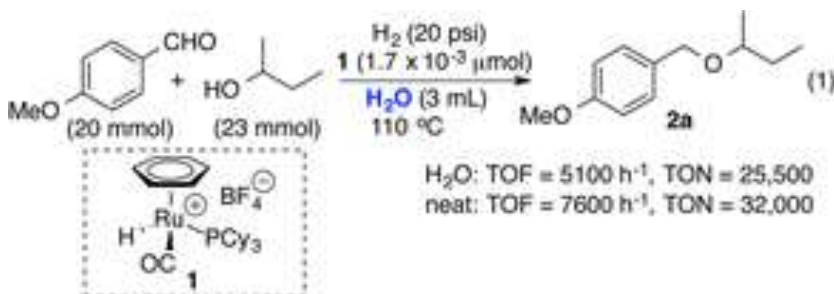
- Broad substrate scope and high functional group tolerance
- High selectivity for unsymmetrical ethers without forming wasteful byproducts
- Employ H_2 as the reducing agent and water as the solvent

A well-defined cationic Ru–H complex catalyzes reductive etherification of aldehydes and ketones with alcohols. The catalytic method employs environmentally benign water as the solvent and cheaply available molecular hydrogen as the reducing agent to afford unsymmetrical ethers in a highly chemoselective manner.

Etherification of oxygenated organic compounds is an ubiquitous organic transformation in both industrial and fine chemical syntheses.¹ Strong Brønsted acid and heterogeneous acid catalysts are commonly employed for industrial-scale etherification of alcohols,² while the Williamson ether synthesis has long been used for laboratory-scale synthesis of unsymmetrically substituted ethers.³ Seminal catalytic C–O bond formation methods such as Ullmann- and Mitsunobu-type coupling reactions have been extensively utilized for the synthesis of aryl-substituted ethers.⁴ More recently, a number of highly effective catalytic methods for unsymmetrical ethers have been developed from use of hydroalkoxylation of alkenes⁵ and oxidative C–H alkoxylation of arenes.⁶ The reductive etherification of carbonyl compounds has also been shown to be a synthetically powerful etherification method, but this method requires a stoichiometric amount of silane as the reducing agent.⁷ Despite such remarkable progress, these catalytic etherification methods pose major synthetic and environmental problems in that they employ reactive reagents such as inorganic acids and organic alkoxide substrates, which result in the formation of copious amounts of wasteful byproducts. From the viewpoint of achieving green and sustainable catalysis, the development of an efficient and broadly applicable catalytic etherification process that

does not form any wasteful byproducts remains a high priority goal, particularly for the synthesis of unsymmetrically substituted ethers.⁸

We recently discovered that a well-defined cationic ruthenium hydride complex $[(C_6H_6)(PCy_3)(CO)RuH]^+BF_4^-$ (**1**) is a highly selective catalyst precursor for the etherification of two different alcohols to form unsymmetrically substituted ethers.⁹ While this etherification provides unsymmetrical ethers without forming any wasteful byproducts, it was not effective for the coupling between electronically similar or sterically demanding aliphatic alcohols, as it gave a mixture of symmetrical and unsymmetrical ethers. In an effort to extend the scope of the etherification reaction, we explored the analogous reductive coupling reactions of carbonyl compounds. Herein, we report a highly chemoselective formation of unsymmetrically substituted ether products from the reductive coupling of aldehydes and ketones with alcohols. The “green” features of the catalytic method are that it employs cheaply available molecular hydrogen as the reducing agent, tolerates a number of common functional groups, and uses environmentally benign water as the solvent.



We initially screened the catalyst activity of the ruthenium complex **1** for the reductive coupling reaction of 2-butanol with 4-methoxybenzaldehyde (eq 1). While searching for a suitable set of conditions, we were delighted to discover that H₂ (1–2 atm) can be used as the reducing agent and water as the solvent. Under these conditions, complex **1** was found to exhibit distinctively high activity and selectivity in forming the ether product **2a** among screened ruthenium and acid catalysts, as analyzed by both GC and NMR spectroscopic methods (Table S1, Supporting Information (SI)). Since most reductive etherifications of carbonyl compounds require a stoichiometric amount of silane or borane as the reducing agent,⁷ our

catalytic method on using molecular H₂ is quite beneficial from both synthetic and environmental points of view.

We measured the catalytic activity of **1** for the etherification reaction. In a Fisher–Porter pressure bottle, the treatment of 4-methoxybenzaldehyde (20 mmol) with 2-butanol (23 mmol) and H₂ (20 psi) in the presence of **1** (1.7×10^{-3} μmol) in water (3 mL) was stirred at 110 °C. The initial turnover frequency (TOF) of 5100 h⁻¹ after 30 min and the turnover number (TON) of 25500 after 18 h were obtained as measured by both GC and NMR spectroscopic methods. The etherification reaction under neat conditions led to a considerably higher activity for **2a** (TOF = 7600 h⁻¹ and TON = 32000). The salient feature of the catalytic method is that it employs cheaply available H₂ as the reducing agent in an aqueous solution.

Substrate scope of the etherification reaction was explored by using the catalyst **1** (Table 1). Both aliphatic and aryl-substituted aldehydes readily reacted with both primary and secondary alcohols to form the ether products **2** (entries 1–13). In the case of 1,2-hexanediol, exclusive etherification to the primary alcohol was observed in yielding the ether product **2i** (entry 9). The coupling between aliphatic alcohol and aldehyde substrates was sluggish, leading to a lower yield than with benzylic ones (entries 12 and 13). In this case, extending the reaction time to 24 h did not increase the product yield significantly.

The etherification of ketones also proceeded smoothly to give the α-substituted ether products. The aryl-substituted ketones with both primary and secondary alcohols led to the corresponding ether products **2n–x** (entries 14–24). The coupling with a linear aliphatic ketone was found to be considerably slower than with benzylic ketones (entry 25). The treatment of a chiral alcohol with 4-methoxyacetophenone led to a 1:1 diastereomeric mixture of ether product **2z** (entry 26). In most cases, using 2 equiv of alcohol substrate (second equivalent alcohol is served as the hydrogen donor) was found to be convenient for forming the ether products, but 1 equiv of alcohol substrate can be used with H₂ (1–2 atm) without sacrificing the product yields. In addition, a 1:1 toluene/H₂O was used as the solvent system in most cases, and pure water was used for water-soluble substrates. The catalytic method achieves a highly

chemoselective etherification of aldehydes and ketones without using any reactive reagents, and employs environmentally sustainable and cheaply available alcohol substrates.

Table 1. Etherification of Alcohols with Aldehydes and Ketones^a

entry	carbonyl compd	alcohol	product(s)	time (h)	yield (%)
1	X = H				
2	X = OMe				
3	X = OBn				
4	X = Cl				
5	X = NHCOMe				
6	MeO	R-OH	2f	12	98 ^b
7		R = Cyclopentyl	2g	16	95 ^b
8		R = (R)-CH ₂ CHMeCO ₂ Me	(R)-2h	16	91 ^b
9		n-Bu	2i	16	91 ^b
10	R-CHO	MeO	2j	12	86
11	R = i-Butyl		2k	12	88
12	c-C ₆ H ₁₁ CHO	Ethanol	2l	12	71
13	c-C ₆ H ₁₁ CHO	1-Butanol	2m	12	76
14		R-OH	2n	16	88
15		R = n-Butyl	2o	16	93
16		R = Cyclopentyl	2p	16	55
17	Ph	R-OH	2q	16	94
18		R = Cyclopentyl	2r	16	92
19		R = CH ₂ C ₆ H ₄ -4-OMe	2s	16	65
20		R-OH	2t	16	89
21		R = Cyclopentyl	2u	16	82
22		R-OH	2v	16	85
23		R = n-Butyl	2w	12	80
24		R = CH ₂ CH ₂ CH ₂ Ph	2x	16	98
25		PhCH ₂ CH ₂ CH ₂ OH	2y	16	55 ^b
26		MeO ₂ C	2z (1:1 dr)	16	78 ^b

Table aReaction conditions: carbonyl compound (1.0 mmol), alcohol (2.0 mmol), toluene/H₂O (v/v = 1:1, 3 mL), **1** (3 mol %), 110 °C.

Table bReaction in pure water (3 mL).

To further illustrate the synthetic versatility of the catalytic method, we next surveyed the etherification reaction of functionalized alcohol substrates of biological importance (Figure 1). The etherification of (–)-menthol and 2',3'-isopropylidenedeoxyuridine with 4-methoxybenzaldehyde smoothly formed the ether product **3a** and **3b** without any epimerization or side products. The etherification reaction of an amino acid and steroid derivatives with 4-

methoxybenzaldehyde also proceeded predictively to give the products **3c–e**, while displaying high chemoselectivity toward the ether product formation. An aliphatic aldehyde was successfully used for fenofibrate and chloroamphenicol, where in the latter case, a selective etherification to the primary alcohol was achieved over the secondary one in forming the ether product **3h**. In these cases, a nonprotic solvent chlorobenzene was found to be most suitable for the coupling reaction, as the substrates become insoluble in toluene/H₂O solvent. The structure of **3e** was determined by X-ray crystallography (Figure S6, SI).

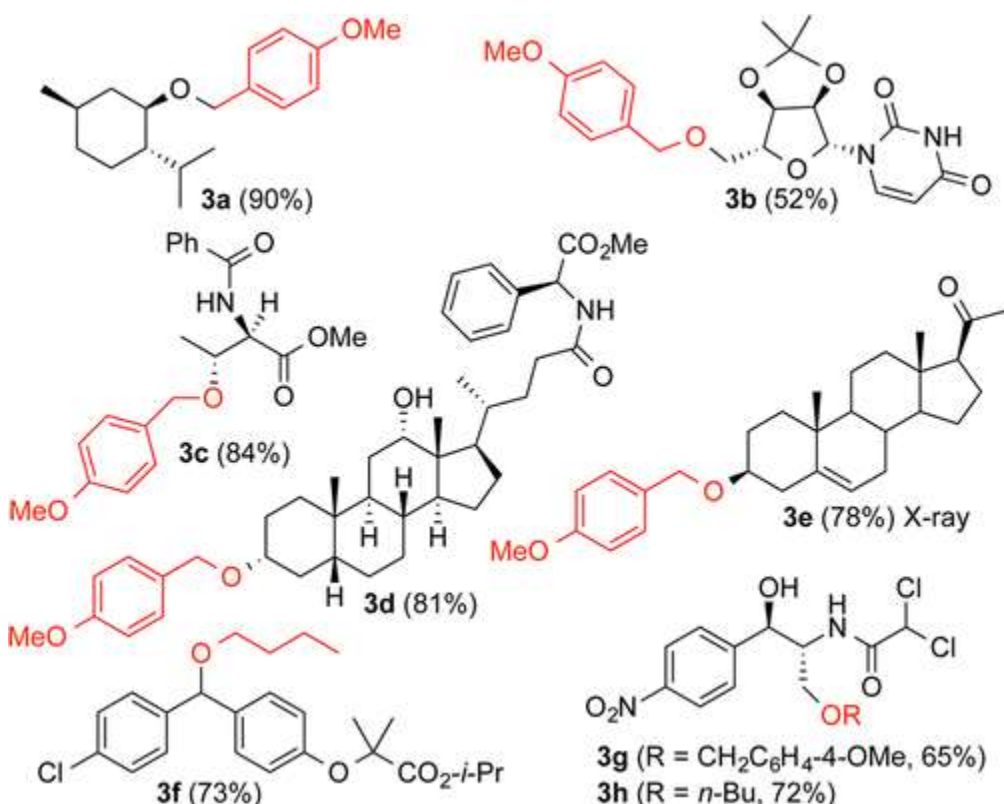
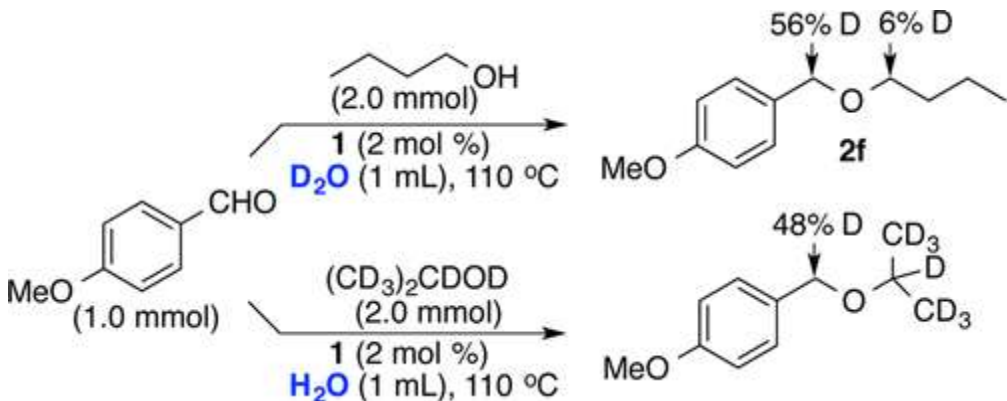


Figure 1. Etherification biologically active alcohols with aldehydes. Reaction conditions: alcohol (1.0 mmol), aldehyde (1.0 mmol), H₂ (1 atm), C₆H₅Cl (2 mL), **1** (3 mol %), 110 °C.

A series of kinetic experiments were performed to gain mechanistic insights for the etherification reaction. First, the H/D exchange pattern on the coupling reaction was examined. The treatment of 4-methoxybenzaldehyde with 1-butanol (2 equiv) in D₂O led to the selective deuterium incorporation to benzylic position of the product **2f** (Scheme 1). Conversely, 4-methoxybenzaldehyde with 2-

propanol-*d*₈ (2 equiv) in H₂O gave the product with ~50% of deuterium on the benzylic position. In a control experiment, the treatment of 2-propanol with D₂O in the presence of **1** (2 mol %) led to a rapid H/D exchange to form (CH₃)₂CHOD at room temperature. These results suggest that an extensive H/D exchange between the solvent molecules and the alcohol substrate led to the deuterium incorporation to the benzylic position of the ether product during the C=O hydrogenolysis step.



Scheme 1

To probe the involvement of solvent molecules, the solvent isotope effect was measured on the catalytic reaction. The initial rates of the reaction between 4-methoxybenzaldehyde with 2-butanol (2 equiv) were separately measured in H₂O and D₂O. The first order plots showed a relatively high normal isotope effect of $k_{\text{H}_2\text{O}}/k_{\text{D}_2\text{O}} = 2.9 \pm 0.2$ (Figure 2). A similar solvent isotope effect was obtained from 2-propanol/2-propanol-*d*₈ ($k_{\text{PROH}}/k_{\text{PROD}} = 2.0 \pm 0.2$, Figure S3, SI). A relatively large solvent isotope effect suggests that the water molecules are intricately involved in C–O bond cleavage and hydrogenolysis steps via extensive hydrogen-bonding-network interactions.¹⁰

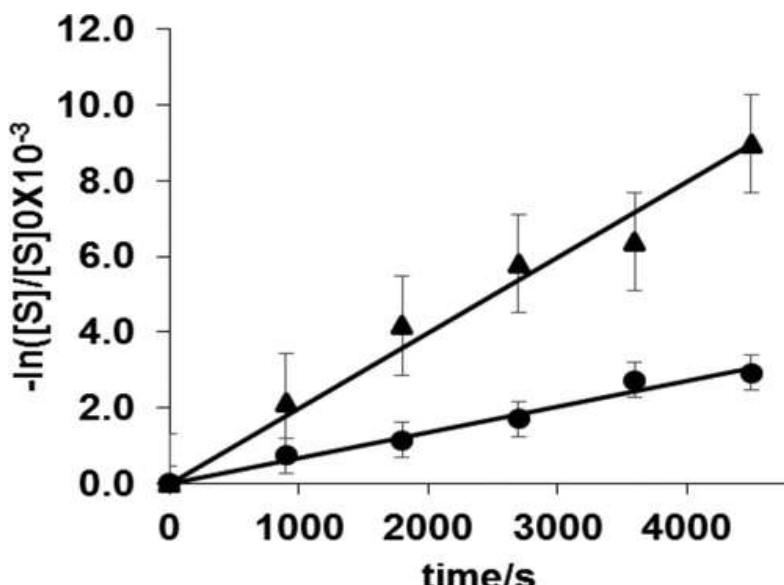


Figure 2. First-order plot of the 4-methoxybenzaldehyde (S) with 2-butanol in H₂O (\blacktriangle) and in D₂O (\bullet).

To probe the electronic effect on the aldehyde substrate, we constructed a Hammett plot from measuring the rate of a series of *para*-substituted benzaldehydes *p*-X-C₆H₄CHO (X = OMe, Me, H, F, Cl) with 2-butanol. A linear correlation from the relative rate vs Hammett σ_p led to a negative ρ value of -1.6 ± 0.1 (Figure 3). The result is consistent with the notion that an electron-releasing group promotes the C–O bond hydrogenolysis step but not during the formation of hemiacetal species. Similar Hammett ρ values have been observed in the catalytic coupling reactions of arenes.¹¹

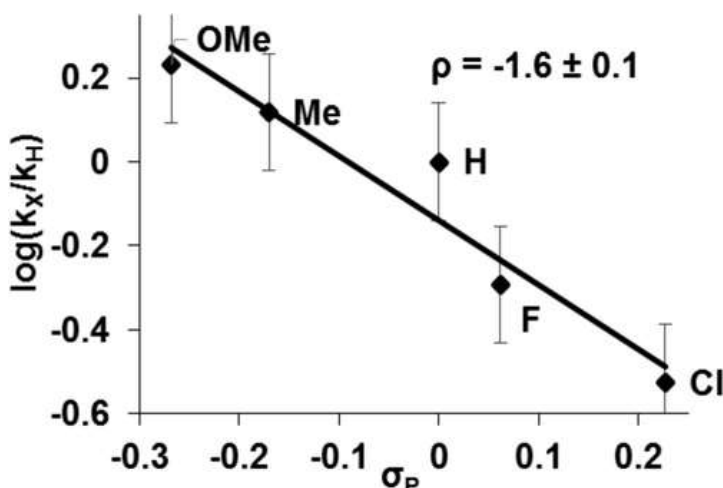
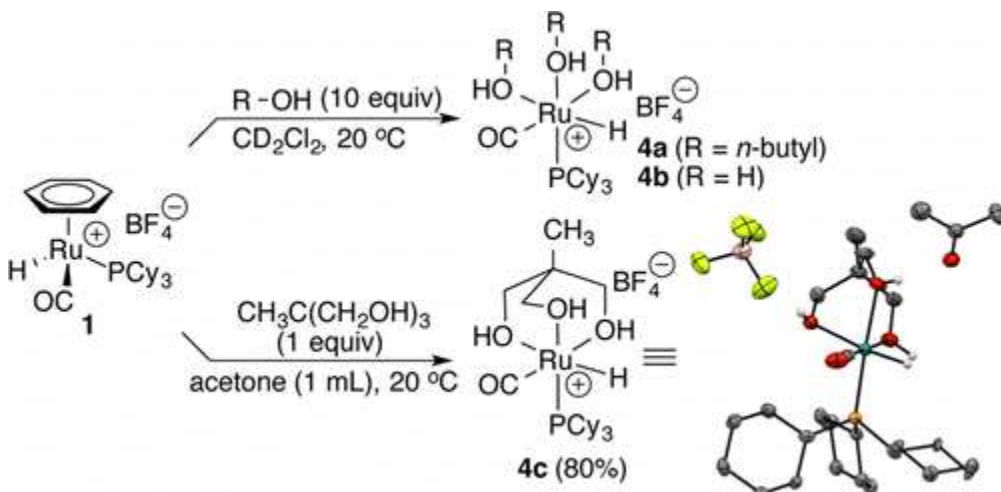


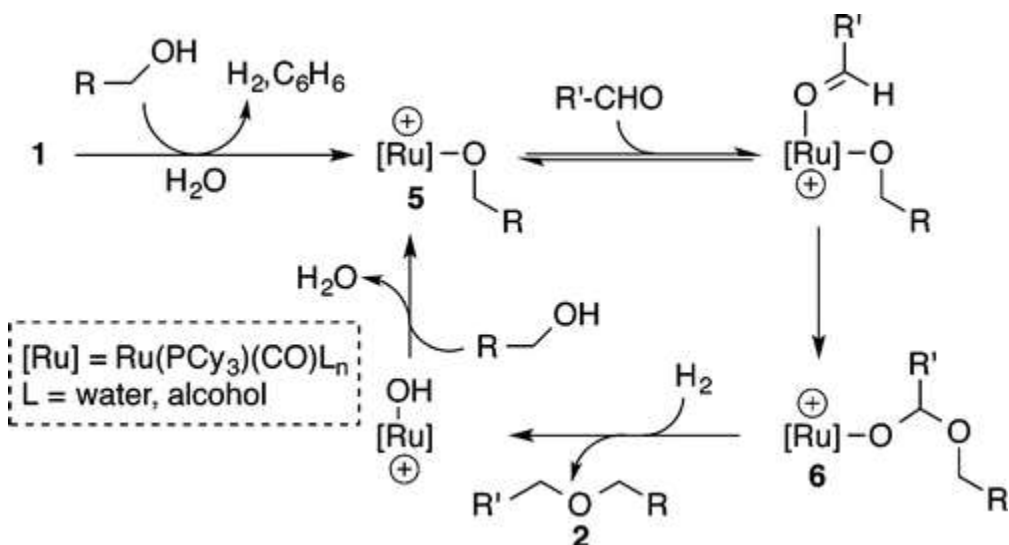
Figure 3. Hammett plot from the reaction of *p*-XC₆H₄CHO (X = OMe, Me, H, F, Cl) with 2-butanol.

To discern the structure of catalytically relevant species, we explored the reactions of **1** with alcohols and water. The treatment of the complex **1** (0.07 mmol) with excess 1-butanol (0.7 mmol) in CD_2Cl_2 (0.6 mL) led to the formation of a new Ru–H species within 30 min at room temperature (Scheme 2). The appearance of a new set of peaks was observed along with the formation of free benzene molecule as monitored by NMR (^1H NMR: δ –18.8 (d, $J_{\text{PH}} = 31.3$ Hz) ppm; $^{31}\text{P}\{\text{H}\}$ NMR: δ 76.0 ppm). We tentatively assign the new species to the alcohol-coordinated complex $[(1\text{-butanol})_3(\text{PCy}_3)(\text{CO})\text{RuH}]^+\text{BF}_4^-$ (**4a**), in light of the previously observed arene exchange reaction of **1**.¹² The analogous reaction with excess water also formed the water-coordinated complex **4b** (^1H NMR: δ –17.7 (d, $J_{\text{PH}} = 30.3$ Hz) ppm; $^{31}\text{P}\{\text{H}\}$ NMR: δ 73.0 ppm), which steadily decomposed within 1 h at room temperature. The catalytic activity of complex **4a** was found to be identical to **1** for the etherification of 4-methoxybenzaldehyde with 2-butanol under the conditions described in eq 1.



Scheme 2

We next examined the reaction of complex **1** with diols and triols as a way to form a stable alcohol-coordinated complex. Thus, the treatment of **1** with 1,1,1-tris(hydroxymethyl)ethane in acetone at room temperature led to the triol-coordinated complex **4c**, which was isolated in 80% after recrystallization in acetone/pentane. The X-ray crystal structure of **4c** showed a distorted octahedral geometry with a facial arrangement between the triol and the ancillary ligands. A number of ruthenium–hydride complexes have been successfully utilized as catalysts for the alcohol-coupling reactions.¹³



Scheme 3. Possible Mechanism for the Reductive Etherification of an Alcohol with an Aldehyde

We present a possible mechanism of the catalytic reaction on the basis of these results (Scheme 3). We propose that an unsaturated cationic Ru-alkoxy (or Ru-alcohol) species **5** is initially generated from the benzene ligand displacement and the dehydrogenation steps. In support of this notion, we have been able to detect/isolate the formation of alcohol-coordinated cationic Ru-H complex **4** from the reaction of **1** with alcohols and water. The coordination of a carbonyl substrate followed by the nucleophilic addition of an alkoxy group is envisioned for the formation of hemiacetoxo species **6**. The observed H/D exchange pattern on the α -carbon of the ether product **2** as well as a normal solvent isotope effect indicates that the solvent molecules are intricately involved in the C–O bond hydrogenolysis step. The Hammett correlation study, where the reaction is promoted by electron-releasing group of the aldehyde, supports the notion that the hydrogenolysis step is likely the turnover-limiting step of the catalytic reaction.¹⁴

In conclusion, we successfully developed a highly chemoselective catalytic etherification method of aldehydes and ketones with alcohols. The ruthenium hydride catalyst exhibits a uniquely high activity as well as broad substrate scope in promoting the reductive etherification reaction of carbonyl compounds in an aqueous solution without using any reactive reagents or forming

wasteful byproducts. We anticipate that the catalytic etherification method provides an environmentally sustainable and cost-effective protocol for forming unsymmetrical ether compounds.

The authors declare no competing financial interest.

Acknowledgment

Financial support from the National Science of Foundation (CHE-1358439) and National Institute of Health General Medical Sciences (R15 GM109273) is gratefully acknowledged. We thank Dr. Sergey Lindeman (Marquette University) for the X-ray crystal structure determination of **3e** and **4c**.

References

- ¹ Reviews:(a) Mitsunobu, O. In *Comprehensive Organic Synthesis*; Trost, B. M., Fleming, J., Eds.; Pergamon Press: New York, 1991; Vol. 6, pp 1–31. (b) Lee, C.; Matunas, R. In *Comprehensive Organometallic Chemistry III*; Crabtree, R. H., Mingos, D. M., Eds.; Elsevier: Boston, 2007; Vol. 10, pp 649– 693.
- ² (a) Olah, G. A.; Molnár, A. *Hydrocarbon Chemistry*, 2nd ed.; Wiley: Hoboken, NJ, 2003. (b) Klier, K.; Beretta, A.; Sun, Q.; Feeley, O. C.; Herman, R. G. *Catal. Today* 1997, 36, 3– 14. (c) Nowak, I.; Ziolek, M. *Chem. Rev.* 1999, 99, 3603– 3624. (d) Tanabea, K.; Hölderich, W. F. *Appl. Catal., A* 1999, 181, 399– 434
- ³ (a) Smith, M. B.; March, J. *March's Advanced Organic Chemistry*, 5th ed.; Wiley: New York, 2001. (b) Baggett, N. In *Comprehensive Organic Synthesis*; Barton, D.; Ollins, W. D., Eds.; Pergamon: Oxford, 1979; Vol. 1.
- ⁴ (a) Ley, S. V.; Thomas, A. W. *Angew. Chem., Int. Ed.* 2003, 42, 5400– 5449. (b) Ma, D.; Cai, Q. *Acc. Chem. Res.* 2008, 41, 1450– 1460. (c) Swamy, K. C. K.; Kumar, N. N. B.; Balaraman, E.; Kumar, K. V. P. P. *Chem. Rev.* 2009, 109, 2551– 2651
- ⁵ (a) Sassaman, M. B.; Kotian, K. D.; Prakash, G. K. S.; Olah, G. A. *J. Org. Chem.* 1987, 52, 4314– 4319. (b) Sakai, N.; Moriya, T.; Konakahara, T. *J. Org. Chem.* 2007, 72, 5920– 5922. (c) Haibach, M. C.; Guan, C.; Wang, D. Y.; Li, B.; Lease, N.; Steffens, A. M.; Krogh-Jespersen, K.; Goldman, A. S. *J. Am. Chem. Soc.* 2013, 135, 15062– 15070
- ⁶ (a) Wang, X.; Lu, Y.; Dai, H.-X.; Yu, J.-Q. *J. Am. Chem. Soc.* 2010, 132, 12203– 12205. (b) Jiang, T.-S.; Wang, G.-W. *J. Org. Chem.* 2012, 77, 9504– 9509. (c) Li, W.; Sun, P. *J. Org. Chem.* 2012, 77, 8362– 8366. (d) Zhang, S.-Y.; He, G.; Zhao, Y.; Wright, K.; Nack, W. A.; Chen, G. *J. Am. Chem. Soc.* 2012, 134, 7313– 7316. (e) Chen, F.-J.; Zhao, S.;

- Hu, F.; Chen, K.; Zhang, Q.; Zhang, S.-Q.; Shi, B.-F. *Chem. Sci.* 2013, 4, 4187– 4192. (f) Roane, J.; Daugulis, O. *Org. Lett.* 2013, 15, 5842– 5845
- ⁷ (a) Lee, S. H.; Park, Y. J.; Yoon, C. M. *Tetrahedron Lett.* 1999, 40, 6049– 6050. (b) Evans, P. A.; Cui, J.; Gharpure, S. J.; Hinkle, R. J. *J. Am. Chem. Soc.* 2003, 125, 11456– 11457. (c) Yang, W.-C.; Lu, X.-A.; Kulkarni, S. S.; Hung, S.-C. *Tetrahedron Lett.* 2003, 44, 7837– 7840. (d) Iwanami, K.; Seo, H.; Tobita, Y.; Oniyama, T. *Synthesis* 2005, 183– 186. (e) Barluenga, J.; Tomás-Gamasa, M.; Aznar, F.; Valdøs, C. *Angew. Chem., Int. Ed.* 2010, 49, 4993– 4996. (f) Gharpure, S. J.; Prasad, J. V. K. *J. Org. Chem.* 2011, 76, 10325– 10331
- ⁸ (a) Min, B. K.; Friend, C. M. *Chem. Rev.* 2007, 107, 2709– 2724. (b) Sheldon, R. A. *Chem. Commun.* 2008, 3352– 3365. (c) Li, C.-J.; Trost, B. M. *Proc. Natl. Acad. Sci. U.S.A.* 2008, 105, 13197– 13202
- ⁹ Kim, J.; Lee, D.-H.; Kalutharage, N.; Yi, C. S. *ACS Catal.* 2014, 4, 3881– 3885
- ¹⁰ Selected recent examples: (a) Gómez-Gallego, M.; Sierra, M. A. *Chem. Rev.* 2011, 111, 4857– 4963. (b) Gregory, M. C.; Denisov, I. G.; Grinkova, Y. G.; Khatri, Y.; Sligar, S. G. *J. Am. Chem. Soc.* 2013, 135, 16245– 16247. (c) Waugh, M. W.; Marsh, E. N. G. *Biochemistry* 2014, 53, 5537– 5543
- ¹¹ (a) Nakagawa, Y.; Mizuno, N. *Inorg. Chem.* 2007, 46, 1727– 1736. (b) Fedorov, A.; Chen, P. *Organometallics* 2010, 29, 2994– 3000. (c) Chakraborty, S.; Blacque, O.; Fox, T.; Berke, H. *ACS Catal.* 2013, 3, 2208– 2217. (d) Ball, L. T.; Lloyd-Jones, G. C.; Russell, C. A. *J. Am. Chem. Soc.* 2014, 136, 254– 264
- ¹² (a) Kwon, K.-H.; Lee, D. W.; Yi, C. S. *Organometallics* 2010, 29, 5748– 5760. (b) Lee, H.; Yi, C. S. *Eur. J. Org. Chem.* 2015, 1899– 1904
- ¹³ (a) Sieffert, N.; Bühl, M. *J. Am. Chem. Soc.* 2010, 132, 8056– 8070. (b) Denichoux, A.; Fukuyama, T.; Doi, T.; Horiguchi, J.; Ryu, I. *Org. Lett.* 2010, 12, 1– 3. (c) Fogler, E.; Balaraman, E.; Ben-David, Y.; Leitus, G.; Shimon, L. J. W.; Milstein, D. *Organometallics* 2011, 30, 3826– 3833. (d) Kang, B.; Fu, Z.; Hong, S. H. *J. Am. Chem. Soc.* 2013, 135, 11704– 11707. (e) Tseng, K.-N. T.; Kampf, J. W.; Szymczak, N. K. *Organometallics* 2013, 32, 2046– 2049. (f) Pingen, D.; Lutz, M.; Vogt, D. *Organometallics* 2014, 33, 1623– 1629
- ¹⁴ In light of the recent results as described in ref 9, we have considered an alternative mechanism involving the hydrogenation of carbonyl substrate to the corresponding alcohol and the subsequent dehydrative coupling with the second alcohol substrate. Since both mechanistic pathways should involve an alcohol–ketone hydrogenation–dehydrogenation redox process and a C–O bond hydrogenolysis step,

we cannot distinguish between these two pathways at the present time.

Supporting Information

Experimental procedures and methods, characterization and NMR spectra, and X-ray data of **3e** and **4c** (CIF). This material is available free of charge via the Internet at <http://pubs.acs.org>.

Supporting Information

Chemoselective Formation of Unsymmetrically Substituted Ethers from Catalytic Reductive Coupling of Aldehydes and Ketones with Alcohols in Aqueous Solution

Nishantha Kalutharage and Chae S. Yi*

Department of Chemistry, Marquette University, Milwaukee, Wisconsin 53201-1881 United States

Table of Contents

1. General Information	S2
2. Experimental Procedures (Table S1)	S2
3. Hammett Study (Figure S1)	S3
4. Solvent Isotope Effect Study (Figures S2 and S3)	S4
5. H/D Exchange Reaction of 3-Methoxybenzaldehyde with 1-Butanol in D ₂ O (Figure S4)	S5
6. Detection and Synthesis of the Alcohol Complexes 4a-4c (Figure S5)	S6
7. X-Ray Crystallographic Determination of 3e and 4c (Figures S6 and S7)	S7
8. Characterization Data of the Products	S9
9. ¹ H and ¹³ C NMR Spectra of the Products	S17
10. X-Ray Crystallographic Data of 3e and 4c (Tables S8-S23)	S35

1. General Information. All operations were carried out in a nitrogen-filled glove box or by using standard high vacuum and Schlenk techniques unless otherwise noted. Solvents were freshly distilled over the appropriate drying reagents. Tetrahydrofuran, benzene, toluene, hexanes and dioxane were distilled from purple solutions of sodium and benzophenone immediately prior to use. Dichloromethane and chlorobenzene (C_6H_5Cl) were dried over calcium hydride. The 1H , 2H , ^{13}C and ^{31}P NMR spectra were recorded on a Varian 300 or 400 MHz FT-NMR spectrometer, and the data are reported as: s = singlet, d = doublet, t = triplet, q = quartet, p = pentet, m = multiplet, br = broad, app = apparent; coupling constant(s) in Hz; integration. Mass spectra were recorded from a Agilent 6850 GC-MS spectrometer with a HP-5 (5% phenylmethylpolysiloxane) column (30 m, 0.32 mm, 0.25 μm). The conversion of organic products was measured from a Hewlett-Packard HP 6890 GC spectrometer. High resolution mass spectra were obtained at the Center of Mass Spectrometry, Washington University, St. Louis, MO and at the Mass Spectrometry/ICP Lab, Department of Chemistry and Biochemistry, University of Wisconsin-Milwaukee, Milwaukee, WI. Elemental analyses were performed at the Midwest Microlab, Indianapolis, IN.

2. Experimental Procedures

General Procedure for the Catalytic Reaction. Method A: In a glove box, complex **1** (17 mg, 3 mol %), carbonyl compound (1.0 mmol) and an alcohol (2.5 mmol) were dissolved in C_6H_5Cl (1 mL) in a 25 mL Schlenk tube equipped with a Teflon stopcock and a magnetic stirring bar. The tube was brought out of the box, and was stirred for 8-16 h in an oil bath which was preset at 110 °C. The reaction tube was taken out of the oil bath, and was cooled to room temperature. After the tube was open to air, the solution was filtered through a short silica gel column (CH_2Cl_2), and the filtrate was analyzed by GC and GC-MS. Analytically pure product was isolated by a simple column chromatography on silica gel (280-400 mesh, hexanes/ Et_2O or hexanes/ $EtOAc$).

Method B: In a glove box, complex **1** (17 mg, 3 mol %), a carbonyl compound (1.0 mmol) and an alcohol (1.3 mmol) were added into a 25 mL Schlenk tube equipped with a Teflon stopcock and a magnetic stirring bar. The tube was brought out of the box, and H_2O (1 mL) was added (0.5 mL of toluene for water insoluble substrates). The tube was evacuated, filled with H_2 (1 atm), and was stirred for 8-16 h in an oil bath which was preset at 110 °C. The reaction tube was taken out of the oil bath, and was cooled to room temperature. After the tube was open to air, the solution was filtered through a short silica gel column (CH_2Cl_2), and the filtrate was analyzed by GC and GC-MS. Analytically pure product was isolated by a simple column chromatography on silica gel (280-400 mesh, hexanes/ Et_2O or hexanes/ $EtOAc$).

Catalyst Screening. In a glove box, 4-methoxybenzaldehyde (136 mg, 1.0 mmol), 1-butanol (185 mg, 2.5 mmol) and a catalyst (2 mol %) were dissolved in toluene/ H_2O (1:1, 1 mL) in a 25 mL Schlenk tube equipped with a Teflon stopcock and a magnetic stirring bar. The tube was brought out of the box, and was stirred for 12

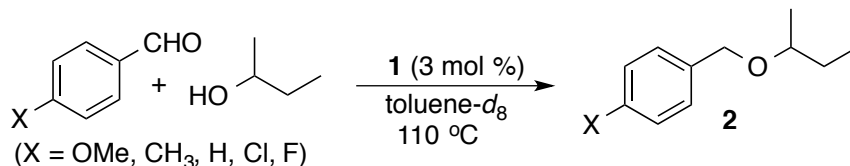
h in an oil bath which was preset at 110 °C. The reaction tube was taken out of the oil bath and the solution mixture was analyzed by GC and GC-MS. The results are summarized in Table S1.

Determination of TON. In a glove box, 4-methoxybenzaldehyde (2.72 g, 20 mmol), 2-butanol (1.48 g, 23 mmol) and the ruthenium catalyst **1** (0.2 µg, 1.7 x 10⁻³ mol %) were dissolved in water (3 mL) in a 100 mL Fisher-Porter pressure tube. The reaction tube was brought out of the box, and H₂ (20 psi) was added. The tube was stirred in an oil bath at 110 °C. A small aliquot was drawn from the reaction mixture after 1 h and after 18 h, and was analyzed by GC and NMR spectroscopic methods.

Table S1. Catalyst Survey for the Coupling Reaction of 4-Methoxybenzaldehyde with 1-Butanol.^a

entry	catalyst	additive	yield (%)
1	[$(\text{C}_6\text{H}_6)(\text{PCy}_3)(\text{CO})\text{RuH}]^+\text{BF}_4^-$ (1)		95
2	[$\text{RuH}(\text{CO})(\text{PCy}_3)_4(\text{O})(\text{OH})_2$		0
3	[$\text{RuH}(\text{CO})(\text{PCy}_3)_4(\text{O})(\text{OH})_2$	HBF ₄ ·OEt ₂	72
4	RuCl ₃ ·3H ₂ O	HBF ₄ ·OEt ₂	0
5	RuCl ₂ (PPh ₃) ₃	HBF ₄ ·OEt ₂	trace
6	RuH ₂ (CO)(PPh ₃) ₃		3
7	RuH ₂ (CO)(PPh ₃) ₃	HBF ₄ ·OEt ₂	10
8	[$\text{RuCl}_2(\text{COD})_x$	HBF ₄ ·OEt ₂	0
9	[$\text{RuH}(\text{CO})(\text{PCy}_3)_2(\text{CH}_3\text{CN})_2]^+\text{BF}_4^-$		20
10	[$(\text{COD})\text{RuCl}_2)_x$	HBF ₄ ·OEt ₂	0
11	Ru ₃ (CO) ₁₂	NH ₄ PF ₆	0
12	Cy ₃ PH ⁺ BF ₄ ⁻		trace
13	BF ₃ ·OEt ₂		trace
14	AlCl ₃		7
15	FeCl ₃ ·H ₂ O		trace
16	HBF ₄ ·OEt ₂		6
17	CF ₃ SO ₃ H		trace

^a Reaction conditions: 4-methoxybenzaldehyde (1.0 mmol), 1-butanol (2.5 mmol), catalyst (2 mol %), additive (1.0 equiv to catalyst), toluene/H₂O (1 mL, 1:1), 12 h, 110 °C. The product yield was determined by GC and GC-MS.



3. Hammett Study. In a glove box, *para*-substituted benzaldehyde *p*-X-C₆H₅CHO (X = OCH₃, CH₃, H, Cl, F) (0.25 mmol), 2-butanol (0.75 mmol) and complex **1** (3 mol %) were dissolved in toluene-*d*₈ (0.5 mL) in six separate J-Young NMR tubes. The tubes were brought out of the box, and stirred in an oil bath set at 110 °C. Each reaction tube was taken out of the oil bath in 20 min intervals, was immediately cooled in an ice water

bath, and was analyzed by ^1H NMR. The k_{obs} was determined from a first-order plot of $-\ln([p\text{-X-C}_6\text{H}_5\text{CHO}]_t/p\text{-X-C}_6\text{H}_5\text{CHO}]_0)$ vs. time.

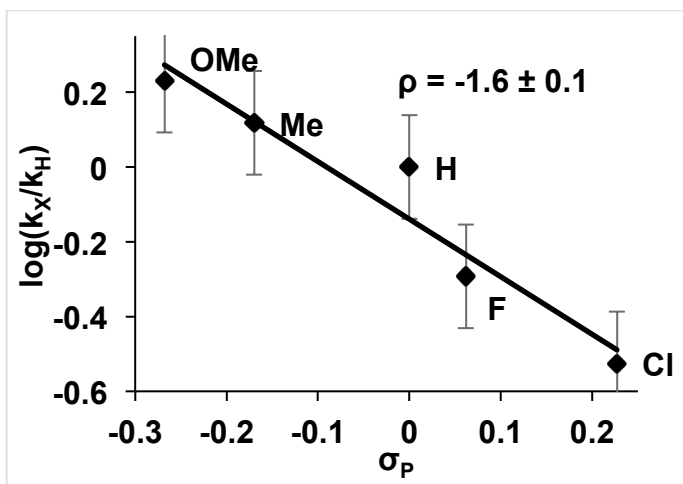


Figure S1. Hammett Plot from the Reaction of $p\text{-X-C}_6\text{H}_4\text{CHO}$ ($\text{X} = \text{OMe}, \text{Me}, \text{H}, \text{F}, \text{Cl}$) with 2-Butanol.

4. Solvent Isotope Effect Study. In a glove box, 4-methoxybenzaldehyde (340 mg, 1.5 mmol), 2-butanol (463 mg, 6.6 mmol) and complex **1** (40 mg, 2 mol %) were mixed in a vial, and the solution was divided into five separate 25 mL Schelenk tubes equipped with magnetic stirring bar. After adding H_2O (0.5 mL), each tube was evacuated, and refilled with N_2 gas. The tubes were stirred in an oil bath set at 110 °C. Each reaction tube was taken out of the oil bath in 15 min intervals, was immediately cooled in liquid N_2 bath, and hexamethylbenzene (10 mg, internal standard) dissolved in CDCl_3 (1 mL) was added. After shaking the reaction tube for 5 min, CDCl_3 layer was separated and was analyzed by ^1H NMR. The $k_{\text{H}_2\text{O}}$ was determined from a first-order plot of $-\ln([p\text{-OMe-C}_6\text{H}_5\text{CHO}]_t/p\text{-OMe-C}_6\text{H}_5\text{CHO}]_0)$ vs. time. The $k_{\text{D}_2\text{O}}$ was determined from the analogous experiment by using D_2O . The $k_{\text{H}_2\text{O}}/k_{\text{D}_2\text{O}}$ was calculated from the ratio of slopes (Figure S2).

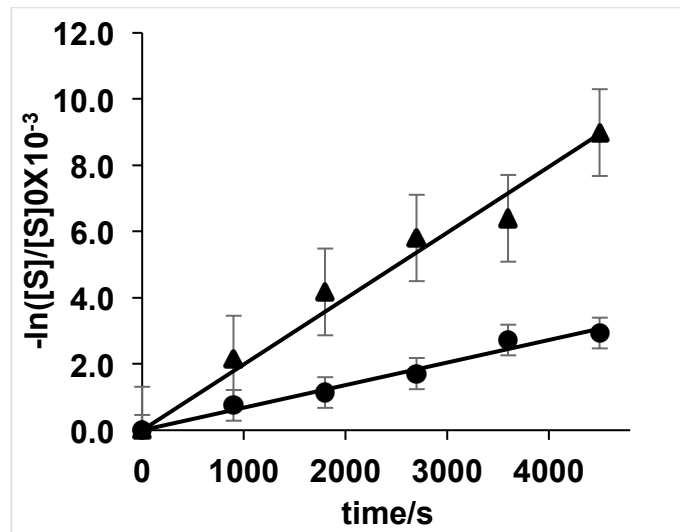


Figure S2. First Order Plot of the 4-Methoxybenzaldehyde with 2-Butanol in H_2O (triangle) and in D_2O (circle).

In a glove box, 4-methoxybenzaldehyde (340 mg, 1.5 mmol), 2-propanol (0.5 mL) and complex **1** (50 mg, 2 mol %) were mixed in a vial, and the solution was divided into five separate 25 mL Schlenk tubes equipped with magnetic stirring bar. The tubes were stirred in an oil bath set at 110 °C. Each reaction tube was taken out of the oil bath in 15 min intervals, was immediately cooled in liquid N₂ bath, hexamethylbenzene (10 mg, internal standard) in benzene-*d*₆ (0.5 mL) was added, and the resulting mixture was analyzed by ¹H NMR. The *k_{PrOH}* was determined from a first-order plot of $-ln([p\text{-OMe-C}_6\text{H}_5\text{CHO}]_t/p\text{-OMe-C}_6\text{H}_5\text{CHO}_0)$ vs. time. The experiment was repeated by using 2-propanol-*d*₁ as the solvent to determine *k_{PrOD}*. The *k_{PrOH}/k_{PrOD}* was calculated from the ratio of slopes.

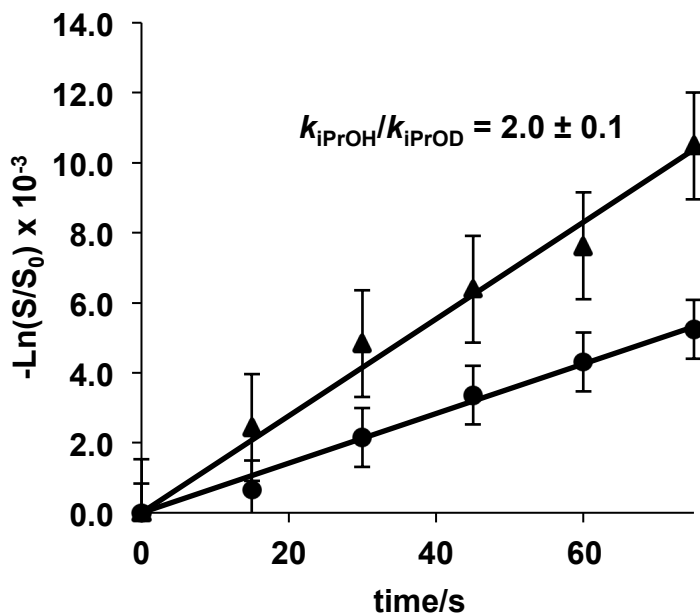


Figure S3. First Order Plot of the 4-Methoxybenzaldehyde with 2-Propanol (triangle) and in 2-Propanol-*d*₁ (circle).

5. H/D Exchange Reaction of 4-Methoxybenzaldehyde with 1-Butanol in D₂O. In a glove box, complex **1** (17 mg, 3 mol %) was placed into a 25 mL Schlenk tube equipped with a Teflon stopcock and a magnetic stirring bar. The tube was brought out of the glove box, and 4-methoxybenzaldehyde (136 mg, 1.0 mmol), 1-butanol (185 mg, 2.5 mmol) and D₂O (99% D, 1 mL) were added to the tube. The tube was filled with N₂, and was stirred in an oil bath set at 110 °C for 12 h. The reaction tube was taken out of the oil bath, and was cooled to room temperature. After the tube was open to air, the organic layer was extracted with CH₂Cl₂ (2 mL). The organic layer was filtered through a short silica gel column by eluting with CH₂Cl₂ (10 mL), and the filtrate was analyzed by GC and GC-MS. Analytically pure product was isolated by a simple column chromatography

on silica gel (280-400 mesh, hexanes/Et₂O = 40:1). The deuterium content of the product **2f** was determined by ¹H and ²H NMR (Figure S4).

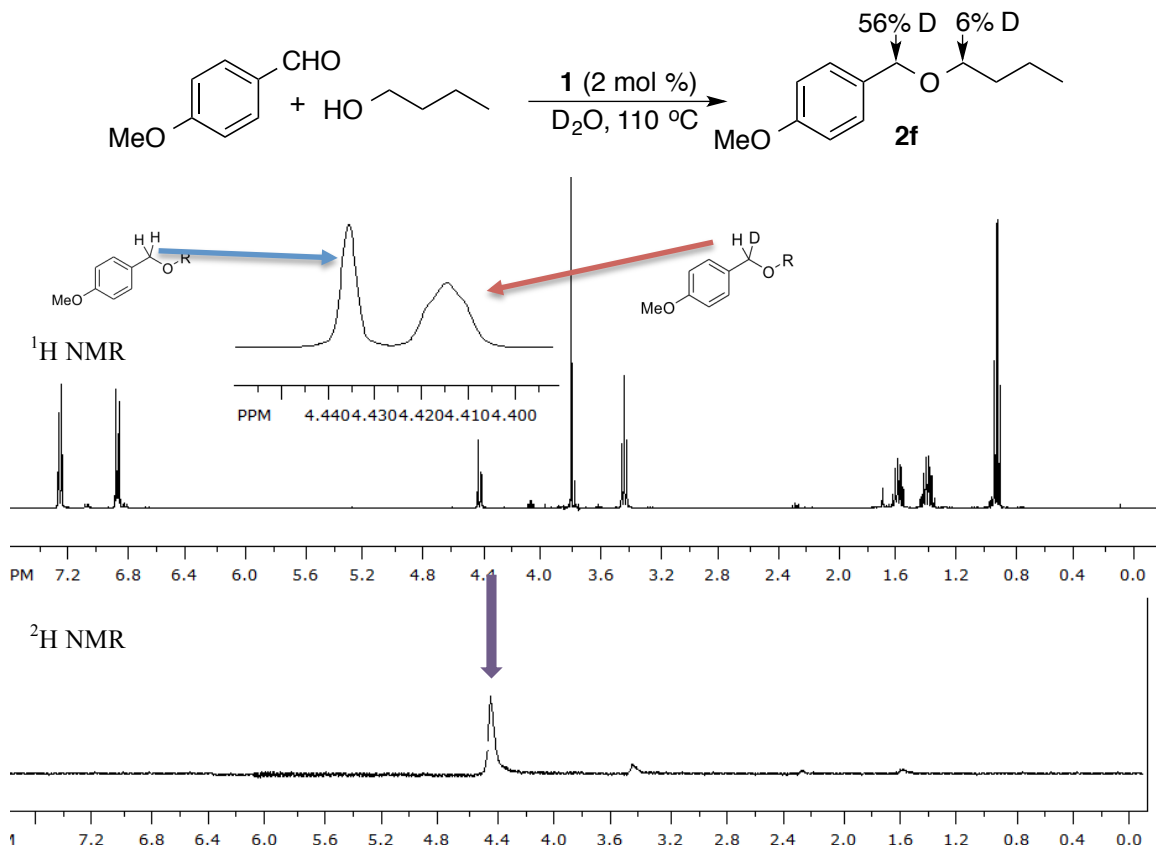
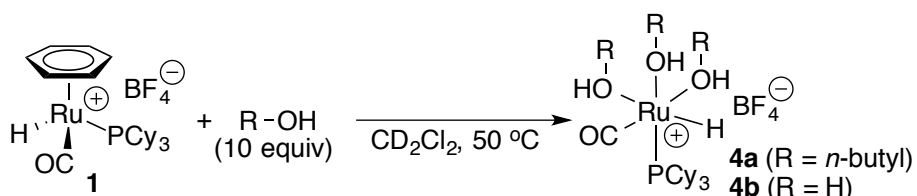


Figure S4. ¹H and ²H NMR Spectra of the Product **2f** Isolated from the Reaction of 4-Methoxybenzaldehyde with 1-Butanol in D₂O.



6. Detection and Synthesis of the Alcohol Complexes 4a-4c. In a glove box, complex **1** (40 mg, 0.07 mmol) was dissolved in CD₂Cl₂ (1 mL) in a NMR tube. 1-Butanol (52 mg, 10 equiv) was added via syringe, and the tube was shaken for 5-10 min at room temperature. The reaction progress was monitored by ¹H NMR and ³¹P NMR at 50 °C. After 5 min, the appearance of new ruthenium hydride species as indicated by a new Ru-H signal (δ -18.8 (d, J_{PH} = 31.3 Hz) ppm) and free benzene molecule (δ 7.26 ppm) was detected by ¹H NMR (Figure S5).

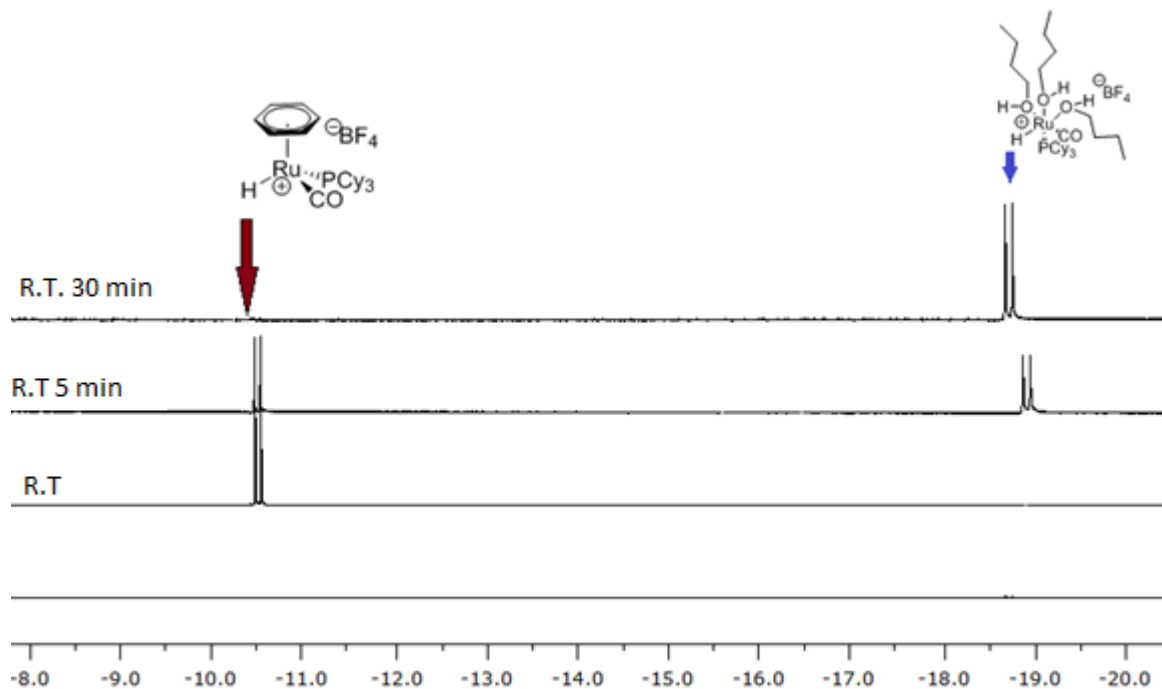


Figure S5. ^1H NMR Spectra of the Reaction of **1** with 1-Butanol.

The analogous treatment of **1** (40 mg) with H_2O (13 mg, 10 equiv) was monitored by NMR. After 5 min at room temperature, the appearance of **4b** was detected by ^1H and ^{31}P NMR. Because the complex decomposes within 1 h at room temperature, both ^1H NMR and ^{31}P NMR spectra were recorded at -10°C in this case (^1H NMR: δ -17.7 (d, $J_{\text{H}-\text{P}} = 30.3$ Hz) ppm, ^{31}P NMR: δ 73.0 ppm). Synthesis of **4c**: The treatment of complex **1** (115 mg, 0.2 mmol) with 1,1,1-tris(hydroxymethyl)ethane (24 mg, 0.2 mmol) in acetone (2 mL), and the mixture was stirred for 30 min at room temperature. The solution was layered with *n*-pentane (5 mL) to obtain single crystals of **4c** as colorless crystals in 80% yield.

7. X-Ray Crystallographic Determination of **3e** and **4c**.

For **3e**: Colorless single crystals of **3e** were grown in CH_2Cl_2 at room temperature. A suitable crystal with the dimension of $0.42 \times 0.12 \times 0.05$ mm³ was selected and mounted on an Oxford SuperNova diffractometer equipped with dual microfocus Cu/Mo X-ray sources, X-ray mirror optics, and Atlas CCD area detector. A total of 11497 reflection data were collected by using MoK α ($\lambda = 1.54184$) radiation while the crystal sample was cooled at 100.00 K during the data collection. Using Olex2, the molecular structure was solved with the ShelXS structure solution program by using Direct Methods, and the data was refined with the XL refinement package using Least Squares minimization. The molecular structure of **3e** is shown in Figure S6.

For **4c**: Colorless single crystals of **4c** were grown in acetone/*n*-pentane at room temperature. A suitable crystal with the dimension of $0.3068 \times 0.2254 \times 0.0989$ mm³ was selected and mounted on an Oxford

SuperNova diffractometer equipped with dual microfocus Cu/Mo X-ray sources, X-ray mirror optics, and Atlas CCD area detector. A total of 55980 reflection data were collected by using MoK α ($\lambda = 1.54184$) radiation while the crystal sample was cooled at 100.00 K during the data collection. Using Olex2, the molecular structure was solved with the ShelXS structure solution program by using Direct Methods, and the data was refined with the XL refinement package using Least Squares minimization. The molecular structure of **4c** is shown in Figure S7.

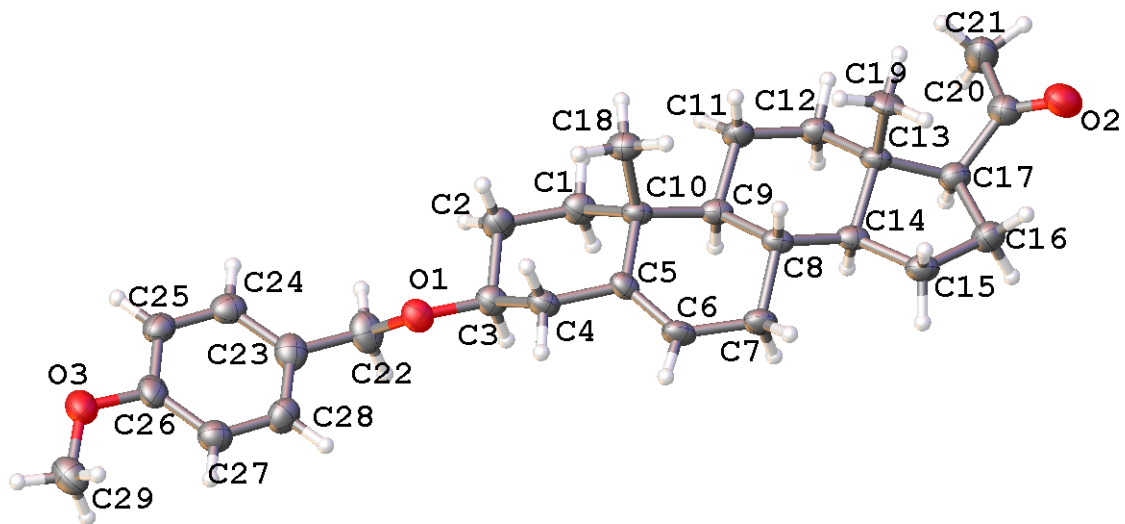


Figure S6. Molecular Structure of **3e**.

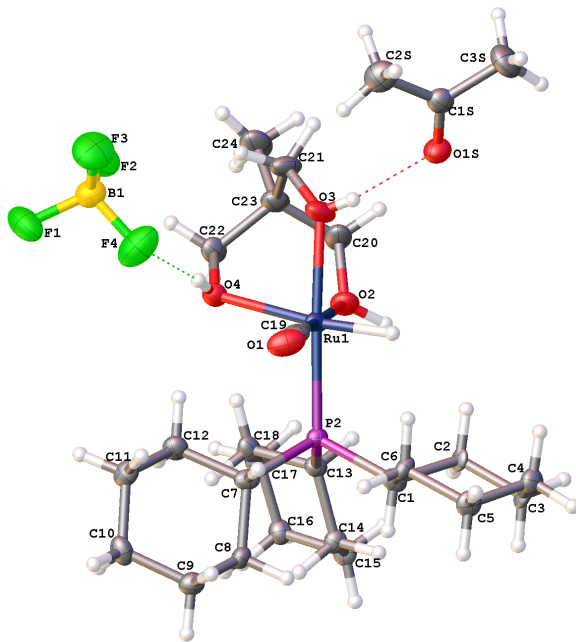
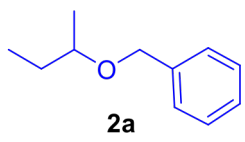


Figure S7. Molecular Structure of **4c**.

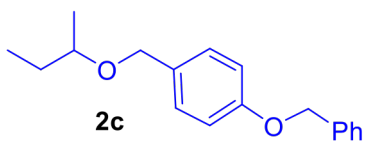
8. Characterization Data of the Products.



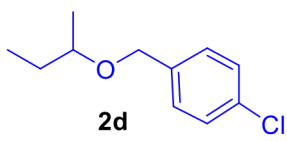
Data for **2a**: Colorless oil (82%, 134 mg). ^1H NMR (400 MHz, CDCl_3) δ 7.77-7.95 (m, 3H), 7.42-7.59 (m, 2H), 4.57 (d, $J = 11.9$ Hz, 1H), 4.49 (d, $J = 11.9$ Hz, 1H), 3.52 (sextet, $J = 6.1$ Hz, 1H), 1.63-1.74 (m, 1H), 1.47-1.61 (m, 1H), 1.25 (d, $J = 6.1$ Hz, 3H), 0.97 (t, $J = 7.4$ Hz, 3H) ppm; $^{13}\text{C}\{\text{H}\}$ NMR (100 MHz, CDCl_3) δ 138.2, 128.4, 127.8, 127.6, 72.1, 70.2, 29.2, 19.2, 9.8 ppm; GC-MS $m/z = 164$ (M^+). ^1H and ^{13}C NMR spectral data are in good agreement with the literature data.^{S1}



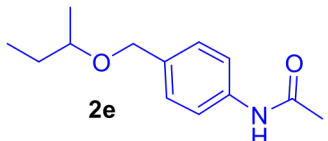
Data for **2b**: Colorless oil (95%, 184 mg). ^1H NMR (400 MHz, CDCl_3) δ 7.29 (d, $J = 8.3$ Hz, 2H), 6.89 (d, $J = 8.3$ Hz, 2H), 4.51 (d, $J = 11.7$ Hz, 1H), 4.42 (d, $J = 11.7$ Hz, 1H), 3.81 (s, 3H), 3.44 (sextet, $J = 7.0$ Hz, 1H), 1.61 (dq, $J = 14.7, 7.9$ Hz, 1H), 1.49 (qd, $J = 14.0, 7.9$ Hz, 1H), 1.19 (d, $J = 6.1$ Hz, 3H), 0.93 (t, $J = 7.9$ Hz, 3H) ppm; $^{13}\text{C}\{\text{H}\}$ NMR (100 MHz, CDCl_3) δ 158.9, 131.2, 129.1, 113.7, 75.8, 69.9, 55.2, 29.2, 19.2, 9.8 ppm; GC-MS $m/z = 194$ (M^+). ^1H and ^{13}C NMR spectral data are in good agreement with the literature data.^{S2}



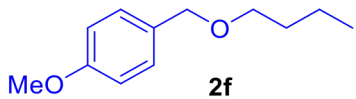
Data for **2c**: White solid (97%, 261 mg). ^1H NMR (400 MHz, CDCl_3) δ 7.27-7.47 (m, 7H), 6.95-6.99 (m, 2H), 5.09 (s, 2H), 4.52 (d, $J = 11.3$ Hz, 1H), 4.43 (d, $J = 11.3$ Hz, 1H), 3.46 (sextet, $J = 5.9$ Hz, 1H), 1.58-1.74 (m, 1H), 1.45-1.56 (m, 1H), 1.20 (d, $J = 6.3$ Hz, 3H), 0.94 (t, $J = 7.4$ Hz, 3H) ppm; $^{13}\text{C}\{\text{H}\}$ NMR (100 MHz, CDCl_3) δ 158.1, 137.0, 131.5, 129.1, 128.5, 127.8, 127.4, 114.6, 75.9, 69.9, 69.9, 29.2, 19.2, 9.8 ppm; GC-MS $m/z = 270$ (M^+); Anal. Calcd for $\text{C}_{18}\text{H}_{22}\text{O}_2$: C, 79.96; H, 8.20. Found: C, 79.88; H, 8.31.



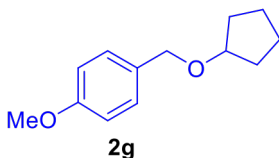
Data for **2d**: Colorless liquid (68%, 134 mg). ^1H NMR (400 MHz, CDCl_3) δ 7.20-7.23 (m, 4H), 4.45 (d, $J = 12.2$ Hz, 1H), 4.36 (d, $J = 12.2$ Hz, 1H), 3.36 (sextet, $J = 6.1$ Hz, 1H), 1.51-1.61 (m, 1H), 1.35-1.47 (m, 1H), 1.11 (d, $J = 6.4$ Hz, 3H), 0.85 (t, $J = 7.5$ Hz, 3H) ppm; $^{13}\text{C}\{\text{H}\}$ NMR (100 MHz, CDCl_3) δ 137.7, 133.0, 128.8, 128.4, 76.4, 69.5, 29.2, 19.1, 9.8 ppm; GC-MS $m/z = 198$ (M^+); Anal. Calcd for $\text{C}_{11}\text{H}_{15}\text{ClO}$: C, 66.50; H, 7.61. Found: C, 66.48; H, 7.52.



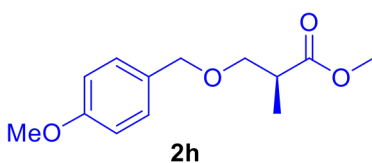
Data for **2e**: White solid (85%, 187 mg). ^1H NMR (400 MHz, CDCl_3) δ 7.55 (br s, 1H), 7.47 (d, $J = 8.61$ Hz, 2H), 7.30 (d, $J = 8.2$ Hz, 2H), 4.52 (d, $J = 11.7$ Hz, 1H), 4.43 (d, $J = 11.7$ Hz, 1H), 3.44 (sextet, $J = 6.1$ Hz, 1H), 2.16 (s, 3H), 1.61 (ddd, $J = 13.7, 7.4, 6.3$ Hz, 1H), 1.48 (ddd, $J = 13.7, 7.4, 5.8$ Hz, 1H), 1.18 (d, $J = 6.3$ Hz, 3H), 0.92 (t, $J = 7.4$ Hz, 3H) ppm; $^{13}\text{C}\{\text{H}\}$ NMR (100 MHz, CDCl_3) δ 168.4, 137.0, 135.0, 128.3, 199.8, 76.1, 69.8, 29.1, 24.5, 19.1, 9.8 ppm; GC-MS $m/z = 221$ (M^+); Anal. Calcd for $\text{C}_{13}\text{H}_{19}\text{NO}_2$: C, 70.56; H, 8.65. Found: C, 70.48; H, 8.61.



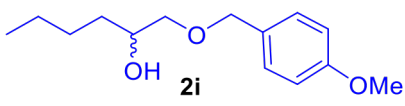
Data for **2f**: Yellow oil (98%, 190 mg). ^1H NMR (400 MHz, CDCl_3) δ 7.28 (d, $J = 8.5$ Hz, 2H), 6.90 (d, $J = 8.5$ Hz, 2H), 4.45 (s, 2H), 3.81 (s, 3H), 3.46 (t, $J = 6.6$ Hz, 2H), 1.60 (quintet, $J = 6.2$ Hz, 2H), 1.41 (sextet, $J = 7.4$ Hz, 2H), 0.93 (t, $J = 7.4$ Hz, 3H) ppm; $^{13}\text{C}\{\text{H}\}$ NMR (100 MHz, CDCl_3) δ 159.0, 130.7, 129.1, 113.6, 72.4, 69.8, 55.1, 31.8, 19.3, 13.9 ppm; GC-MS $m/z = 194$ (M^+); ^1H and ^{13}C NMR spectral data are in good agreement with the literature data.^{S2}



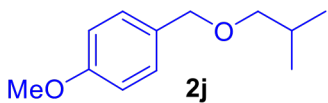
Data for **2g**: Colorless oil (95%, 195 mg). ^1H NMR (400 MHz, CDCl_3) δ 7.16-7.22 (m, 2H), 6.77-6.82 (m, 2H), 4.33 (s, 2H), 3.87-3.94 (m, 1H), 3.72 (s, 3H), 1.59-1.71 (m, 6H), 1.39-1.49 (m, 2H) ppm; $^{13}\text{C}\{\text{H}\}$ NMR (100 MHz, CDCl_3) δ 158.9, 131.0, 129.2, 129.1, 113.7, 80.5, 70.3, 55.2, 32.3, 23.6, 23.5 ppm; GC-MS $m/z = 206$ (M^+); ^1H and ^{13}C NMR spectral data are in good agreement with the literature data.^{S3}



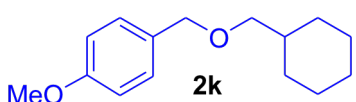
Data for **2h**: Colorless oil (91%, 216 mg). ^1H NMR (400 MHz, CDCl_3) δ 7.14-7.18 (m, 2H), 6.77-6.81 (m, 2H), 4.37 (dd, $J = 14.0, 12.0$ Hz, 2H), 3.71 (s, 3H), 3.60 (s, 3H), 3.54 (dd, $J = 9.0, 7.4$ Hz, 1H), 3.37 (dd, $J = 9.2, 6.1$ Hz, 1H), 2.68 (qt, $J = 7.5, 6.1$ Hz, 1H), 1.08 (d, $J = 7.0$ Hz, 3H) ppm; $^{13}\text{C}\{\text{H}\}$ NMR (100 MHz, CDCl_3) δ 175.2, 159.1, 130.1, 129.1, 113.6, 72.6, 71.5, 55.1, 51.6, 40.1, 13.9 ppm; GC-MS $m/z = 238$ (M^+); ^1H and ^{13}C NMR spectral data are in good agreement with the literature data.^{S4}



Data for **2i**: Colorless oil (91%, 216 mg). ^1H NMR (400 MHz, CDCl_3) δ 7.24-7.30 (m, 2H), 6.87-6.92 (m, 2H), 4.49 (s, 2H), 3.81 (s, 3H), 3.49 (dd, $J = 9.4, 3.1$ Hz, 1H), 3.3 (dd, $J = 9.4, 7.8$ Hz, 1H), 2.39 (br s, 1H), 1.26-1.51 (m, 7H), 0.90 (t, $J = 7.4$ Hz, 3H) ppm; $^{13}\text{C}\{\text{H}\}$ NMR (100 MHz, CDCl_3) δ 159.2, 130.0, 129.4, 113.8, 74.3, 72.9, 70.4, 55.2, 32.8, 27.7, 22.7, 14.0 ppm; GC-MS $m/z = 238$ (M^+); ^1H and ^{13}C NMR spectral data are in good agreement with the literature data.^{S5}



Data for **2j**: Colorless oil (86%, 166 mg), ^1H NMR (400 MHz, CDCl_3) δ 7.28 (d, $J = 8.4$ Hz, 2H), 6.90 (d, $J = 8.7$ Hz, 2H), 4.45 (s, 2H), 3.82 (s, 3H), 3.49 (t, $J = 6.8$ Hz, 2H), 1.74 (dt, $J = 13.4, 6.7$ Hz, 1H), 1.52 (qd, $J = 6.8, 0.9$ Hz, 2H), 0.92 (d, $J = 7.7$ Hz, 6H) ppm; $^{13}\text{C}\{\text{H}\}$ NMR (100 MHz, CDCl_3) δ 159.0, 130.7, 129.2, 113.7, 72.5, 68.5, 55.2, 38.5, 22.6 ppm; GC-MS $m/z = 194$ (M^+); ^1H and ^{13}C NMR spectral data are in good agreement with the literature data.^{S6}

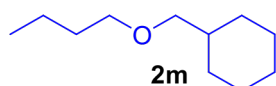


Data for **2k**: Yellow oil (88%, 201 mg). ^1H NMR (400 MHz, CDCl_3) δ 7.13 (d, $J = 8.7$ Hz, 2H), 6.9 (d, $J = 8.6$ Hz, 2H), 4.47 (s, 2H), 3.80 (s, 3H),

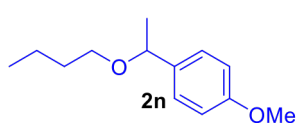
3.29 (d, $J = 6.5$ Hz, 2H), 1.62-1.95 (m, 5H), 1.15-1.49 (m, 4H), 0.92-1.05 (m, 2H) ppm; $^{13}\text{C}\{\text{H}\}$ NMR (100 MHz, CDCl_3) δ 157.8, 133.6, 129.6, 113.7, 75.9, 72.5, 55.1, 55.1, 40.0, 38.0, 30.1, 26.6, 25.8 ppm; GC-MS $m/z = 234$ (M^+); Anal. Calcd for $\text{C}_{15}\text{H}_{22}\text{O}_2$: C, 76.88; H, 9.46. Found: C, 76.48; H, 9.51.



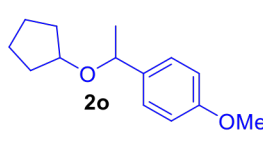
Data for **2l**: Colorless volatile liquid (71%, 92 mg). ^1H NMR (400 MHz, CDCl_3) δ 3.37 (t, $J = 6.5$ Hz, 2H), 3.50 (q, $J = 11.9$ Hz, 2H), 1.31-1.51 (m, 8H), 1.10 (t, $J = 6.5$ Hz, 3H), 0.88 (t, $J = 6.5$ Hz, 3H) ppm; $^{13}\text{C}\{\text{H}\}$ NMR (100 MHz, CDCl_3) δ 70.4, 66.6, 31.8, 30.0, 22.7, 22.6, 15.2, 14.1 ppm; GC-MS $m/z = 130$ (M^+); ^1H and ^{13}C NMR spectral data are in good agreement with the literature data.⁵⁷



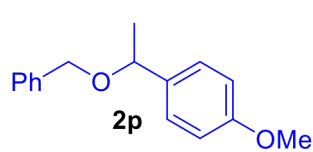
Data for **2m**: Colorless liquid (76%, 129 mg). ^1H NMR (400 MHz, CDCl_3) δ 3.29 (t, $J = 6.6$ Hz, 2H), 3.08 (d, $J = 6.0$ Hz, 2H), 1.52-1.71 (m, 5H), 1.41-1.52 (m, 2H), 1.22-1.34 (m, 2H), 0.98-1.22 (m, 4H), 0.73-0.89 (m, 5H) ppm; $^{13}\text{C}\{\text{H}\}$ NMR (100 MHz, CDCl_3) δ 76.8, 70.8, 38.0, 31.8, 30.1, 26.7, 25.9, 19.3, 13.9 ppm; GC-MS $m/z = 170$ (M^+). ^1H and ^{13}C NMR spectral data are in good agreement with the literature data.⁵⁸



Data for **2n**: Colorless oil (88%, 166 mg). ^1H NMR (400 MHz, CDCl_3) δ 6.93 (d, $J = 8.7$ Hz, 2H), 6.57 (d, $J = 8.8$ Hz, 2H), 4.03 (q, $J = 6.4$ Hz, 1H), 3.49 (s, 3H), 2.96 (t, $J = 6.6$ Hz, 2H), 1.18-1.28 (m, 2H), 1.11 (d, $J = 6.4$ Hz, 3H), 0.98-1.09 (m, 2H), 0.58 (t, $J = 7.4$ Hz, 3H) ppm; $^{13}\text{C}\{\text{H}\}$ NMR (100 MHz, CDCl_3) δ 158.8, 136.3, 127.2, 113.6, 77.3, 68.1, 55.1, 32.0, 24.1 19.3, 13.9 ppm; GC-MS $m/z = 208$ (M^+). ^1H and ^{13}C NMR spectral data are in good agreement with the literature data.⁵⁹



Data for **2o**: Colorless oil (93%, 204 mg). ^1H NMR (400 MHz, CDCl_3) δ 7.26 (d, $J = 8.4$ Hz, 2H), 6.89 (d, $J = 8.5$ Hz, 2H), 4.43 (q, $J = 6.5$ Hz, 1H), 3.82 (s, 3H), 1.41-1.77 (m, 9H), 1.39 (d, $J = 6.5$ Hz, 3H) ppm; $^{13}\text{C}\{\text{H}\}$ NMR (100 MHz, CDCl_3) δ 158.7, 136.7, 127.4, 113.6, 78.3, 74.9, 55.2, 33.0, 31.8, 24.6, 23.5, 23.4 ppm; GC-MS $m/z = 220$ (M^+). ^1H and ^{13}C NMR spectral data are in good agreement with the literature data.⁶⁰

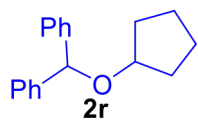


Data for **2p**: White solid (55%, 133 mg). ^1H NMR (400 MHz, CDCl_3) δ 7.10-7.33 (m, 7H), 6.72-6.87 (m, 2H), 4.38 (q, $J = 6.5$ Hz, 1H), 4.35 (d, $J = 11.9$ Hz, 1H), 4.19 (d, $J = 11.9$ Hz, 1H), 3.75 (s, 3H), 1.39 (d, $J = 6.5$ Hz, 3H) ppm; $^{13}\text{C}\{\text{H}\}$ NMR (100 MHz, CDCl_3) δ 159.0, 138.9, 135.7, 128.3, 127.7, 127.6, 127.4, 113.8, 76.7, 70.0, 55.3, 24.1 ppm; GC-MS $m/z = 242$ (M^+); ^1H and ^{13}C NMR spectral data are in good agreement with the literature data.⁶¹

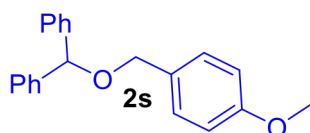


Data for **2q**: White solid (94%, 225 mg). ^1H NMR (400 MHz, CDCl_3) δ 7.27-7.48 (m, 10H), 5.44 (s, 1H), 3.56 (t, $J = 6.5$ Hz, 2H), 1.69-1.79 (m, 2H), 1.48-1.62 (m, 2H),

1.02 (t, $J = 7.4$ Hz, 3H) ppm; $^{13}\text{C}\{\text{H}\}$ NMR (100 MHz, CDCl_3) δ 142.6, 128.3, 128.3, 128.2, 128.2, 127.2, 126.9, 126.9, 126.8, 83.5, 68.9, 32.0, 19.4, 13.9 ppm; GC-MS $m/z = 240$ (M^+); ^1H and ^{13}C NMR spectral data are in good agreement with the literature data.^{S12}

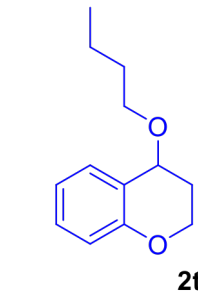


Data for **2r**: White solid (92%, 231 mg). ^1H NMR (400 MHz, CDCl_3) δ 7.23-7.52 (m, 10H), 5.54 (s, 1H), 4.05-4.16 (m, 1H), 1.74-1.96 (m, 6H), 1.54-1.70 (m, 2H) ppm; $^{13}\text{C}\{\text{H}\}$ NMR (100 MHz, CDCl_3) δ 142.8, 128.2, 127.2, 127.1, 80.9, 78.9, 32.5, 23.5 ppm; GC-MS $m/z = 252$ (M^+); Anal. Calcd for $\text{C}_{18}\text{H}_{20}\text{O}$: C, 85.67; H, 7.99. Found: C, 75.48; H, 8.61.

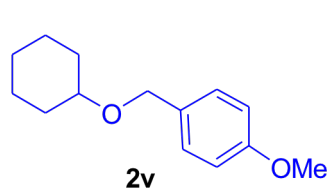
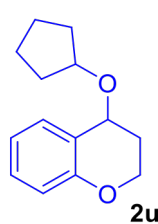


Data for **2s**: White solid (65%, 197 mg). ^1H NMR (400 MHz, CDCl_3) δ 7.13-7.34 (m, 12H), 6.78-6.85 (m, 2H), 5.35 (s, 1H), 4.40 (s, 2H), 3.74 (s, 3H) ppm; $^{13}\text{C}\{\text{H}\}$ NMR (100 MHz, CDCl_3) δ 159.1, 142.2, 130.4, 129.4, 128.4, 127.4, 127.1, 113.7, 82.0, 70.1, 55.3 ppm; GC-MS $m/z = 304$ (M^+); ^1H and ^{13}C NMR spectral data are in good agreement with the literature data.^{S13}

Data for **2t**: Colorless oil (89%, 183 mg). ^1H NMR (400 MHz, CDCl_3) δ 7.27 (dd, $J = 7.6, 1.8$ Hz, 1H), 7.20 (ddd, $J = 8.4, 7.0, 1.8$ Hz, 1H), 6.91 (td, $J = 7.4, 1.2$ Hz, 1H), 6.85 (dd, $J = 8.2, 1.2$ Hz, 1H), 4.38 (t, $J = 3.7$ Hz, 1H), 4.32 (td, $J = 11.0, 3.1$ Hz, 1H), 4.25 (dtd, $J = 11.0, 4.1, 0.8$ Hz, 1H), 3.59 (ttd, $J = 15.7, 12.9, 6.3$ Hz, 2H), 2.10-2.18 (m, 1H), 2.01-2.10 (m, 1H), 1.57-1.66 (m, 2H), 1.37-1.48 (m, 2H), 0.95 (t, $J = 7.4$ Hz, 3H) ppm; $^{13}\text{C}\{\text{H}\}$ NMR (100 MHz, CDCl_3) δ 154.7, 130.5, 29.4, 122.2, 119.9, 116.8, 70.3, 68.0, 62.2, 32.1, 27.6, 19.4, 13.9 ppm; GC-MS $m/z = 206$ (M^+); Anal. Calcd for $\text{C}_{13}\text{H}_{18}\text{O}_2$: C, 75.69; H, 8.80. Found: C, 75.48; H, 8.61.

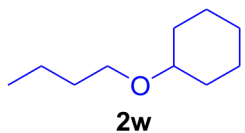


Data for **2u**: Colorless oil (82%, 178 mg). ^1H NMR (400 MHz, CDCl_3) δ 7.24-7.27 (m, 1H), 7.16-7.21 (m, 1H), 6.91 (td, $J = 7.4, 1.2$ Hz, 1H), 6.81-6.85 (m, 1H), 4.48 (t, $J = 3.9$ Hz, 1H), 4.28-4.35 (m, 1H), 4.22-4.28 (m, 1H), 4.16-4.22 (m, 1H), 3.88 (septet, $J = 6.1$ Hz, 1H), 2.04-2.08 (m, 3H), 1.27 (d, $J = 6.0$ Hz, 3H), 1.25 (d, $J = 6.2$ Hz, 3H) ppm; $^{13}\text{C}\{\text{H}\}$ NMR (100 MHz, CDCl_3) δ 154.8, 130.2, 129.4, 122.8, 120.2, 116.8, 68.9, 67.4, 62.3, 28.4, 23.3, 22.4 ppm; GC-MS $m/z = 192$ (M^+); Anal. Calcd for $\text{C}_{12}\text{H}_{16}\text{O}_2$: C, 74.97; H, 8.39. Found: C, 75.48; H, 8.61.

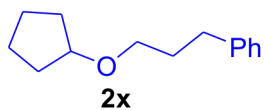


Data for **2v**: Colorless oil (85 %, 187 mg). ^1H NMR (400 MHz, CDCl_3) δ 7.24 (dd, $J = 7.5, 1.6$ Hz, 1H), 7.17 (td, $J = 7.8, 1.8$ Hz, 1H), 6.87-6.92 (m, 1H), 6.79-6.83 (m, 1H), 4.43 (t, $J = 4.0$ Hz, 1H), 4.41-4.45 (m, 1H), 4.36-4.16 (m, 4H), 1.93-2.12 (m, 2H), 1.67 (m, 1H), 1.63-1.88 (m, 5H), 1.51-1.63 (m, 2H) ppm; $^{13}\text{C}\{\text{H}\}$ NMR (100 MHz, CDCl_3) δ 154.8, 130.3, 129.2, 122.8, 120.1,

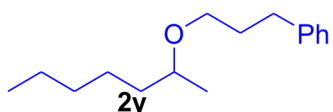
116.8, 78.5, 77.4, 68.0, 62.4, 33.0, 32.8, 28.1, 23.6, 23.4 ppm; GC-MS m/z = 218 (M^+); Anal. Calcd for C₁₄H₂₀O₂: C, 76.33; H, 9.15. Found: C, 76.38; H, 9.13.



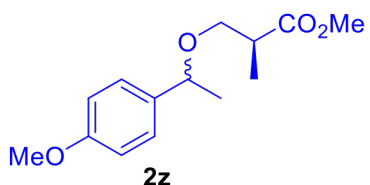
Data for **2w**: Colorless liquid (80%, 124 mg). ¹H NMR (400 MHz, CDCl₃) δ 3.43 (t, J = 6.7 Hz, 2H), 3.13-3.23 (m, 1H), 1.80-1.95 (m, 3H), 1.66-1.77 (m, 3H), 1.47-1.57 (m, 3H), 1.31-1.42 (m, 2H), 1.14-1.31 (m, 6H), 0.91 (t, J = 7.4 Hz, 3H) ppm; ¹³C{¹H} NMR (100 MHz, CDCl₃) δ 77.4, 67.5, 32.3, 32.3, 25.8, 25.8, 24.2, 19.4, 13.9 ppm; GC-MS m/z = 156 (M^+); ¹H and ¹³C NMR spectral data are in good agreement with the literature data.^{S7}



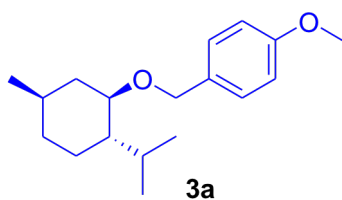
Data for **2x**: Yellow liquid (98%, 199 mg). ¹H NMR (400 MHz, CDCl₃) δ 7.25-7.32 (m, 2H), 7.17-7.23 (m, 3H), 4.28-4.35 (m, 1H), 3.65 (t, J = 6.8 Hz, 2H), 2.70 (t, J = 7.7 Hz, 2H), 1.94-2.04 (m, 2H), 1.84-1.93 (m, 2H), 1.68-1.82 (m, 4H), 1.48-1.65 (m, 2H) ppm; ¹³C{¹H} NMR (100 MHz, CDCl₃) δ 141.8, 128.4, 128.4, 128.4, 128.3, 128.3, 128.3, 125.8, 73.9, 62.1, 35.4, 34.1, 32.0, 23.2 ppm; GC-MS m/z = 234 (M^+); ¹H and ¹³C NMR spectral data are in good agreement with the literature data.^{S14}



Data for **2y**: Colorless oil (55%, 128 mg). ¹H NMR (400 MHz, CDCl₃) 7.17-7.24 (m, 3H), 7.08-7.15 (m, 2H), 3.42 (dt, J = 9.1, 6.4 Hz, 2H), 3.23-3.31 (m, 2H), 2.63 (td, J = 7.8, 1.8 Hz, 2H), 1.76-1.85 (m, 2H), 1.39-1.52 (m, 1H), 1.16-1.35 (m, 6H), 1.05 (d, J = 5.9 Hz, 3H), 0.82 (t, J = 6.8 Hz, 3H) ppm; ¹³C{¹H} NMR (100 MHz, CDCl₃) δ 142.2, 128.5, 128.3, 125.7, 75.4, 67.43, 36.7, 32.5, 32.0, 31.7, 25.3, 22.7, 19.7, 14.1 ppm; GC-MS m/z = 234 (M^+); Anal. Calcd for C₁₆H₂₆O: C, 81.99; H, 11.18. Found: C, 75.48; H, 8.61.

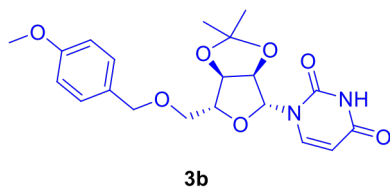


Data for **2z** (1:1 diasteromers): White solid (78%, 196 mg). Isomer **A**: ¹H NMR (400 MHz, CDCl₃) δ 7.21 (d, J = 8.8 Hz, 2H), 6.87 (d, J = 8.8 Hz, 2H), 4.35 (q, J = 6.3 Hz, 1H), 3.80 (s, 3H), 3.67 (s, 3H), 3.46 (t, J = 9.3 Hz, 1H), 3.28 (t, J = 6.4 Hz, 1H), 2.78-2.66 (m, 1H), 1.38 (d, J = 6.3 Hz, 3H), 1.14 (d, J = 7.0 Hz, 3H) ppm; ¹³C{¹H} NMR (100 MHz, CDCl₃) δ 175.5, 143.7, 128.3, 127.4, 126.1, 78.5, 70.5, 51.7, 40.3, 24.1, 14.0 ppm. Isomer **B**: ¹H NMR (100 MHz, CDCl₃) δ 7.20 (d, J = 8.8 Hz, 2H), 6.87 (d, J = 8.8 Hz, 2H), 4.34 (q, J = 6.3 Hz, 1H), 3.80 (s, 3H), 3.68 (s, 3H), 3.48 (t, J = 9.3 Hz, 1H), 3.30 (t, J = 6.4 Hz, 1H), 2.78-2.66 (m, 1H), 1.39 (d, J = 6.3 Hz, 3H), 1.12 (d, J = 7.0 Hz, 3H) ppm; ¹³C{¹H} NMR (100 MHz, CDCl₃) δ 175.3, 143.7, 128.4, 127.4, 126.1, 78.2, 70.4, 51.7, 40.3, 24.1, 14.0 ppm; GC-MS m/z = 252 (M^+); ¹H and ¹³C NMR spectral data are in good agreement with the literature data.^{S15}

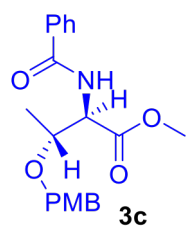


Data for **3a**: Colorless oil (90%, 248 mg). ¹H NMR (400 MHz, CDCl₃) δ 7.26-7.33 (m, 2H), 6.87-6.92 (m, 2H), 4.61 (d, J = 11.0 Hz, 1H), 4.35 (d, J = 11.0 Hz, 1H), 3.81 (s, 3H), 3.17 (td, J = 10.5, 4.2 Hz, 1H), 2.31 (m, J = 2.7 Hz, 1H), 2.20 (m, J = 1.7 Hz, 1H), 1.60-1.71 (m, 2H), 1.39 (s, 2H), 0.95-0.98 (m,

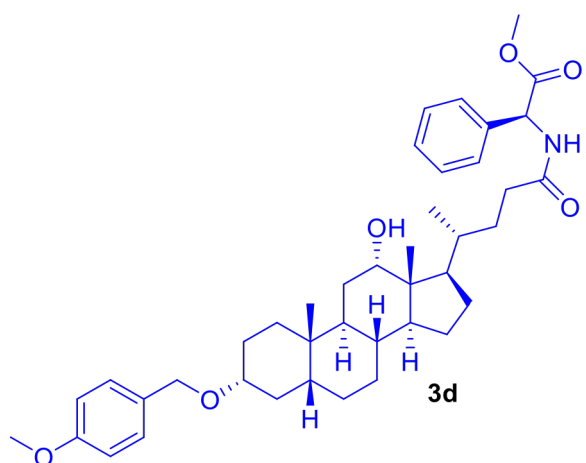
6H), 0.92 (d, J = 7.1 Hz, 3H), 0.73 (d, J = 6.9 Hz, 3H) ppm; $^{13}\text{C}\{\text{H}\}$ NMR (100 MHz, CDCl_3) δ 158.9, 131.2, 129.3, 113.6, 78.3, 70.0, 55.1, 48.2, 40.2, 34.5, 31.5, 25.4, 23.2, 22.3, 21.0, 14.0 ppm; GC-MS m/z = 276 (M^+); ^1H and ^{13}C NMR spectral data are in good agreement with the literature data.^{S16}



Data for **3b**: Yellow solid (52%, 210 mg). ^1H NMR (400 MHz, CDCl_3) δ 8.79 (br s, 1H), 7.59 (d, J = 8.1 Hz, 1H), 7.23 (d, J = 8.9 Hz, 2H), 6.90 (d, J = 8.7 Hz, 2H), 5.96 (d, J = 2.8 Hz, 1H), 5.52 (dd, J = 8.1, 2.3 Hz, 1H), 4.81 (dd, J = 6.2, 2.9 Hz, 1H), 4.7 (dd, J = 6.2, 2.8 Hz, 1H), 4.47 (dd, J = 14.3, 11.1 Hz, 2H), 4.40 (dd, J = 5.6, 2.9 Hz, 1H), 3.82 (s, 3H), 3.76 (dd, J = 10.5, 2.6 Hz, 1H), 3.65 (dd, J = 10.5, 3.4 Hz, 1H), 1.59 (s, 3H), 1.35 (s, 3H) ppm; ^{13}C NMR (100 MHz, CDCl_3) 163.5, 159.4, 150.2, 141.1, 129.5, 129.1, 114.0, 113.8, 102.1, 92.3, 85.5, 84.9, 80.8, 73.2, 69.7, 55.2, 27.1, 25.2 ppm; HRMS (ESI): calcd for $\text{C}_{20}\text{H}_{24}\text{N}_2\text{O}_7$ ($[\text{M}+\text{H}]^+$) 405.1656, found 405.1658. ^1H and ^{13}C NMR spectral data are in good agreement with the literature data.^{S17}

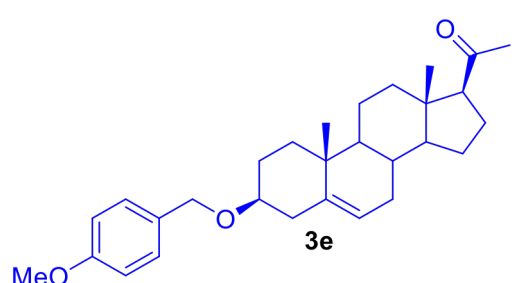


Data for **3c**: White Crystal (84%, 299 mg). ^1H NMR (400 MHz, CDCl_3) δ 7.79-7.86 (m, 2H), 7.46-7.52 (m, 1H), 7.38-7.45 (m, 2H), 7.17-7.22 (m, 2H), 6.84-6.89 (m, 3H), 4.87 (dd, J = 9.1, 2.4 Hz, 1H), 4.54 (d, J = 11.5 Hz, 1H), 4.34 (d, J = 11.5 Hz, 1H), 4.20 (ddd, J = 12.6, 6.3, 2.4 Hz, 1H), 3.78 (d, J = 0.4 Hz, 3H), 3.68 (s, 3H), 1.26 (d, J = 6.2 Hz, 3H) ppm; $^{13}\text{C}\{\text{H}\}$ NMR (100 MHz, CDCl_3) δ 171.0, 167.5, 159.2, 133.7, 131.6, 129.7, 129.3, 128.4, 127.0, 113.6, 73.7, 70.3, 56.9, 55.1, 52.2, 16.2 ppm; HRMS (ESI): calcd for $\text{C}_{20}\text{H}_{23}\text{NO}_5$ ($[\text{M}+\text{Na}]^+$) 380.1668, found 380.1669.



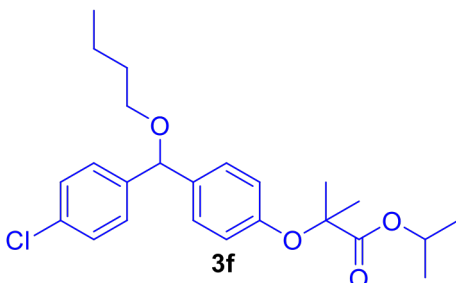
Data for **3d**: Yellow solid (81%, 533 mg). ^1H NMR (400 MHz, CDCl_3) δ 7.33-7.42 (m, 5H), 7.30 (d, J = 8.9 Hz, 2H), 6.90 (d, J = 7.8 Hz, 2H), 6.69 (d, J = 7.2 Hz, 1H), 5.65 (d, J = 6.7 Hz, 1H), 4.50-4.53 (m, 2H), 3.97 (br s, 1H), 3.83 (s, 3H), 3.75 (s, 3H), 3.39 (tt, J = 11.0, 4.4 Hz, 1H), 2.30-2.42 (m, 1H), 1.04-1.94 (m, 24H), 0.95-1.02 (m, 4H), 0.94 (s, 3H), 0.68 (s, 3H) ppm; $^{13}\text{C}\{\text{H}\}$ NMR (100 MHz, CDCl_3) δ 172.8, 171.4, 158.8, 136.5, 131.0, 128.9, 128.8, 128.3, 127.1, 113.6, 78.1, 72.9, 69.2, 56.12, 55.1, 52.6, 48.0, 46.9, 46.3, 41.9, 35.9,

35.1, 34.9, 34.3, 33.4, 33.0, 32.8, 31.1, 28.5, 27.3, 27.1, 26.9, 25.9, 23.5, 23.1, 17.2, 12.6 ppm; HRMS (ESI): calcd for $\text{C}_{41}\text{H}_{57}\text{NO}_6$ ($[\text{M}+\text{H}]^+$) 660.4259, found 660.4262.



Data for **3e**: White crystalline solid (78%, 340 mg). ^1H

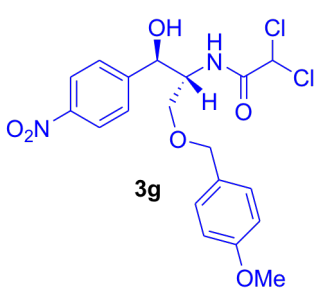
NMR (400 MHz, CDCl₃) δ 7.22-7.30 (m, 2H), 6.81-6.90 (m, 2H), 5.29-5.37 (m, 1H), 4.48 (s, 2H), 3.78 (s, 3H), 3.19-3.31 (m, 1H), 2.47-2.56 (m, 1H), 2.35-2.45 (m, 1H), 2.12-2.30 (m, 2H), 2.11 (s, 3H), 1.77-2.06 (m, 4H), 1.37-1.72 (m, 9H), 1.01-1.31 (m, 3H), 1.00 (s, 3H), 0.61 (s, 3H) ppm; ¹³C NMR (100 MHz, CDCl₃) 209.4, 58.9, 140.9, 131.0, 129.0, 121.1, 113.7, 78.0, 69.5, 63.6, 56.8, 55.2, 49.9, 43.9, 39.0, 38.7, 37.2, 36.8, 31.7, 31.5, 28.3, 24.4, 22.7, 21.0, 19.3, 13.1 ppm; GC-MS *m/z* = 276. ¹H and ¹³C NMR spectral data are in good agreement with the literature data.⁵¹⁸



Data for **3f**: White solid (73%, 305 mg). ¹H NMR (400 MHz,

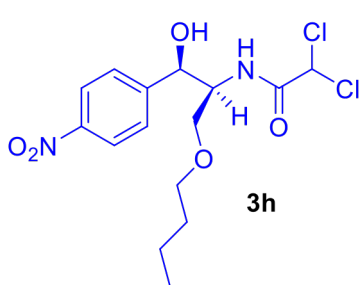
CDCl₃) δ 7.23-7.31 (m, 4H), 7.12-7.20 (m, 2H), 6.77-6.85 (m, 2H), 5.25 (s, 1H), 5.08 (septet, *J* = 6.2 Hz, 1H), 3.60 (dt, *J* = 9.3, 6.6 Hz, 1H), 1.52-1.66 (m, 9H), 1.34-1.47 (m, 2H), 1.20 (d, *J* = 6.5 Hz, 6H), 0.93 (t, *J* = 7.8 Hz, 3H) ppm; ¹³C NMR (100 MHz, CDCl₃) 173.6, 154.9, 141.3, 135.4, 128.3, 128.2, 127.7, 118.6, 102.8, 82.3, 78.9, 68.8, 65.0, 35.5, 31.9, 25.3, 21.4, 19.4, 18.0, 13.8 ppm; GC-

MS *m/z* = 418; HRMS (APCI): calcd for C₂₄H₃₁ClO₄ ([M+H]⁺) 419.1989, found 419.1991.



Data for **3g**: White solid (65%, 287 mg). ¹H NMR (400 MHz, CDCl₃) δ

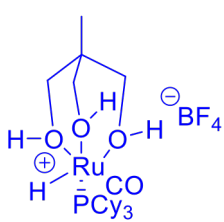
8.02-8.13 (m, 2 H), 7.42 (d, *J* = 8.7 Hz, 2H), 7.18 (d, *J* = 8.7 Hz, 2H), 7.09 (d, *J* = 9.0 Hz, 1H), 6.83 (d, *J* = 8.5 Hz, 2H), 5.70 (s, 1H), 5.13 (d, *J* = 2.4 Hz, 1H), 4.44 (s, 2H), 4.12-4.19 (m, 1H), 3.73 (s, 3H), 3.60-3.69 (m, 3H) ppm; ¹³C{¹H} NMR (100 MHz, CDCl₃) δ 164.1, 159.6, 147.5, 129.6, 128.7, 126.7, 123.5, 114.0, 73.5, 73.3, 70.4, 66.1, 55.3, 54.4 ppm; GC-MS *m/z* = 442 (M⁺); HRMS (APCI): calcd for C₁₉H₂₂Cl₂N₂O₆ ([M+H]⁺) 443.0777; found. 443.0779.



Data for **3h**: Colorless oil (72%, 272 mg). ¹H NMR (400 MHz, CDCl₃)

δ 8.17-8.23 (m, 2H), 7.50-7.55 (m, 2H), 7.08 (d, *J* = 9.7 Hz, 1H), 5.68 (s, 1H), 5.08-5.13 (m, 1H), 4.88 (t, *J* = 5.0 Hz, 1H), 4.32 (dq, *J* = 9.7, 1.8 Hz, 1H), 4.08-4.20 (m, 3H), 1.76-1.85 (m, 3H), 1.49-1.61 (m, 2H), 1.01 (t, *J* = 7.3 Hz, 3H) ppm; ¹³C{¹H} NMR (100 MHz, CDCl₃) δ 163.5, 147.5, 144.4, 126.4, 126.4, 123.5, 123.4, 102.9, 78.4, 77.4, 77.3, 76.7, 76.6, 70.2, 65.9, 47.6, 36.7, 17.0, 14.0 ppm; GC-MS *m/z* = 379 (M⁺); HRMS (APCI): calcd for C₁₅H₂₁Cl₂N₂O₅ ([M+H]⁺) 379.0828; found. 379.0825.

Data for **4c**: Complex **1** (115 mg, 0.2 mmol) and 1,1,1-tris(hydroxymethyl)ethane (24 mg, 0.2 mmol) in acetone (2 mL) were stirred at room temperature for 30 min. Crystallization in acetone/*n*-pentane to obtain the complex as white crystals in 80% yield. ¹H NMR (400 MHz, acetone-*d*₆) δ 3.64 (m, 3H), 3.48-

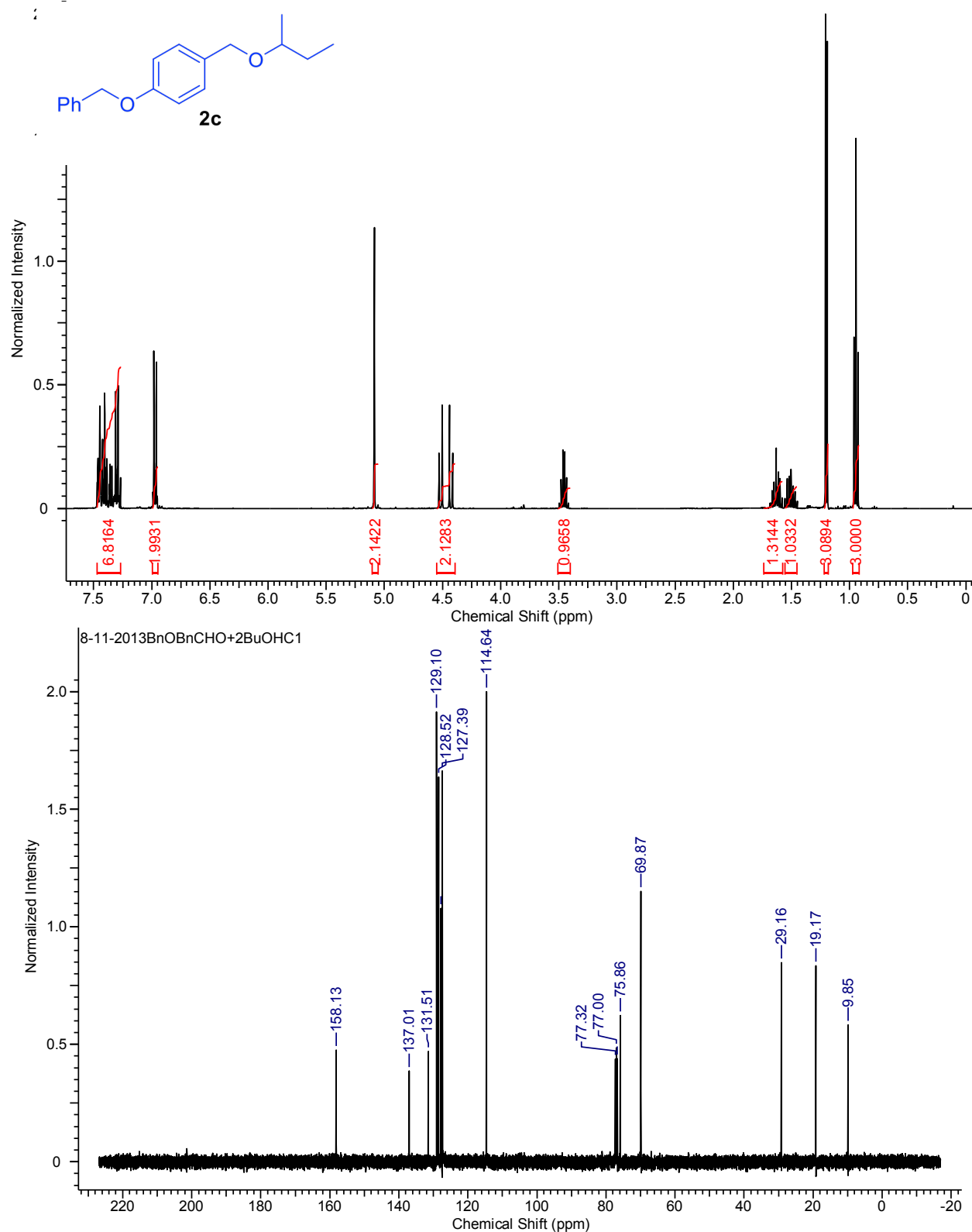


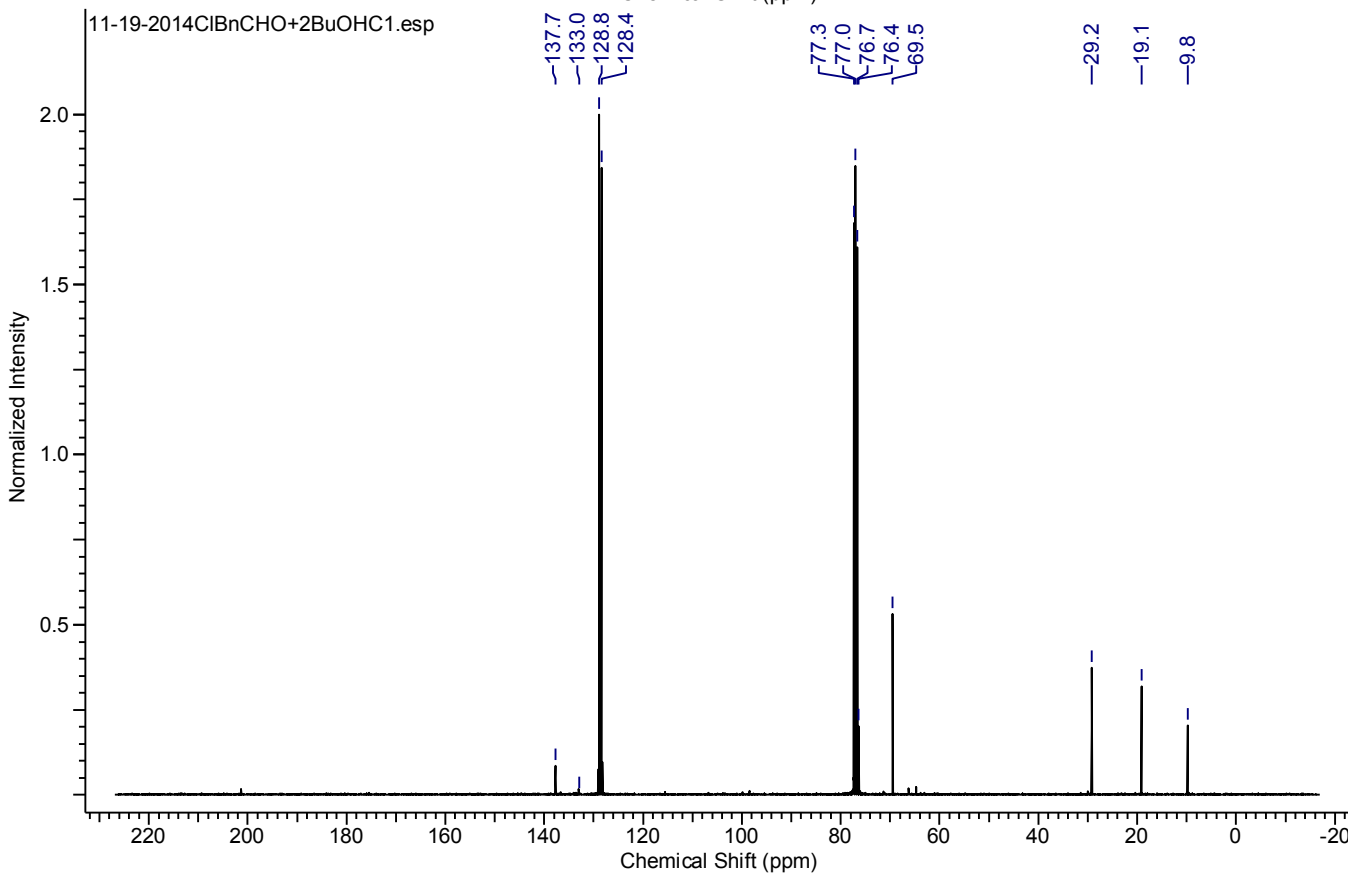
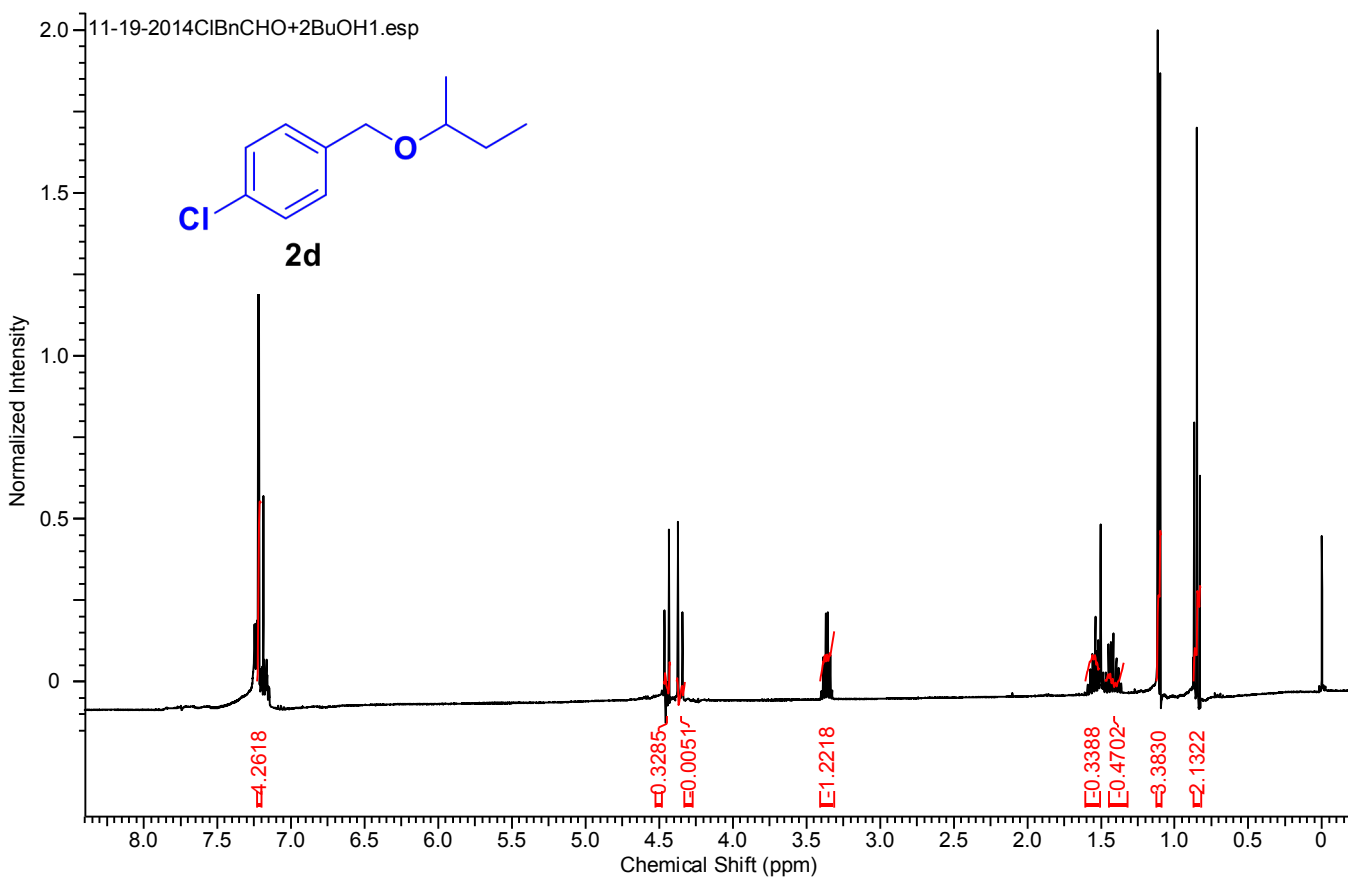
3.55 (m, 6H), 1.17-1.39 (m, 33H), 0.82 (s, 3H), -17.76 (d, $J_{\text{PH}} = 34.2$ Hz, 1H) ppm; $^{13}\text{C}\{\text{H}\}$ NMR (100 MHz, CDCl_3) δ 216.1 (d, $J_{\text{CP}} = 18.3$ Hz), 72.0, 65.7, 64.5, 37.5, 30.8, 30.1, 27.9, 27.8, 26.7 ppm; ^{31}P NMR (100 MHz, CDCl_3) δ 76.4 ppm; FT-IR (pure solid) $\nu_{\text{CO}} = 1915 \text{ cm}^{-1}$.

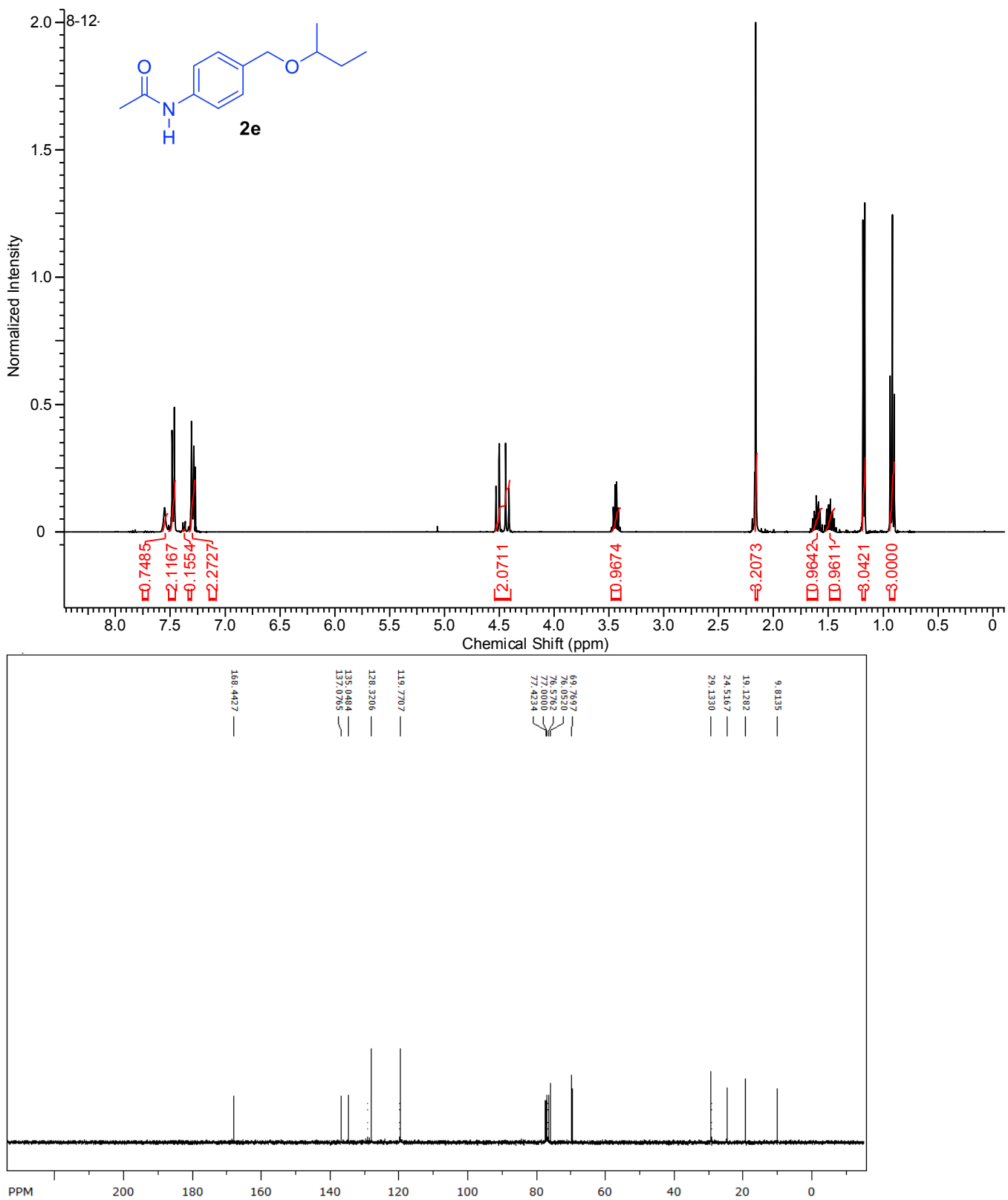
References

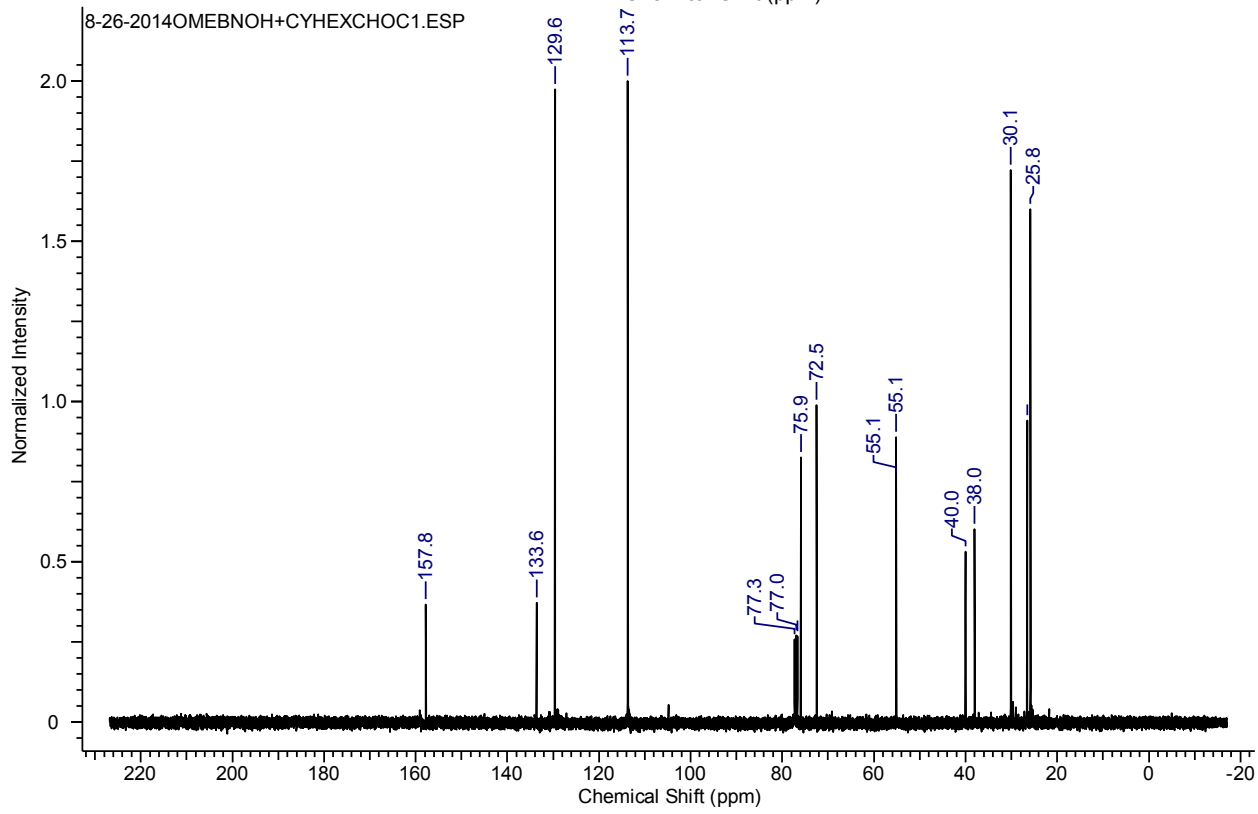
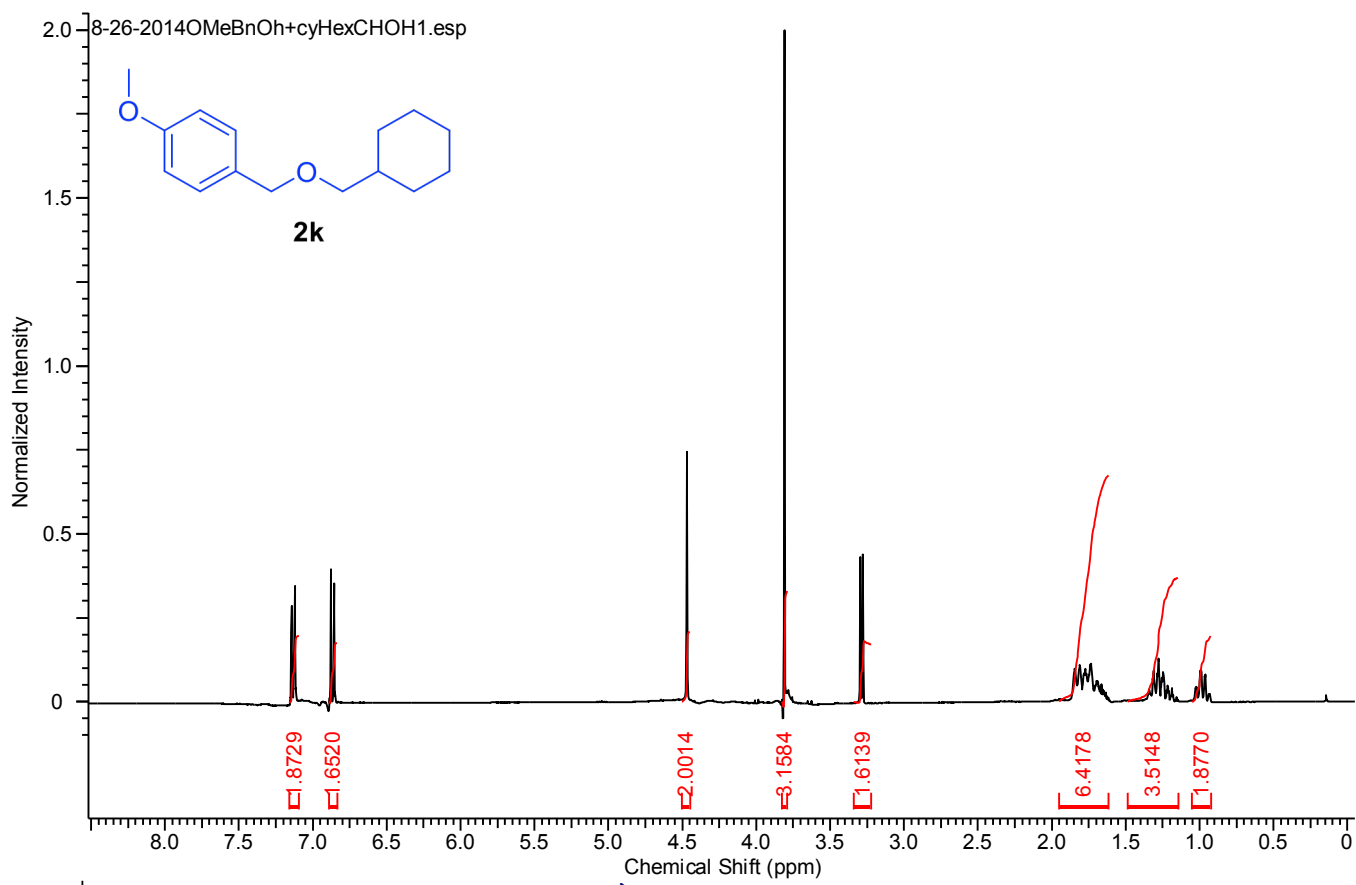
- S1** Dimitriadis, E.; Massy-Westropp, R. A. *Aust. J. Chem.* **1984**, *37*, 619-627.
- S2** Yu, J.-L.; Wang, H.; Zou, K.-F.; Zhang, J.-R.; Gao, X.; Zhang, D.-W.; Li, Z.-T. *Tetrahedron* **2013**, *69*, 310-315.
- S3** Molander, G. A.; Canturk, B. *Org. Lett.* **2008**, *10*, 2135-2138.
- S4** Burke, C. P.; Haq, N.; Boger, D. L. *J. Am. Chem. Soc.* **2010**, *132*, 2157-2159.
- S5** Joseph, M.; Jacobsen, E. N. *J. Am. Chem. Soc.* **2001**, *123*, 2687-2688.
- S6** Shah, S. T. A.; Singh, P. S.; Guiry J. *J. Org. Chem.* **2009**, *74*, 2179-2182.
- S7** Radhakrishnan, S.; Franken, J.; Martens, J. A. *Green Chem.* **2012**, *14*, 1475-1479.
- S8** Sassaman, M. B.; Kotian, K. D.; Prakash, G. K. S.; Olah, G. A. *J. Org. Chem.* **1987**, *52*, 4314-4319.
- S9** Wang, H. *Chinese J. Chem.* **2011**, *29*, 1180-1184.
- S10** Zaccheria, F.; Psaro, R.; Ravasio, N. *Tetrahedron Lett.* **2009**, *50*, 5221-5224.
- S11** Talluri, S. K.; Sudalai, A. *Org. Lett.* **2005**, *7*, 855-857.
- S12** Davies, T. E.; Kean, J. R.; Apperley, D. C.; Taylor, S. H.; Graham, A. E. *ACS Sust. Chem. Eng.* **2014**, *2*, 860-866.
- S13** Yadav, J. S.; Meshram, H. M.; Reddy, G. S.; Sumithra, G. *Tetrahedron Lett.* **1998**, *39*, 3043-3046.
- S14** Huang, H.; Nelson, C. G.; Taber, D. F. *Tetrahedron Lett.* **2010**, *51*, 3545-3546.
- S15** Kim, J.; Lee, D.-H.; Kalutharage, N.; Yi, C. S. *ACS Catal.* **2014**, *4*, 3881-3885.
- S16** Shintou, T.; Mukaiyama, T. *J. Am. Chem. Soc.* **2004**, *126*, 7359-7367.
- S17** Blank, H. U.; Pfleiderer, W. *Justus Liebigs Ann. Chem.* **1970**, *742*, 1-15.
- S18** Piazza, P. V.; Vallee, M.; Felpin, F.-X.; Revest, J.-M.; Fabre, S. *PCT Int. Appl.* **2014**, WO2014083068 A1 20140605.

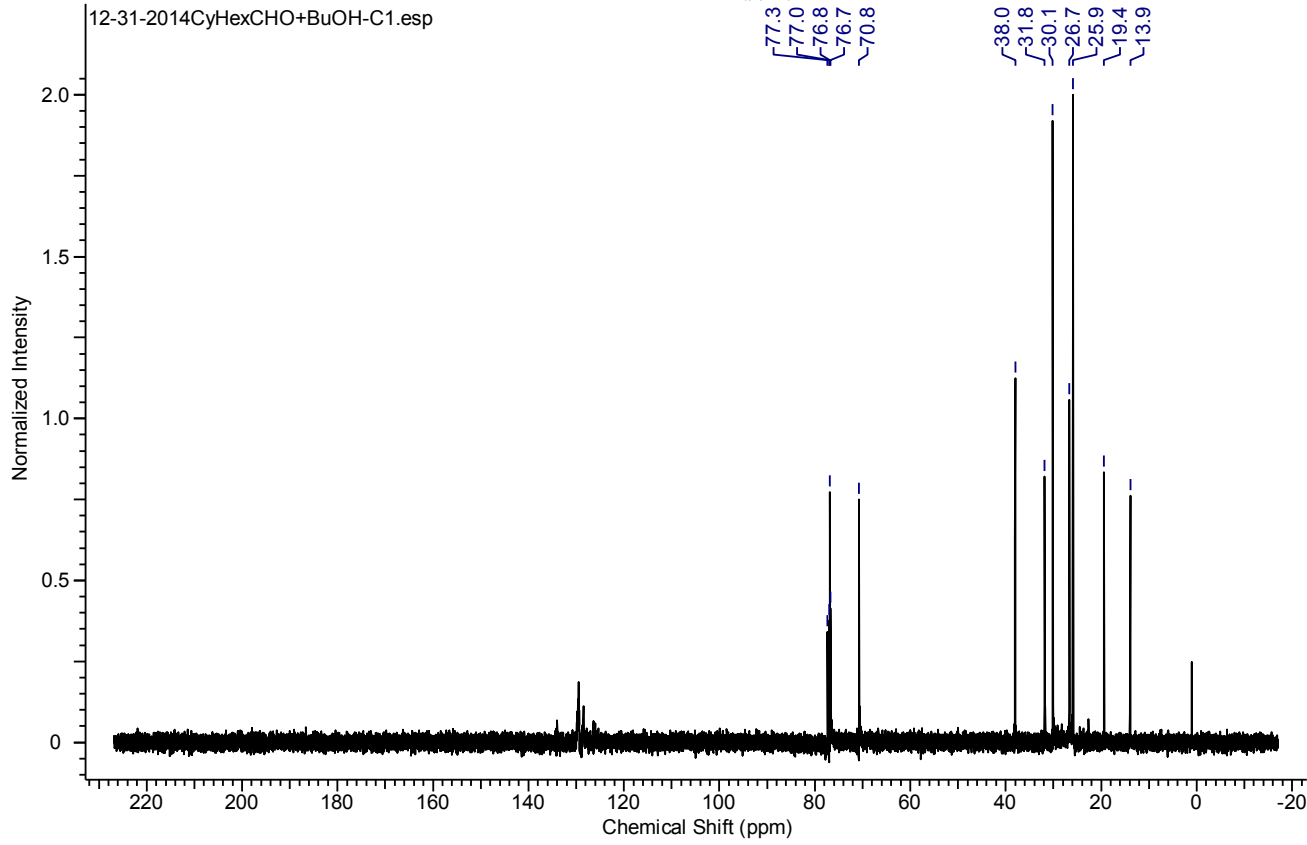
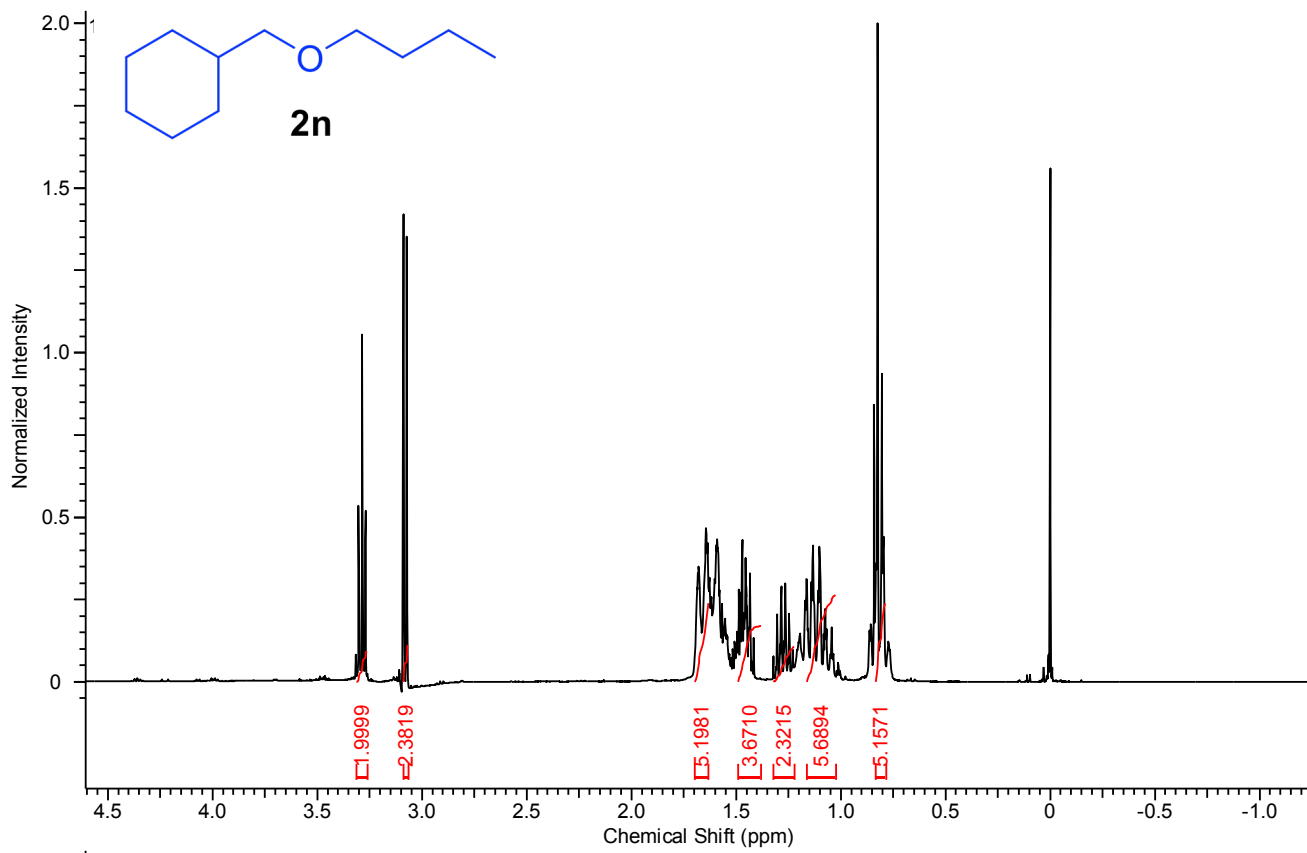
8. ^1H and $^{13}\text{C}\{^1\text{H}\}$ NMR Spectra of New Compounds

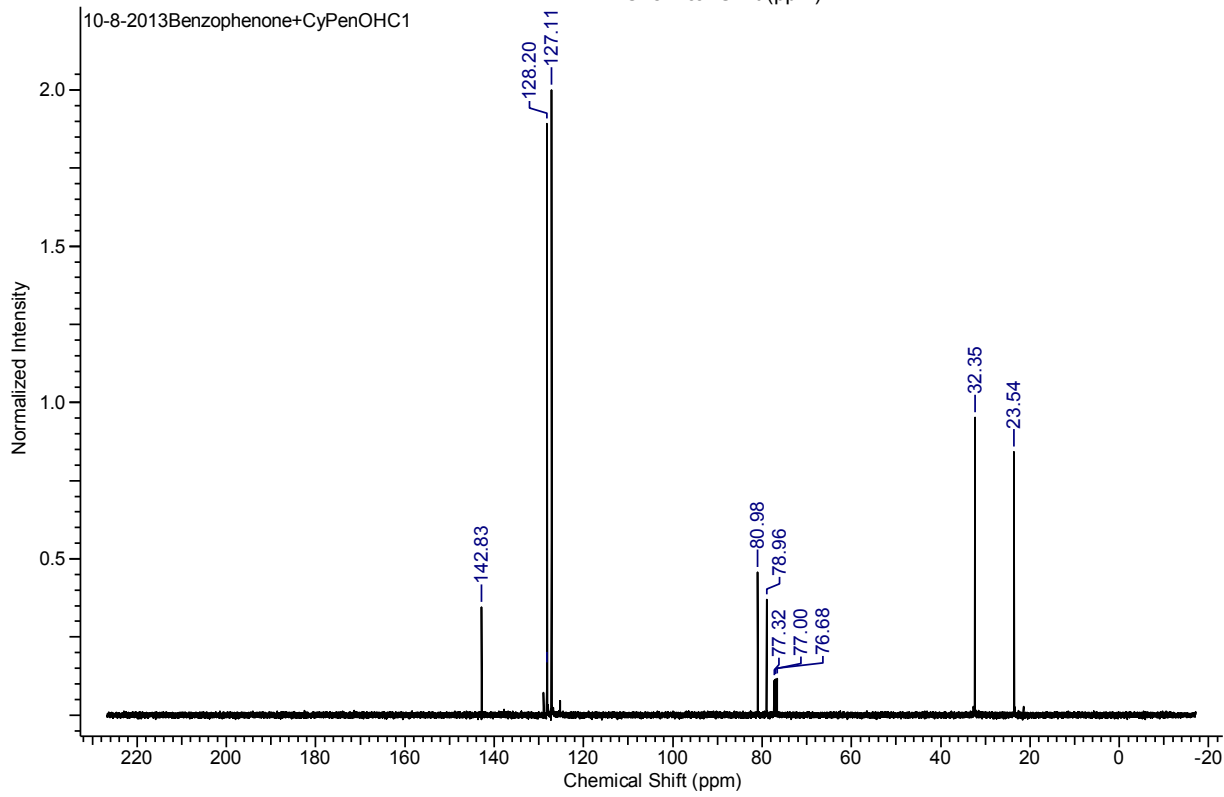
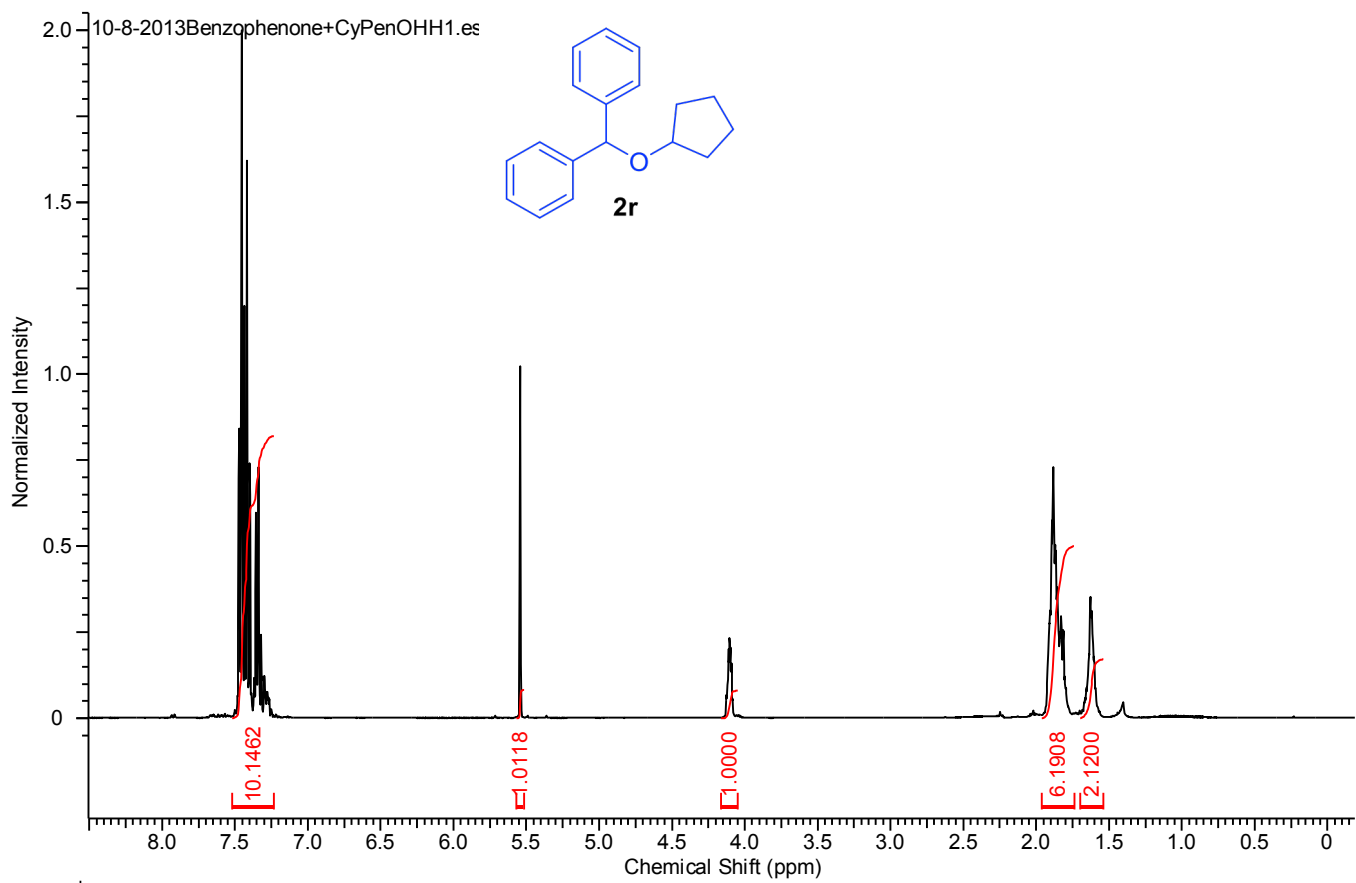


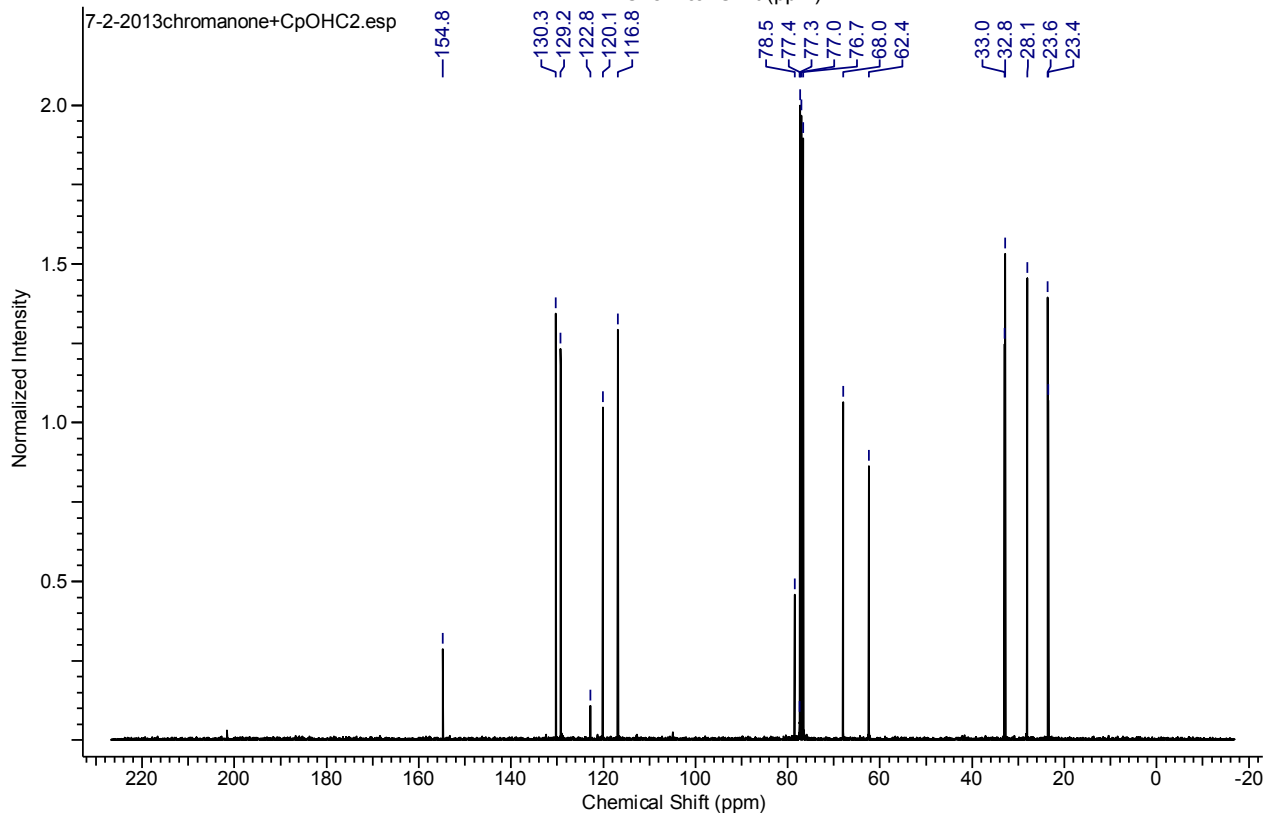
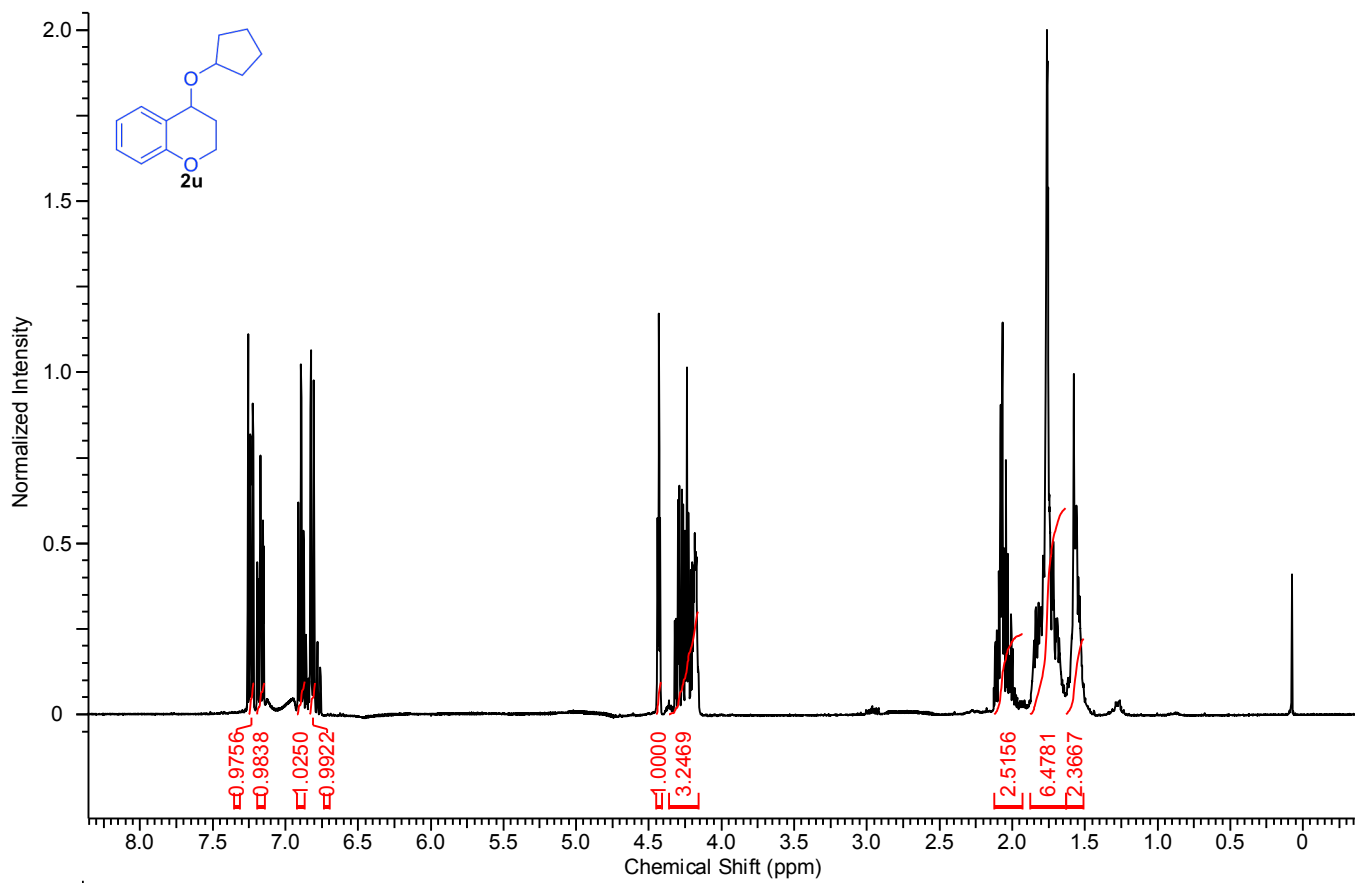


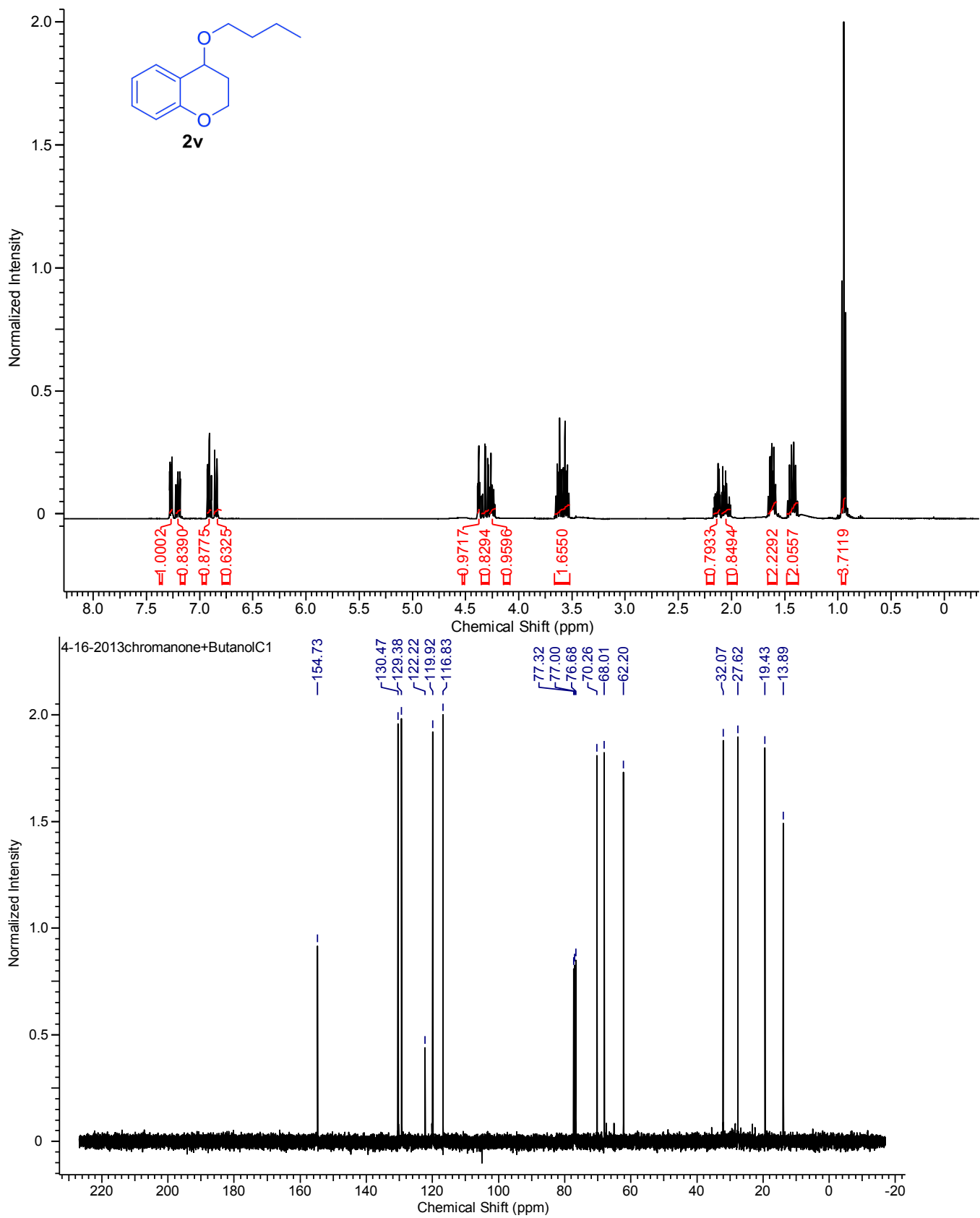


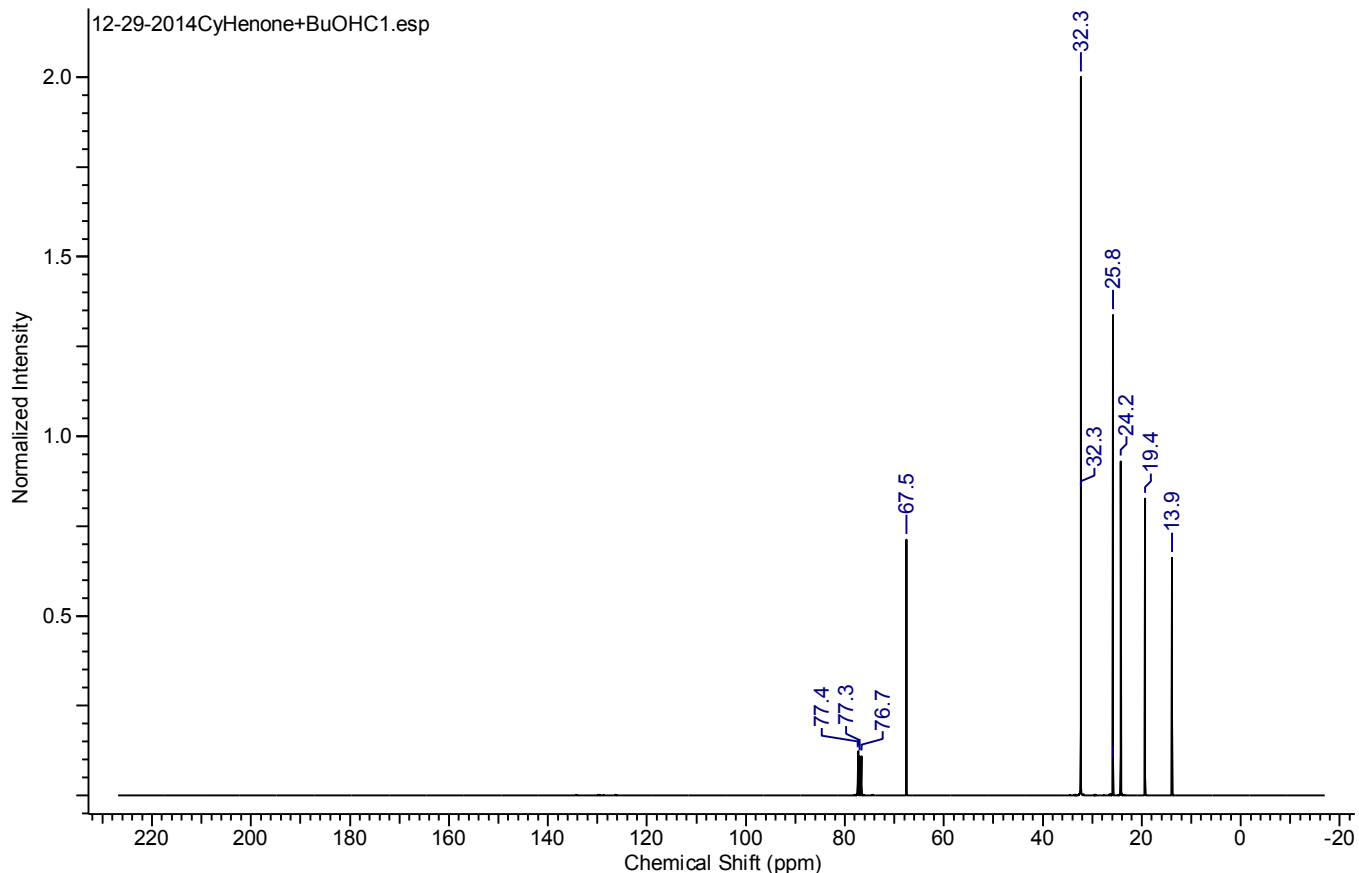
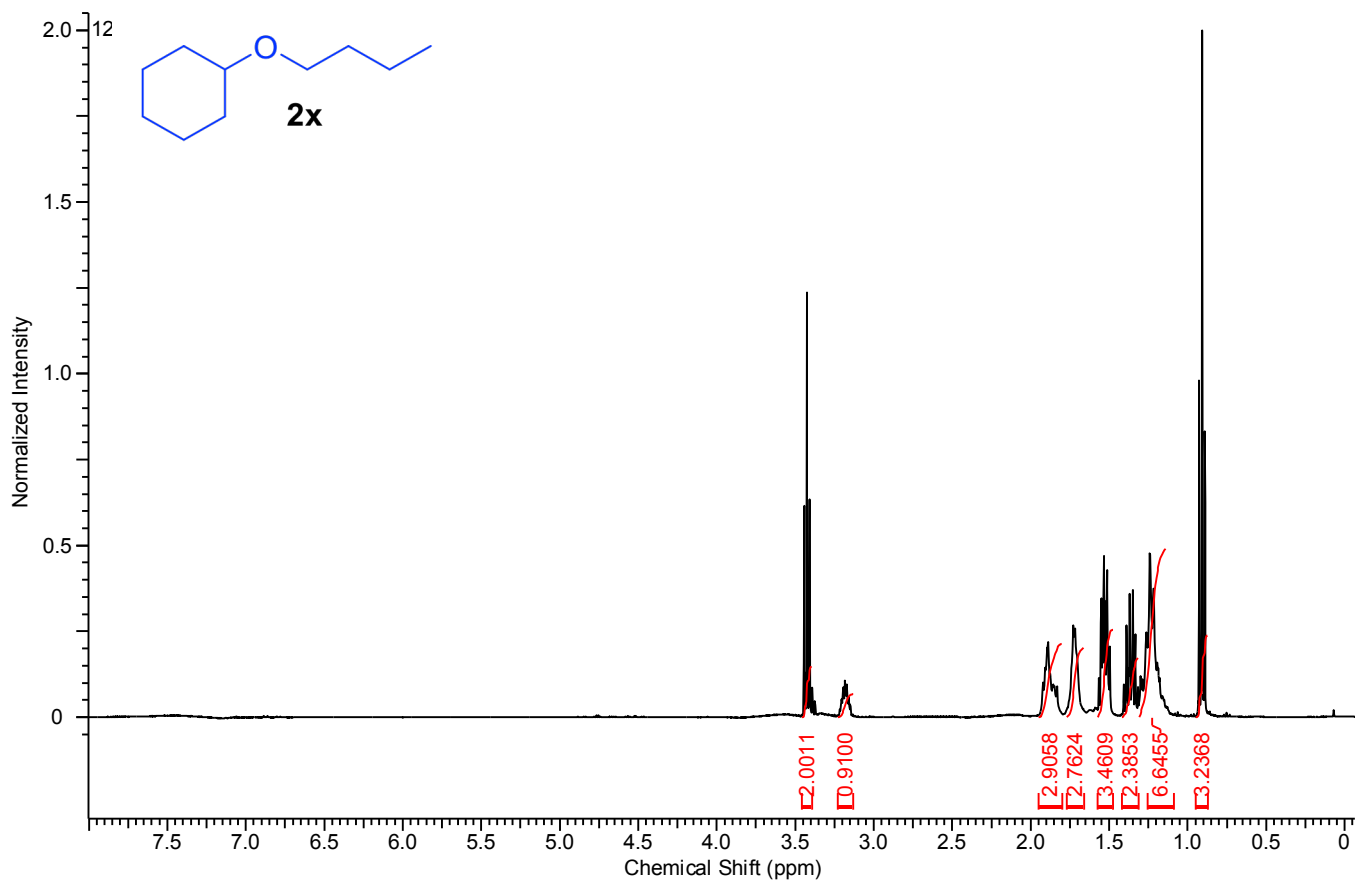


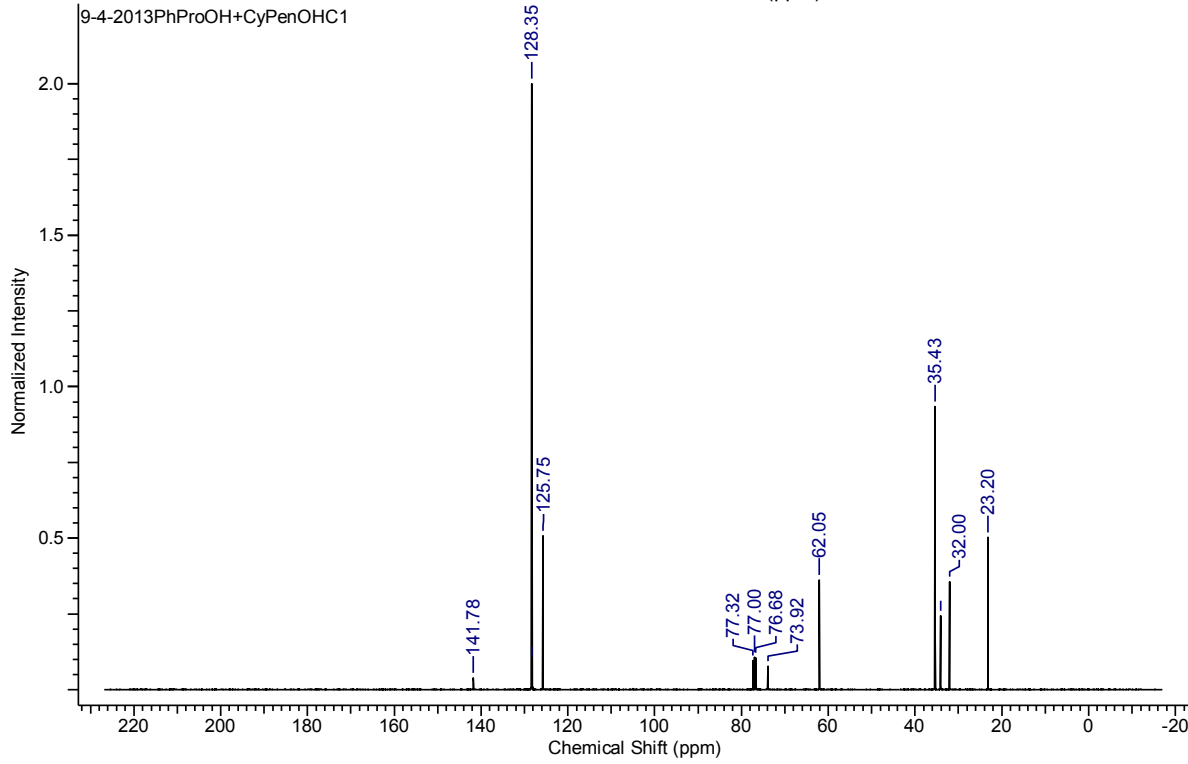
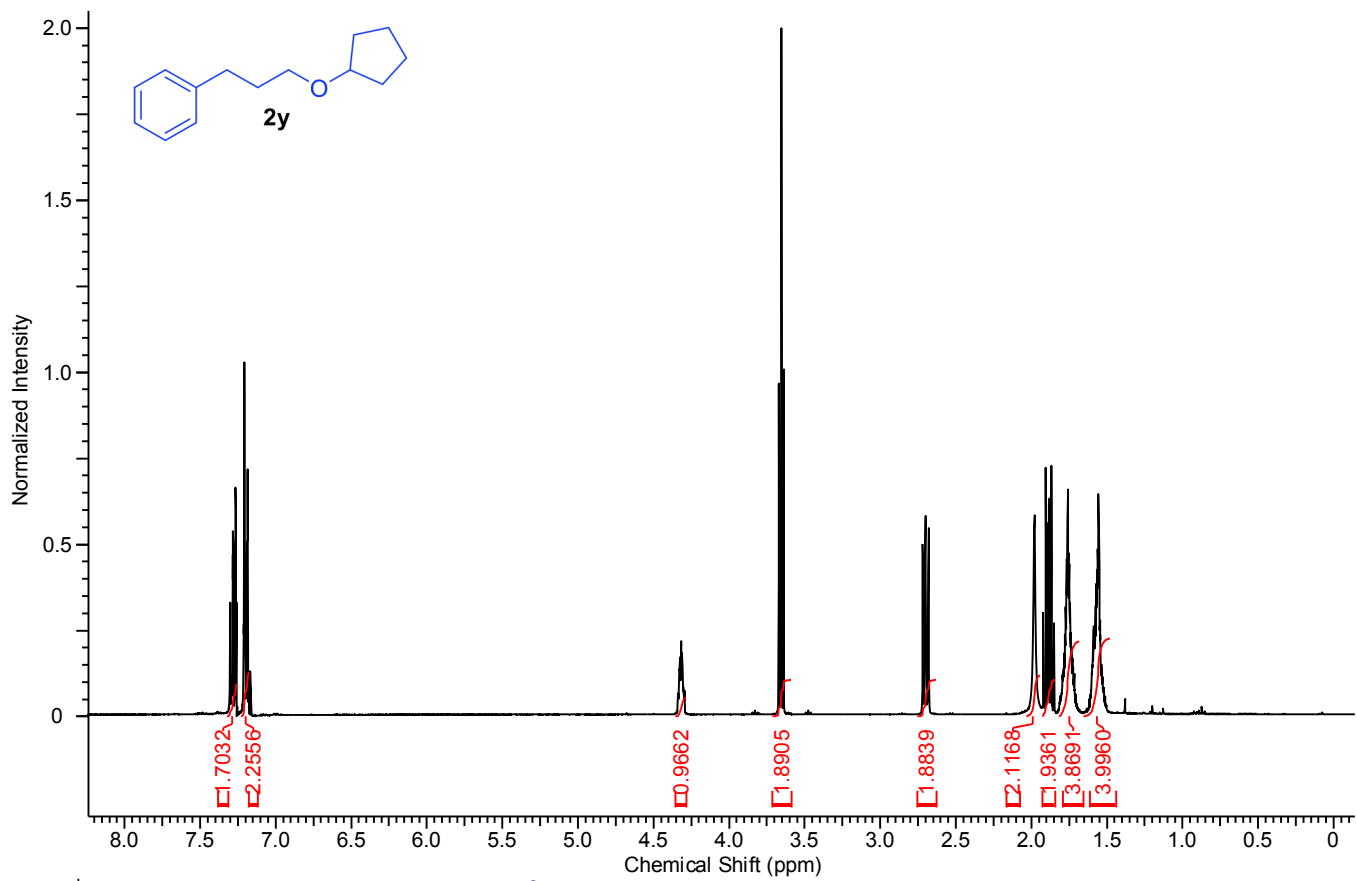


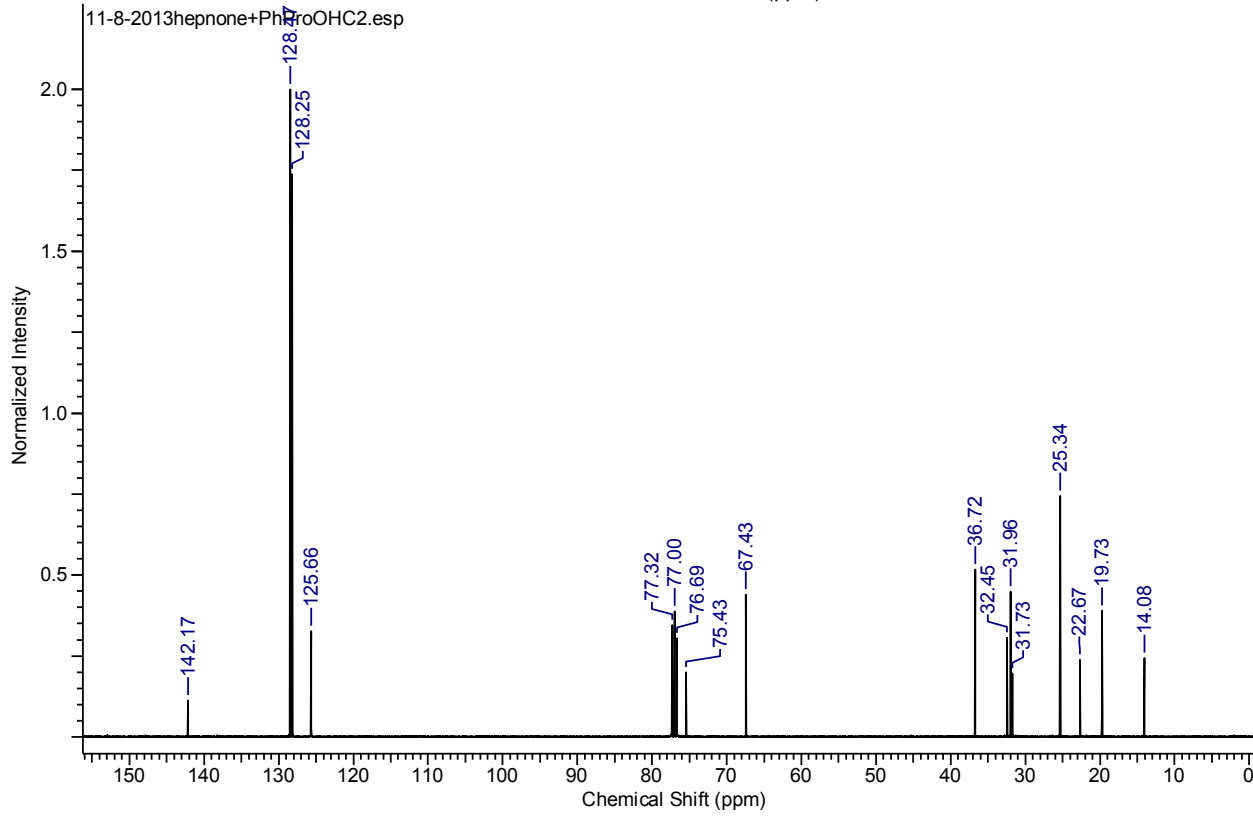
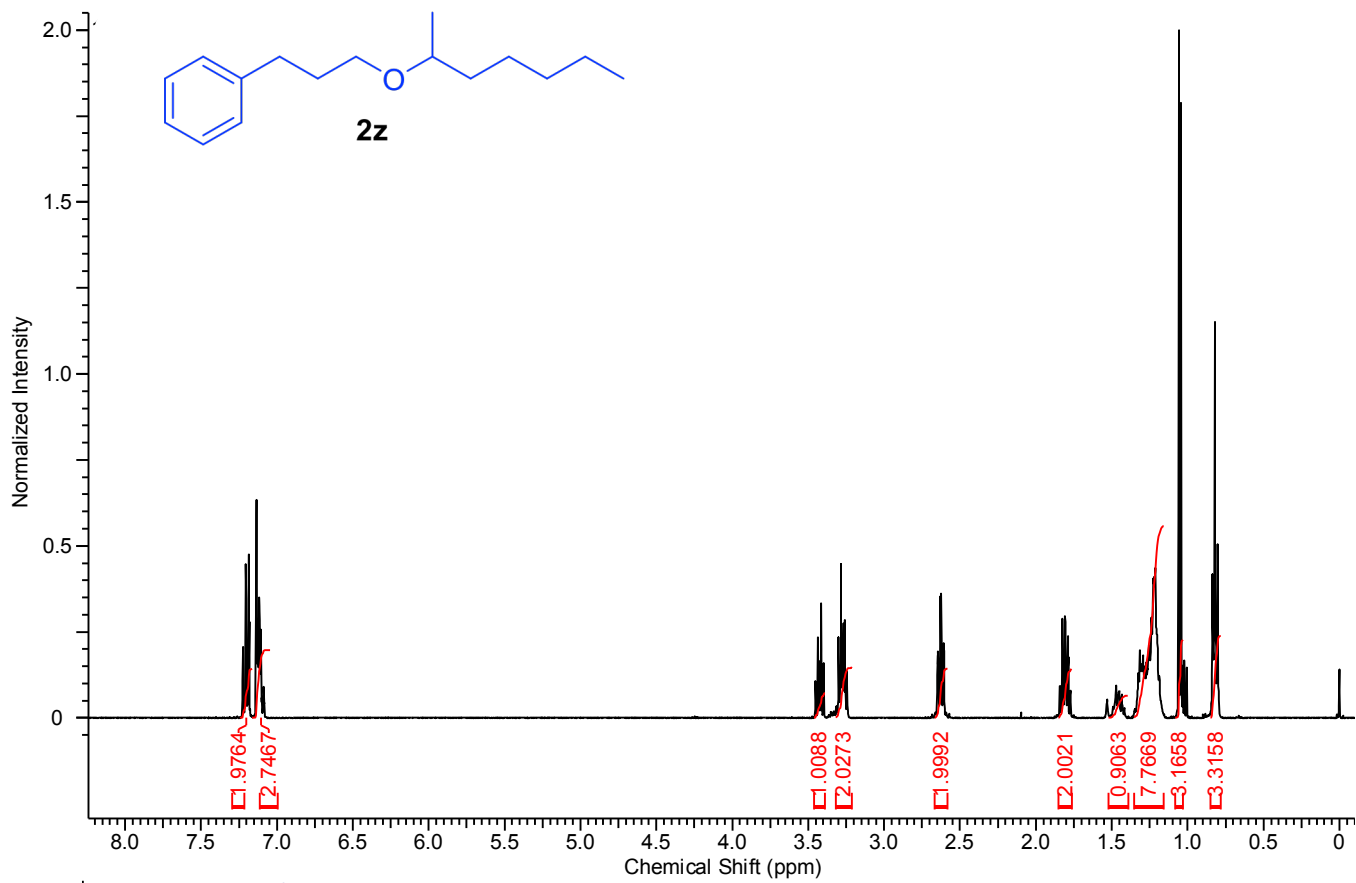


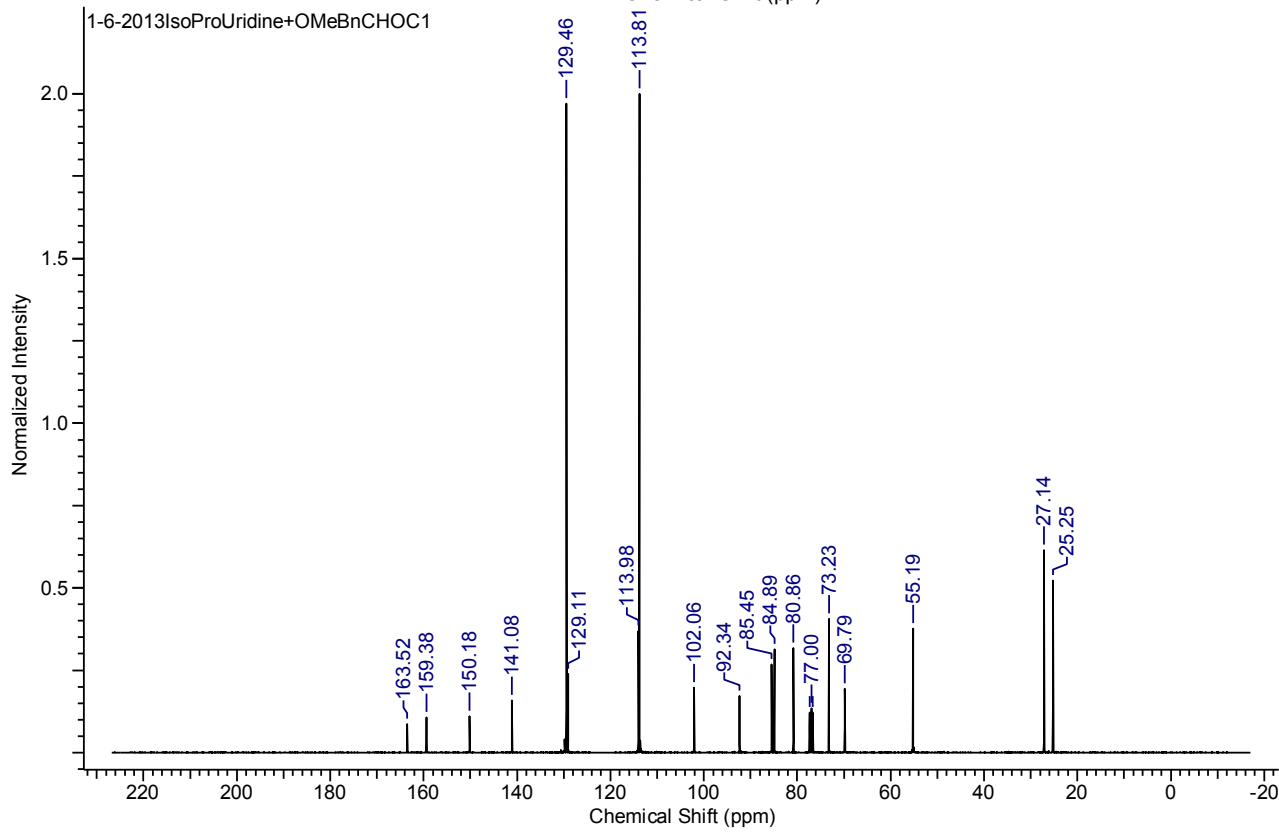
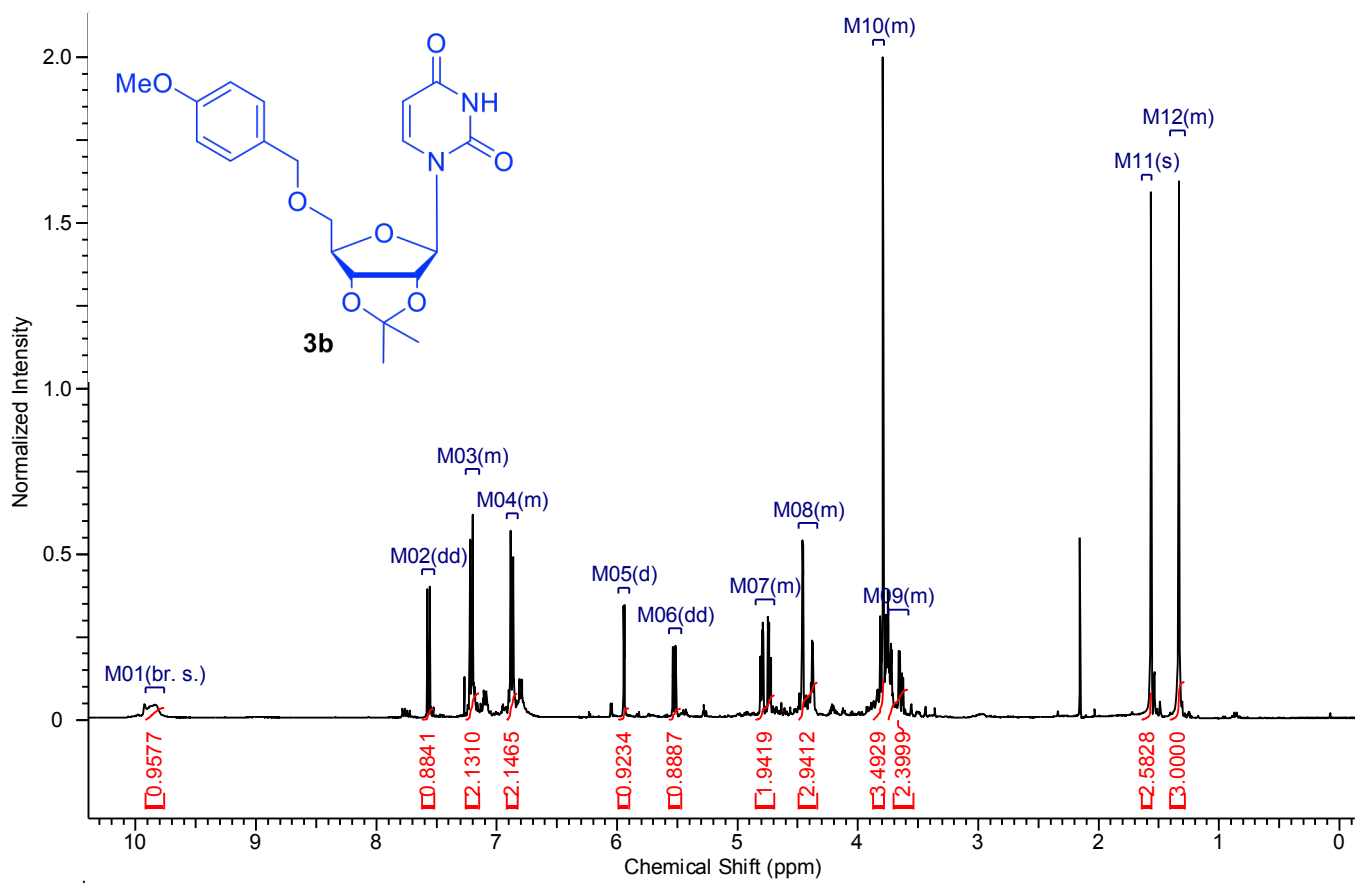


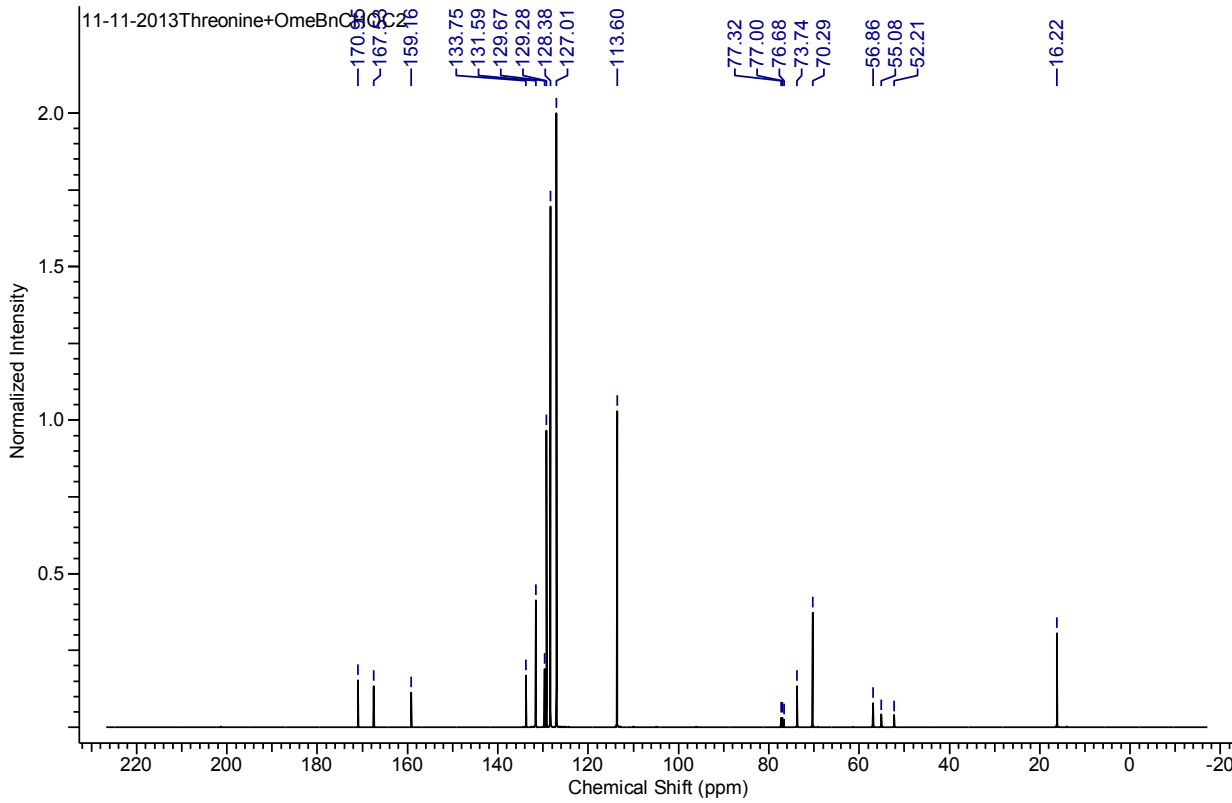
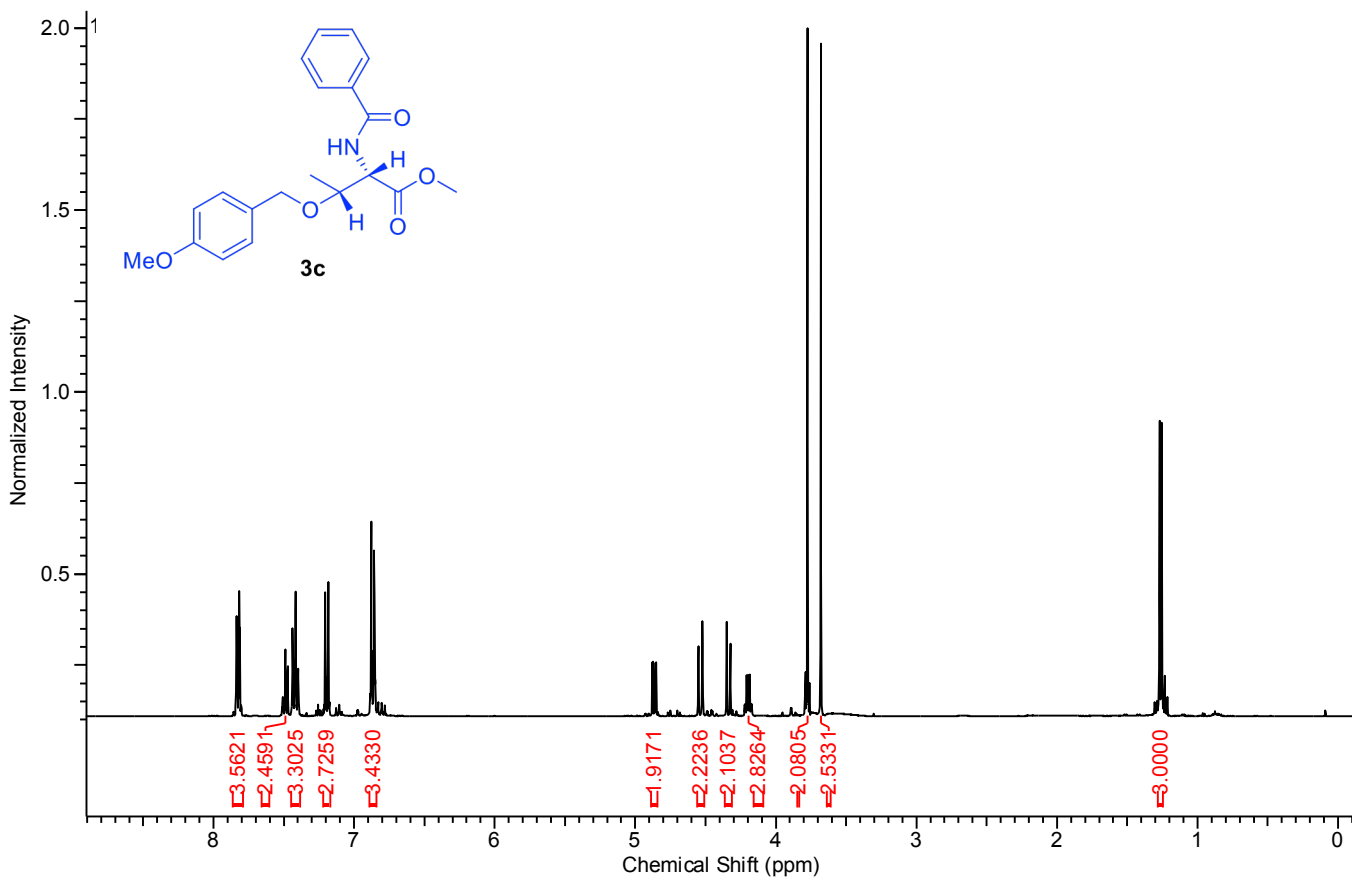


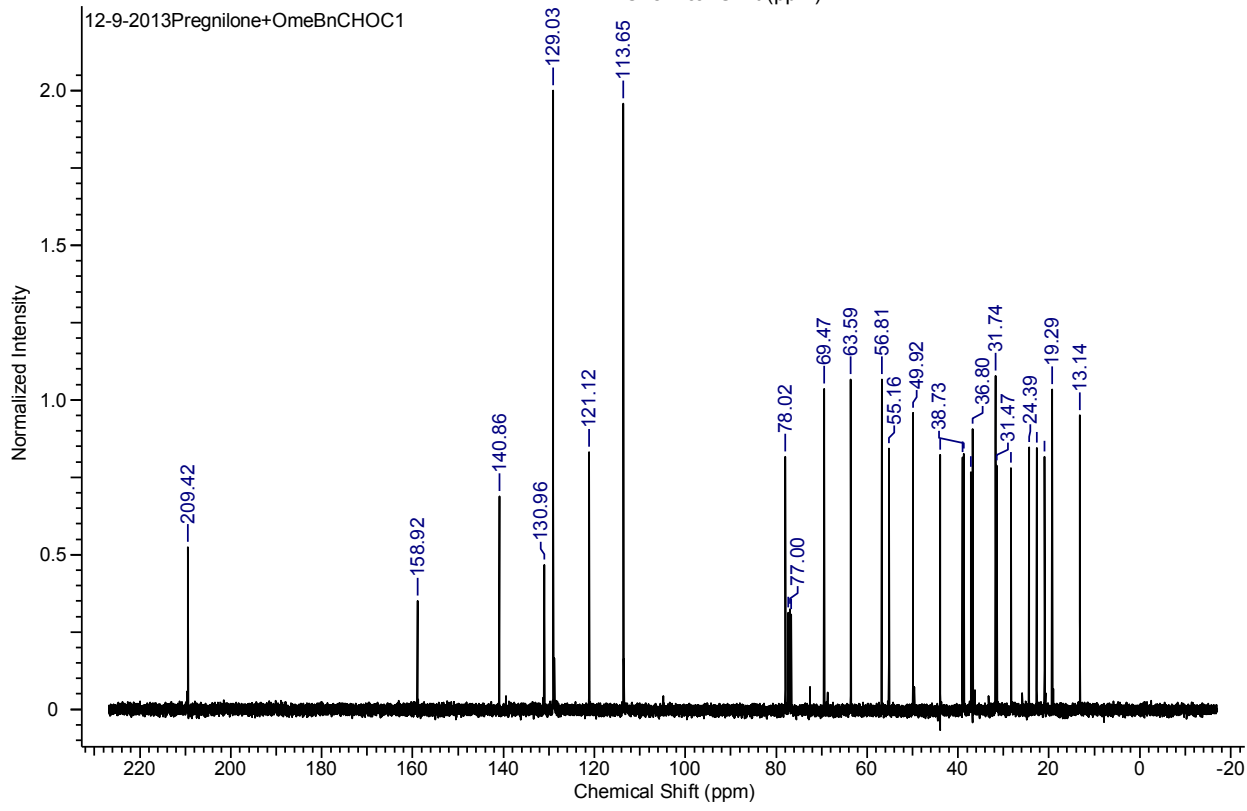
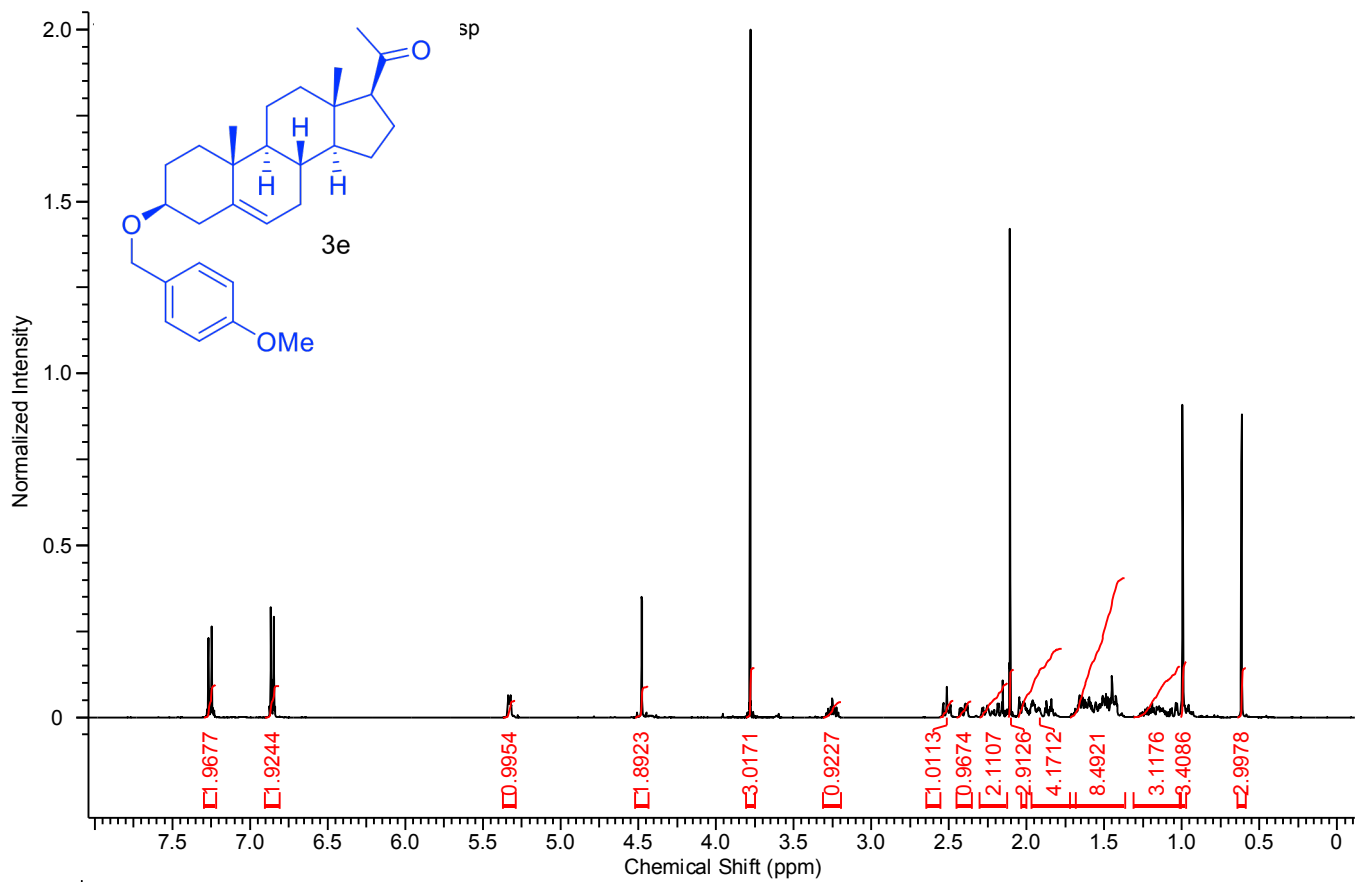


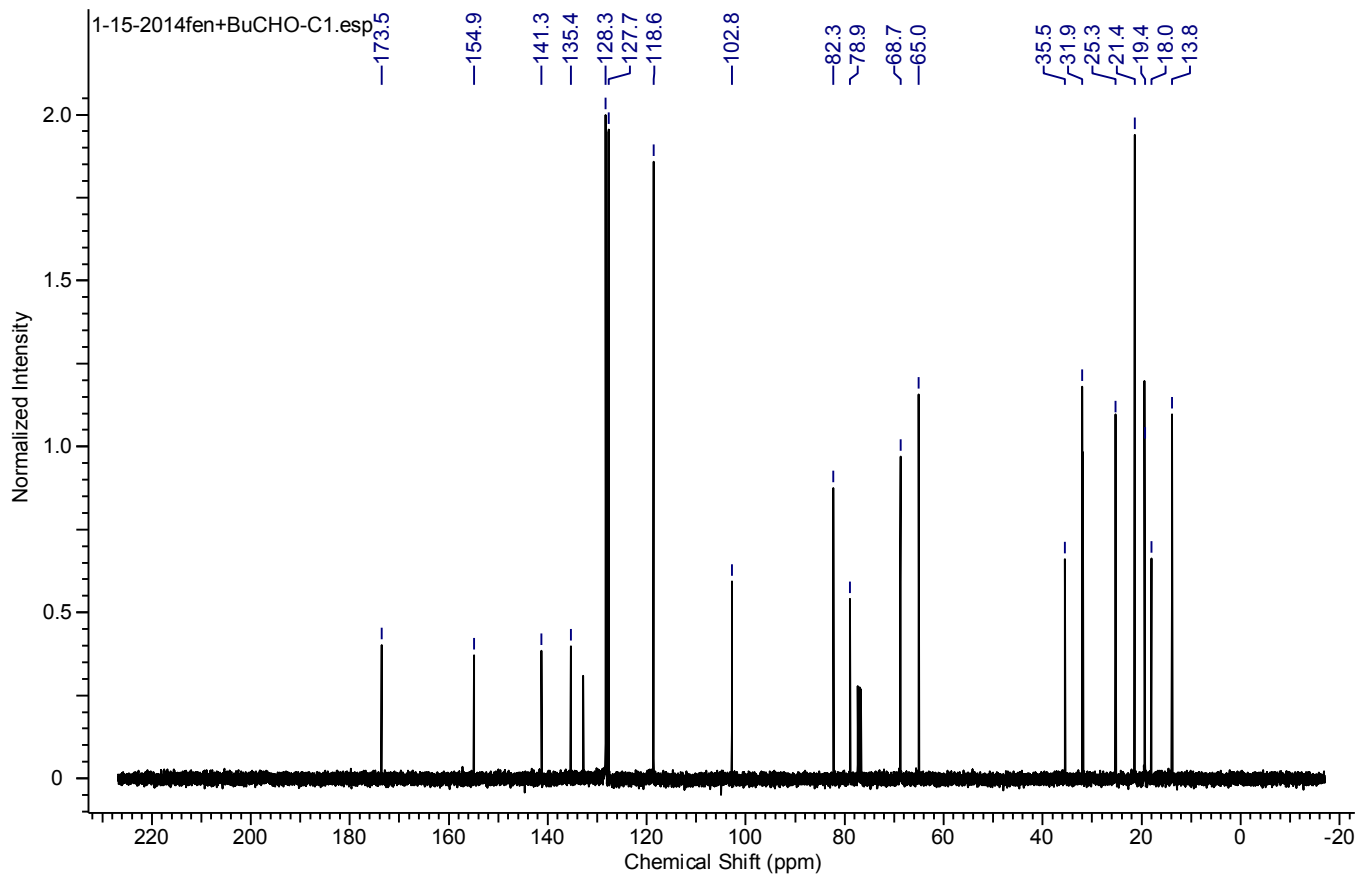
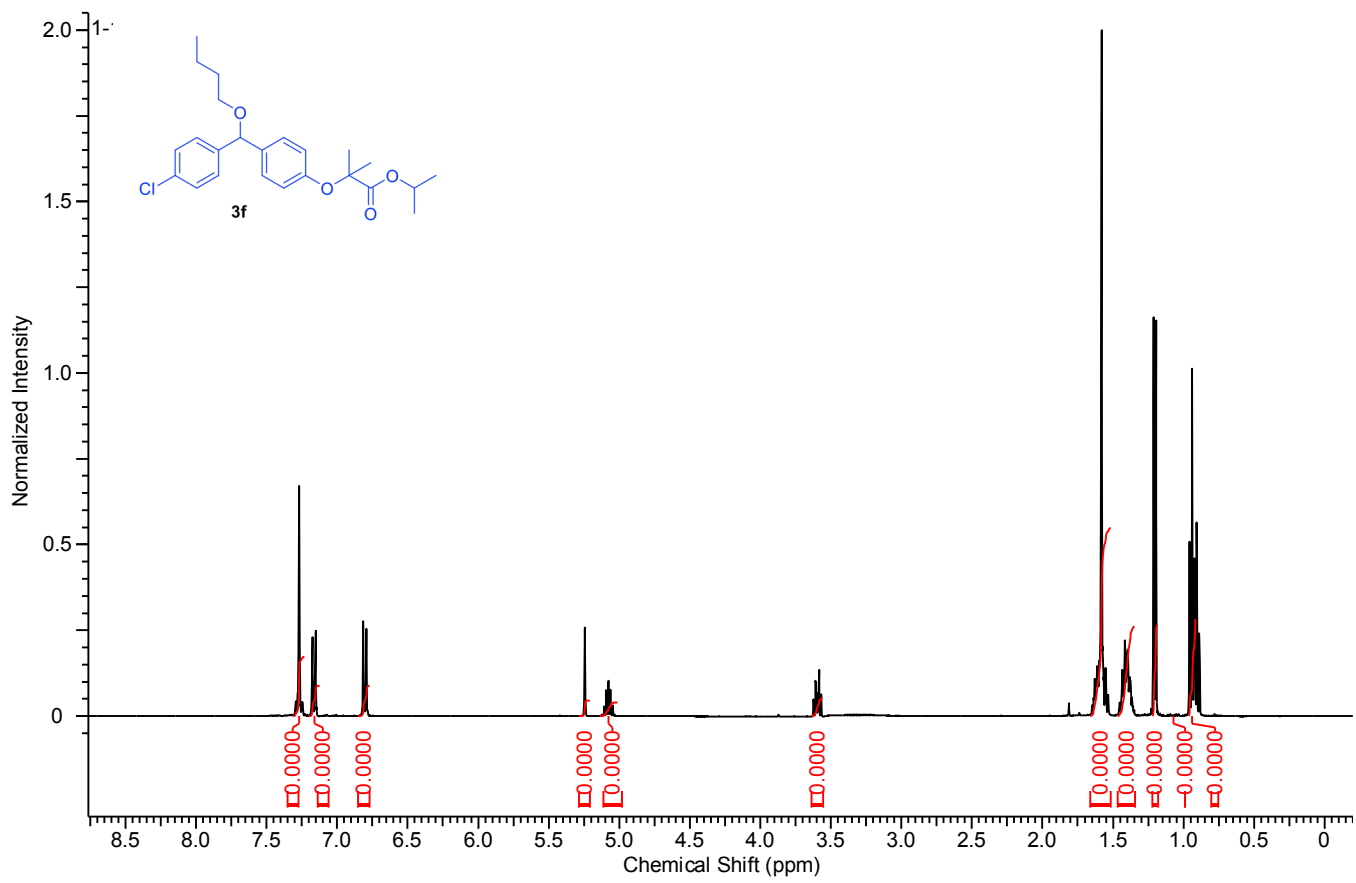


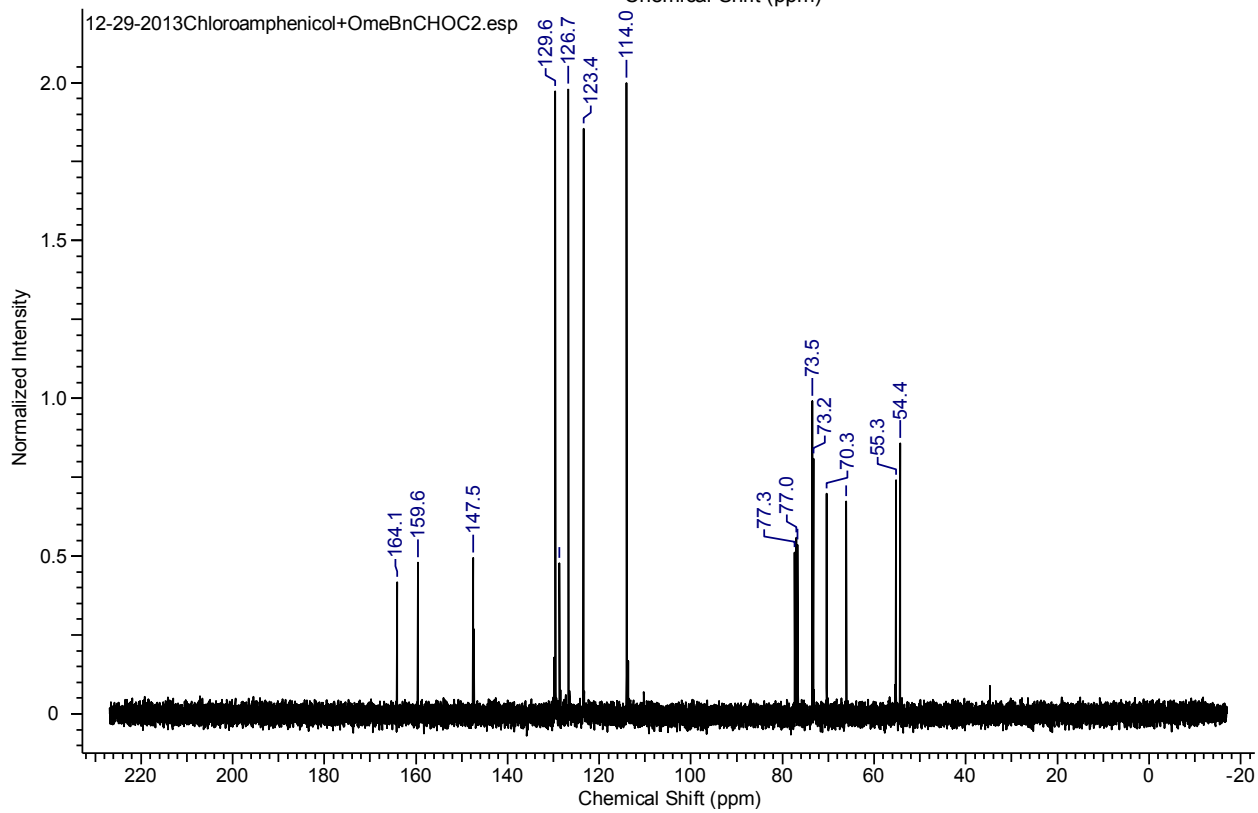
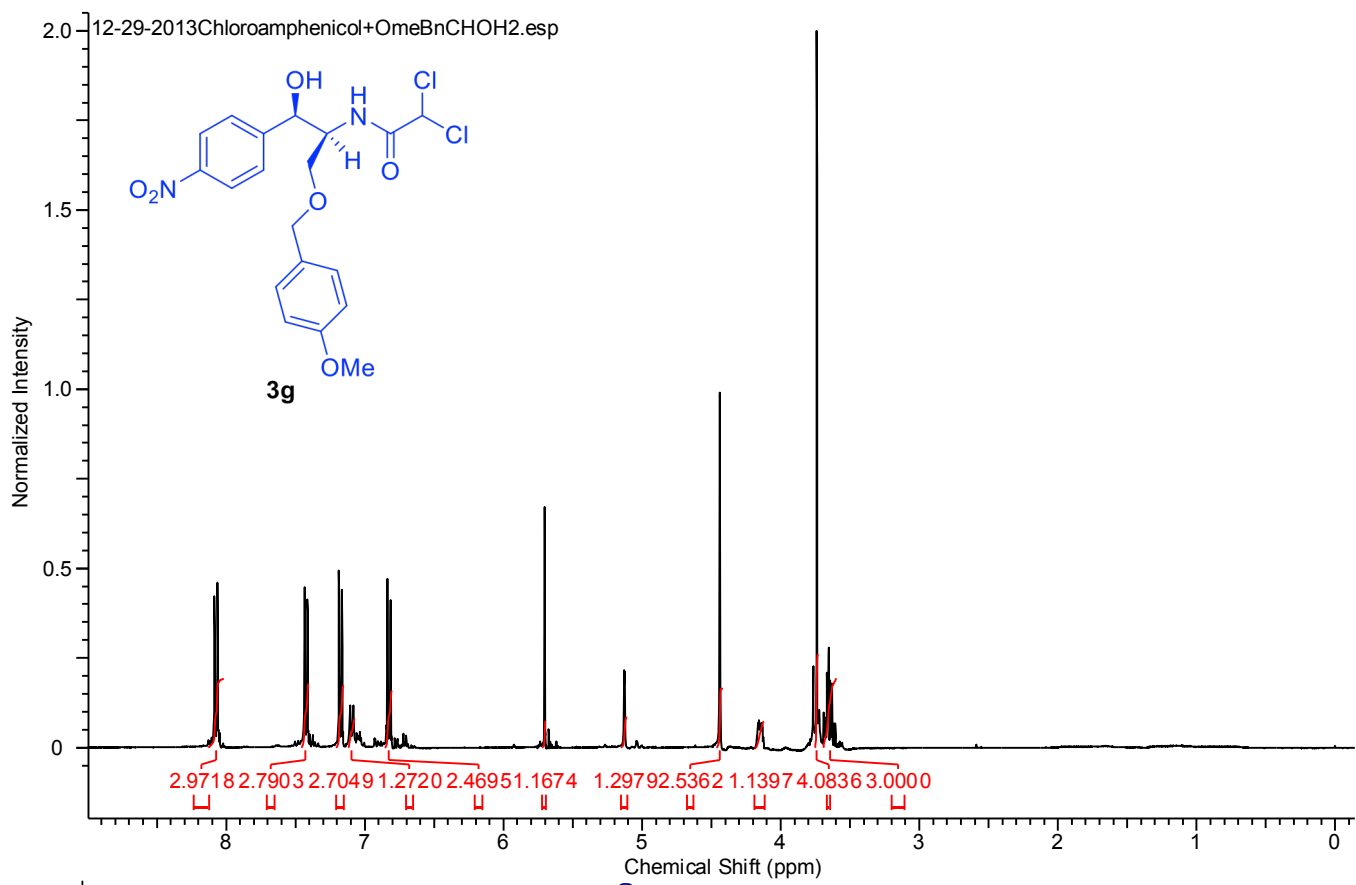


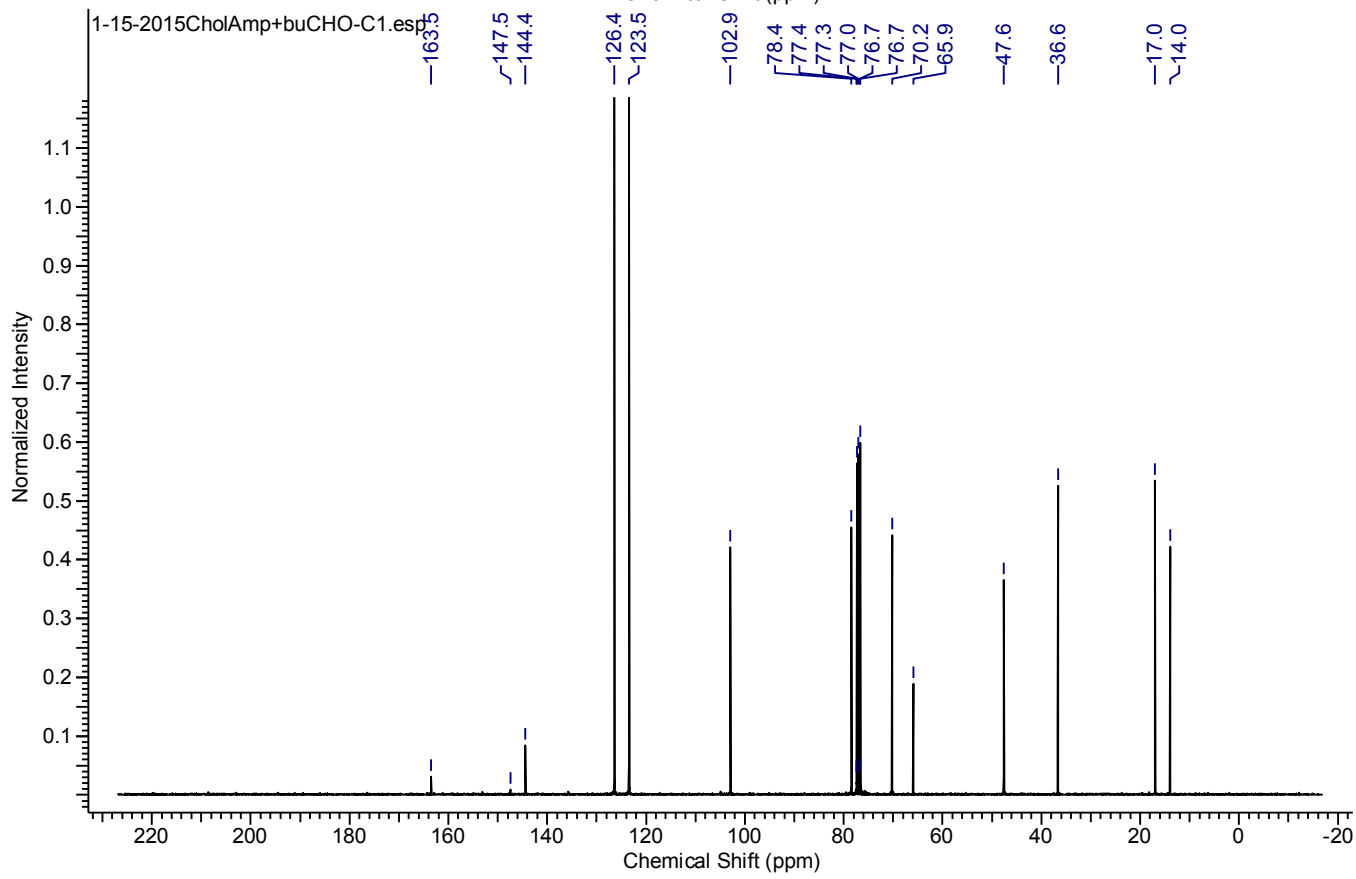
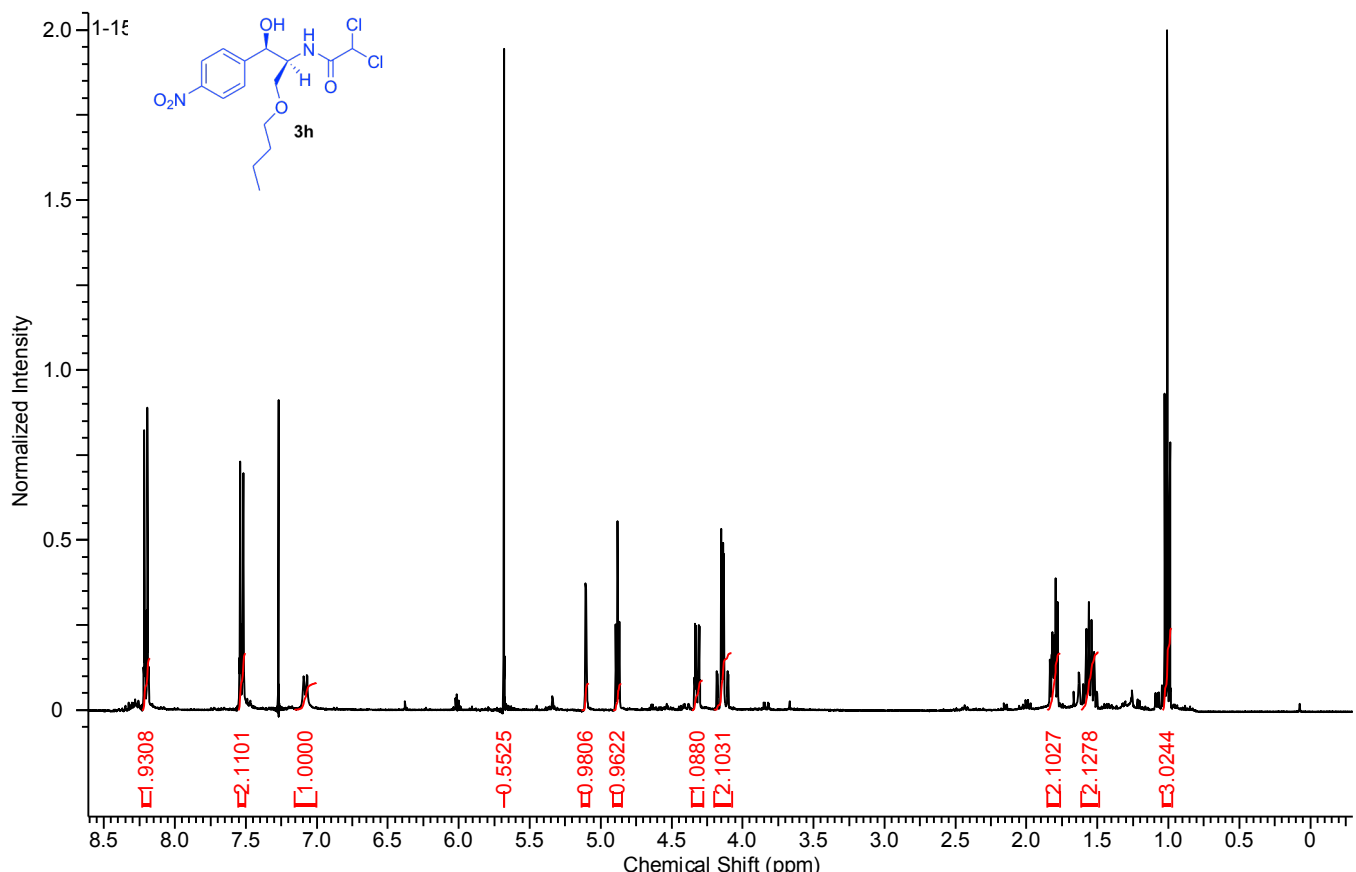


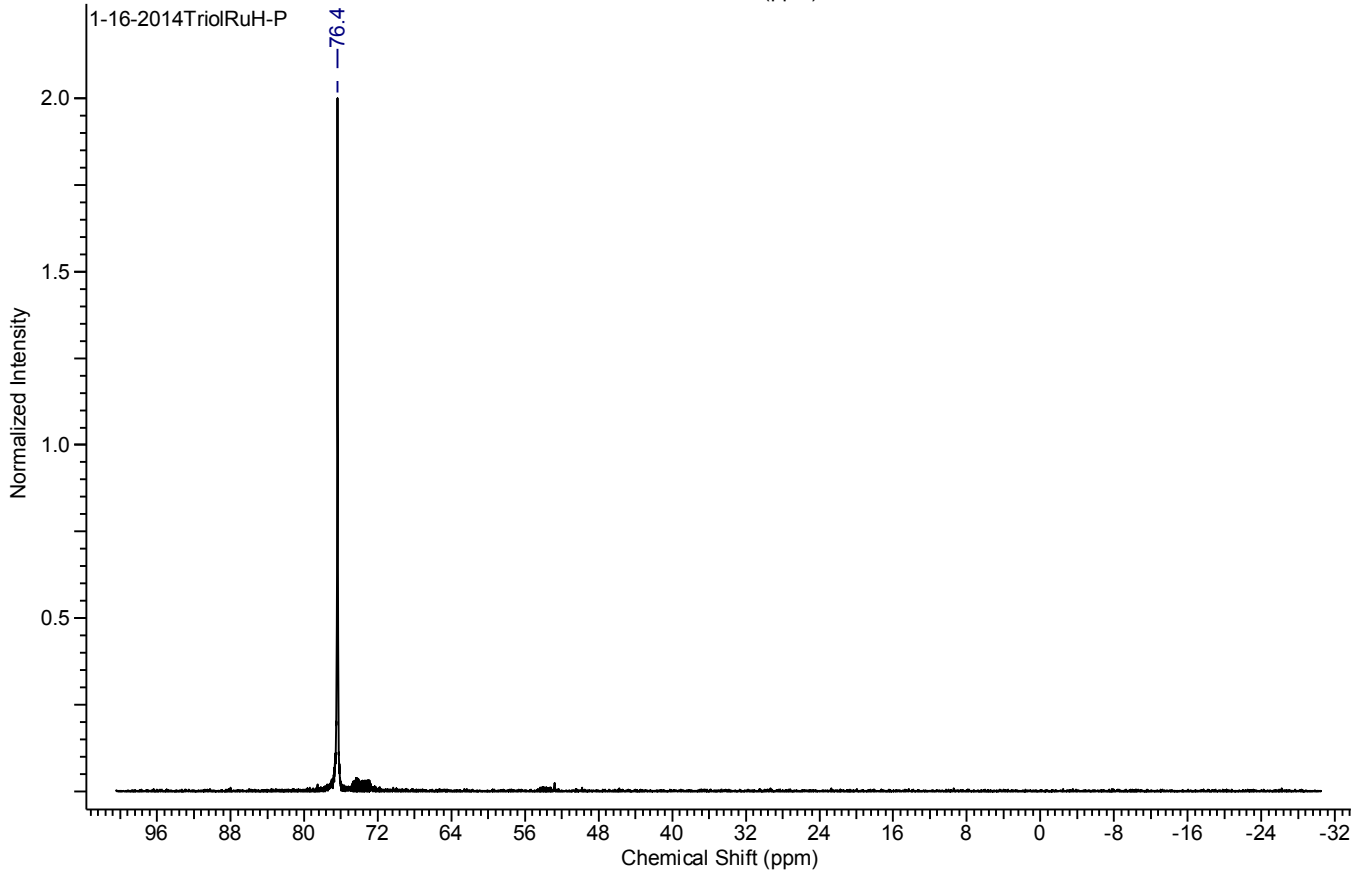
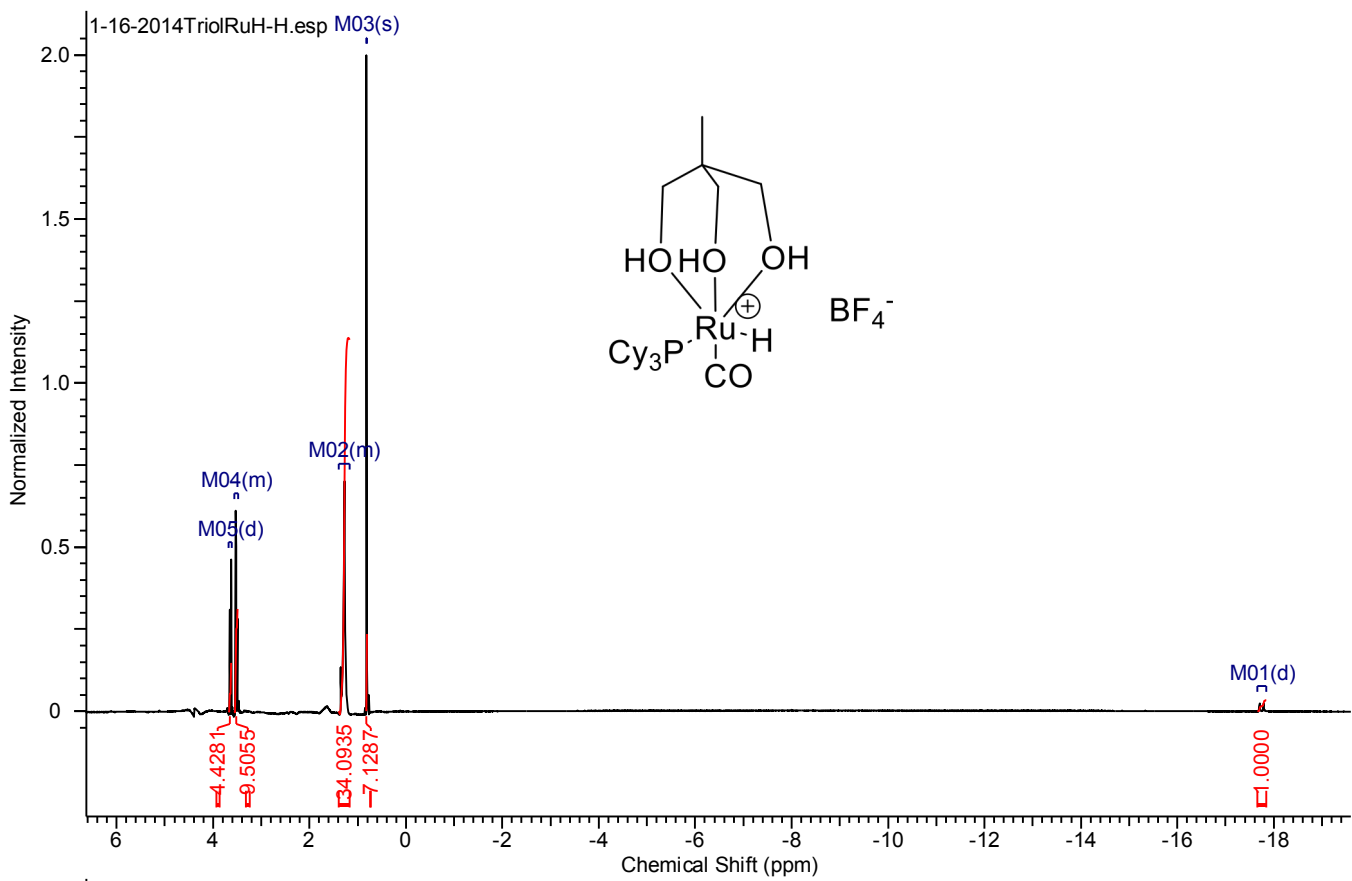












10. X-ray Crystallographic Data of 3e and 4c.

Table S8. Crystal data and structure refinement for 3e.

Identification code	yi2o
Empirical formula	C ₂₉ H ₄₀ O ₃
Formula weight	436.61
Temperature/K	100.00(10)
Crystal system	trigonal
Space group	P3 ₂
a/Å	13.48807(18)
b/Å	13.48807(18)
c/Å	11.6705(2)
α/°	90.00
β/°	90.00
γ/°	120.00
Volume/Å ³	1838.73(5)
Z	3
ρ _{calc} mg/mm ³	1.183
m/mm ⁻¹	0.578
F(000)	714.0
Crystal size/mm ³	0.42 × 0.12 × 0.05
Radiation	CuKα ($\lambda = 1.54184$)
2Θ range for data collection	7.56 to 147.18°
Index ranges	-16 ≤ h ≤ 16, -16 ≤ k ≤ 16, -10 ≤ l ≤ 14
Reflections collected	11497
Independent reflections	4347 [R _{int} = 0.0231, R _{sigma} = 0.0230]
Data/restraints/parameters	4347/274/587
Goodness-of-fit on F ²	1.053
Final R indexes [I>=2σ (I)]	R ₁ = 0.0281, wR ₂ = 0.0734
Final R indexes [all data]	R ₁ = 0.0282, wR ₂ = 0.0736
Largest diff. peak/hole / e Å ⁻³	0.08/-0.10
Flack parameter	-0.09(18)

Table S9. Fractional Atomic Coordinates ($\times 10^4$) and Equivalent Isotropic Displacement Parameters ($\text{\AA}^2 \times 10^3$) for 3e. U_{eq} is defined as 1/3 of the trace of the orthogonalised U_{IJ} tensor.

Atom	x	y	z	U(eq)
O1	5425.6(13)	5635.9(14)	3706.1(14)	35.0(4)
O2	9146(2)	7728(2)	-6082(3)	51.1(6)
O3	3876.0(16)	4818.0(17)	8877.2(16)	45.6(4)
C1	6147.7(19)	7093.9(19)	805(2)	35.9(5)
C2	5954(2)	6983(2)	2099(2)	37.5(5)
C3	5576.2(19)	5762.8(19)	2498(2)	33.0(5)
C4	6500.1(19)	5480.1(19)	2169.7(19)	32.5(5)
C5	6746(5)	5619(4)	884(4)	28.6(9)
C6	6691.3(19)	4764.5(18)	278(2)	33.1(5)
C7	6921(2)	4809.4(18)	-979(2)	34.3(5)
C8	7517.4(16)	6031.8(17)	-1456.4(19)	28.1(4)
C9	6981.9(17)	6709.5(17)	-943(2)	29.5(4)
C10	7044.4(16)	6778.2(17)	379.4(19)	29.1(4)
C11	7477(2)	7893.4(18)	-1518.4(19)	33.4(5)
C12	7427(2)	7854.2(19)	-2830(2)	34.5(5)
C13	7994.7(18)	7208.5(17)	-3314.2(19)	29.1(4)
C14	7410.8(17)	6016.2(16)	-2749.7(19)	29.8(4)
C15	7815.3(19)	5336.6(19)	-3460(2)	35.2(5)
C16	7867(2)	5772(2)	-4698(2)	40.1(5)
C17	7747.4(19)	6850.8(19)	-4599(2)	35.0(5)
C18	8247(2)	7684.0(19)	806(2)	37.2(5)
C19	9290(3)	7886(4)	-3129(4)	34.8(8)
C20	8444(2)	7778(2)	-5457(2)	40.1(5)
C21	8244(3)	8776(2)	-5541(2)	49.6(6)
C22	4416(2)	5614(3)	4096(2)	44.8(6)
C23	4298(5)	5403(6)	5373(5)	40.7(11)
C24	4328.4(19)	6206(2)	6125(2)	39.0(5)
C25	4192(2)	5994(2)	7291(2)	38.3(5)
C26	4012(5)	4964(5)	7701(5)	39.3(10)
C27	3983(2)	4136(2)	6967(2)	39.2(5)
C28	4119(2)	4372(2)	5799(2)	40.5(5)
C29	3592(2)	3730(3)	9346(2)	47.8(6)
O1A	7865(3)	6902(3)	-1698(3)	38.3(8)
O2A	4063(9)	5155(9)	8007(8)	66(3)

O3A	9386(3)	7584(4)	-6864(3)	50.8(10)
C1A	7125(5)	7595(4)	1202(4)	40.2(11)
C2A	7316(5)	7694(4)	-88(5)	42.6(12)
C3A	7683(5)	6855(4)	-492(4)	38.4(11)
C4A	6774(5)	5636(4)	-173(5)	42.2(12)
C5A	6525(11)	5517(9)	1128(10)	32(2)
C6A	6584(4)	4720(4)	1693(5)	39.2(11)
C7A	6353(5)	4517(4)	2947(5)	41.0(12)
C8A	5748(4)	5128(4)	3455(4)	34.6(10)
C9A	6308(4)	6353(4)	2962(4)	35.4(10)
C10A	6226(4)	6375(4)	1618(4)	35.9(11)
C11A	5846(5)	7066(5)	3533(4)	39.9(11)
C12A	5903(4)	7058(4)	4854(4)	34.5(10)
C13A	5316(4)	5836(4)	5324(4)	36.8(10)
C14A	5871(4)	5208(4)	4753(4)	34.5(10)
C15A	5442(5)	4112(4)	5459(4)	40.3(11)
C16A	5394(6)	4490(5)	6687(5)	47.4(13)
C17A	5550(4)	5704(4)	6608(4)	36.9(10)
C18A	5022(4)	6077(5)	1214(5)	40.2(11)
C19A	4042(8)	5249(11)	5119(10)	34(2)
C20A	4822(6)	5931(5)	7449(5)	46.9(13)
C21A	5096(6)	7159(5)	7564(5)	55.6(15)
C22A	8845(5)	7918(5)	-2072(5)	52.2(14)
C23A	8955(7)	7802(9)	-3339(8)	43(2)
C24A	9004(4)	8614(5)	-4119(5)	40.4(11)
C25A	9139(5)	8502(6)	-5274(5)	46.6(13)
C26A	9309(7)	7663(8)	-5650(5)	47(2)
C27A	9281(5)	6830(5)	-4930(5)	46.1(12)
C28A	9137(5)	6944(5)	-3779(4)	42.5(11)
C29A	9681(5)	6786(6)	-7293(5)	50.9(14)

Table S10. Anisotropic Displacement Parameters ($\text{\AA}^2 \times 10^3$) for 3e. The Anisotropic displacement factor exponent takes the form: $-2\pi^2[\mathbf{h}^2\mathbf{a}^{*2}\mathbf{U}_{11}+2\mathbf{h}\mathbf{k}\mathbf{a}^{*}\mathbf{b}^{*}\mathbf{U}_{12}+\dots]$.

Atom	\mathbf{U}_{11}	\mathbf{U}_{22}	\mathbf{U}_{33}	\mathbf{U}_{23}	\mathbf{U}_{13}	\mathbf{U}_{12}
O1	30.5(7)	38.8(9)	40.0(9)	3.9(7)	3.6(7)	20.6(7)
O2	45.0(14)	41.8(11)	61.0(19)	6.8(12)	15.6(14)	17.5(10)

O3	38.3(9)	45(1)	42.8(11)	-1.0(8)	8.5(8)	12.8(8)
C1	36.2(12)	34.3(11)	43.5(13)	3.8(10)	1.9(9)	22.4(10)
C2	43.5(12)	35.5(11)	41.3(13)	4.2(10)	5.3(10)	25.5(10)
C3	31.0(11)	32.8(11)	37.9(12)	3.2(9)	1.8(10)	18(1)
C4	30.5(10)	28(1)	38.6(14)	6.8(9)	5.6(9)	14.3(8)
C5	24(2)	29.0(16)	33(2)	6.6(12)	6.7(14)	14.0(16)
C6	31.6(10)	22.1(9)	46.1(13)	7.0(8)	6.7(9)	13.9(8)
C7	33.4(11)	22.8(10)	46.1(13)	2.7(8)	4.4(9)	13.7(8)
C8	23.2(9)	22.2(10)	38.5(12)	3.1(8)	1.9(8)	11.0(8)
C9	23.9(9)	22.9(9)	41.1(12)	1.7(8)	-0.2(9)	11.1(7)
C10	26.7(9)	21.2(9)	37.5(11)	2.5(8)	2.0(8)	10.6(8)
C11	39.4(11)	23.7(9)	37.8(12)	2.4(9)	2.9(9)	16.3(9)
C12	33.9(11)	25.6(10)	43.9(13)	3.9(9)	2.6(9)	14.9(8)
C13	25.6(11)	21.3(9)	36.9(12)	2.7(8)	1.7(8)	9.0(9)
C14	21.4(9)	22.8(9)	43.1(12)	2.0(9)	1.7(8)	9.5(8)
C15	32.2(10)	26.1(10)	45.1(13)	1.8(9)	5.1(9)	13.0(9)
C16	44.6(13)	31.6(11)	43.8(13)	-2.2(10)	2.3(10)	18.9(10)
C17	33.2(10)	28.9(10)	41.8(13)	-0.7(9)	2.6(9)	14.8(9)
C18	34.3(11)	29.3(10)	43.1(12)	1.1(9)	-2.0(9)	12.2(9)
C19	17.2(17)	27.1(13)	46.3(19)	3.8(13)	2.8(13)	0.7(14)
C20	40.6(14)	33.4(12)	42.2(13)	2.4(10)	3.1(11)	15.5(11)
C21	70.9(19)	41.0(13)	41.5(13)	5.5(11)	9.9(13)	31.3(13)
C22	38.9(12)	61.1(16)	44.5(14)	3.0(12)	4.7(11)	32.5(12)
C23	31(2)	51(3)	42(2)	-1.9(17)	0.4(16)	22(2)
C24	27.9(10)	33.6(11)	52.5(14)	-2.1(10)	1.3(9)	13.1(9)
C25	29.2(11)	33.6(11)	46.0(14)	-6.8(10)	2.2(10)	11.1(9)
C26	27.1(15)	43.0(16)	40(2)	-1.0(14)	7.6(14)	11.7(12)
C27	34.7(11)	37.0(12)	46.2(13)	1.6(10)	3.6(10)	18(1)
C28	40.6(12)	42.9(12)	45.1(13)	-6.4(10)	0.5(10)	26.1(11)
C29	39.2(13)	55.3(17)	43.8(15)	9.2(12)	2.4(11)	19.8(13)
O1A	37.3(17)	33.2(18)	37.8(19)	-0.1(14)	7.0(14)	12.6(15)
O2A	65(5)	78(6)	68(6)	31(5)	40(4)	46(4)
O3A	38.1(19)	78(3)	31(2)	5.6(19)	6.8(16)	25(2)
C1A	48(3)	27(2)	46(3)	0.6(18)	8(2)	19(2)
C2A	51(3)	33(2)	42(3)	3(2)	8(2)	19(2)
C3A	45(3)	28(2)	36(3)	3.3(19)	2(2)	13.9(19)
C4A	43(3)	32(2)	53(3)	-8(2)	8(2)	20(2)

C5A	20(4)	24(3)	51(5)	3(3)	14(3)	10(3)
C6A	37(2)	35(2)	49(3)	-7(2)	7(2)	20.6(19)
C7A	42(3)	39(2)	45(3)	6(2)	9(2)	22(2)
C8A	27(2)	32(2)	45(3)	0.4(19)	1.6(19)	14.8(18)
C9A	29(2)	39(2)	39(2)	-1(2)	4(2)	17(2)
C10A	35(2)	29(2)	42(3)	0.6(19)	6(2)	15.0(19)
C11A	49(3)	39(2)	39(3)	-1(2)	2(2)	27(2)
C12A	40(2)	34(2)	32(2)	-3.7(18)	2.9(19)	20.7(19)
C13A	30(2)	34(2)	45(3)	-1(2)	-1(2)	15(2)
C14A	24(2)	33(2)	47(3)	2.4(19)	3.3(18)	14.7(18)
C15A	38(2)	39(2)	45(3)	5(2)	4(2)	20(2)
C16A	57(3)	49(3)	46(3)	6(2)	9(2)	34(3)
C17A	35(2)	46(3)	39(3)	1(2)	4.7(19)	27(2)
C18A	33(2)	42(3)	48(3)	1(2)	3(2)	20(2)
C19A	25(4)	35(3)	48(6)	-5(4)	3(3)	18(3)
C20A	60(4)	45(3)	47(3)	4(2)	9(3)	34(3)
C21A	81(4)	64(3)	43(3)	0(3)	11(3)	52(4)
C22A	55(3)	33(3)	46(3)	-5(2)	2(2)	5(2)
C23A	25(5)	41(3)	46(4)	-8(3)	-4(3)	3(4)
C24A	25(2)	41(3)	48(3)	-2(2)	0.8(19)	11(2)
C25A	35(3)	64(4)	47(3)	7(3)	1(2)	30(3)
C26A	32(3)	91(5)	22(3)	1(3)	-3(2)	35(3)
C27A	35(2)	46(3)	52(3)	2(2)	0(2)	17(2)
C28A	43(3)	33(2)	41(3)	5(2)	3(2)	11(2)
C29A	40(3)	56(4)	38(3)	-5(2)	0(2)	10(3)

Table S11. Bond Lengths for 3e.

Atom	Atom	Length/Å	Atom	Atom	Length/Å
O1	C3	1.423(3)	O1A	C3A	1.425(5)
O1	C22	1.422(3)	O1A	C22A	1.415(6)
O2	C20	1.224(4)	O2A	C20A	1.223(10)
O3	C26	1.386(6)	O3A	C26A	1.428(6)
O3	C29	1.428(4)	O3A	C29A	1.413(8)
C1	C2	1.527(3)	C1A	C2A	1.522(6)
C1	C10	1.551(3)	C1A	C10A	1.555(6)
C2	C3	1.532(3)	C2A	C3A	1.519(7)

C3	C4		1.523(3)	C3A C4A		1.525(6)
C4	C5		1.528(5)	C4A C5A		1.546(11)
C5	C6		1.322(5)	C5A C6A		1.298(10)
C5	C10		1.525(4)	C5A C10A		1.515(9)
C6	C7		1.494(3)	C6A C7A		1.493(7)
C7	C8		1.533(3)	C7A C8A		1.540(6)
C8	C9		1.542(3)	C8A C9A		1.544(6)
C8	C14		1.515(3)	C8A C14A		1.521(6)
C9	C10		1.546(3)	C9A C10A		1.574(6)
C9	C11		1.543(3)	C9A C11A		1.535(6)
C10	C18		1.546(3)	C10A C18A		1.539(6)
C11	C12		1.532(3)	C11A C12A		1.544(6)
C12	C13		1.527(3)	C12A C13A		1.529(6)
C13	C14		1.541(3)	C13A C14A		1.534(6)
C13	C17		1.559(3)	C13A C17A		1.561(6)
C13	C19		1.529(4)	C13A C19A		1.509(9)
C14	C15		1.525(3)	C14A C15A		1.532(6)
C15	C16		1.548(3)	C15A C16A		1.533(7)
C16	C17		1.547(3)	C16A C17A		1.545(7)
C17	C20		1.508(3)	C17A C20A		1.524(7)
C20	C21		1.503(3)	C20A C21A		1.512(7)
C22	C23		1.510(6)	C22A C23A		1.502(10)
C23	C24		1.379(7)	C23A C24A		1.401(11)
C23	C28		1.380(8)	C23A C28A		1.395(11)
C24	C25		1.384(3)	C24A C25A		1.378(7)
C25	C26		1.370(7)	C25A C26A		1.335(10)
C26	C27		1.393(5)	C26A C27A		1.388(9)
C27	C28		1.391(3)	C27A C28A		1.377(7)

Table S12. Bond Angles for 3e.

Atom	Atom	Atom	Angle/ [°]	Atom	Atom	Atom	Angle/ [°]
C22	O1	C3	113.41(17)	C22A	O1A	C3A	113.8(4)
C26	O3	C29	118.3(3)	C29A	O3A	C26A	117.8(5)
C2	C1	C10	114.15(18)	C2A	C1A	C10A	114.2(4)
C1	C2	C3	110.7(2)	C3A	C2A	C1A	110.2(4)
O1	C3	C2	112.39(18)	O1A	C3A	C2A	112.7(4)

O1	C3	C4	107.72(17)	O1A C3A C4A	108.5(4)
C4	C3	C2	108.59(18)	C2A C3A C4A	109.9(4)
C3	C4	C5	111.8(2)	C3A C4A C5A	111.5(6)
C6	C5	C4	120.3(3)	C6A C5A C4A	119.0(7)
C6	C5	C10	124.0(4)	C6A C5A C10A	126.3(8)
C10	C5	C4	115.7(3)	C10AC5A C4A	114.7(7)
C5	C6	C7	124.7(2)	C5A C6A C7A	123.8(6)
C6	C7	C8	112.78(18)	C6A C7A C8A	113.5(4)
C7	C8	C9	110.31(17)	C7A C8A C9A	108.8(4)
C14	C8	C7	110.61(17)	C14AC8A C7A	110.7(4)
C14	C8	C9	109.02(16)	C14AC8A C9A	108.5(4)
C8	C9	C10	113.32(17)	C8A C9A C10A	113.0(4)
C8	C9	C11	110.85(17)	C11AC9A C8A	111.9(4)
C11	C9	C10	112.96(17)	C11AC9A C10A	111.5(4)
C5	C10	C1	108.4(2)	C1A C10AC9A	107.8(4)
C5	C10	C9	110.2(3)	C5A C10AC1A	109.0(5)
C5	C10	C18	108.7(3)	C5A C10AC9A	108.3(6)
C9	C10	C1	108.05(17)	C5A C10AC18A	109.5(7)
C18	C10	C1	109.49(19)	C18AC10AC1A	110.1(4)
C18	C10	C9	111.92(17)	C18AC10AC9A	112.0(4)
C12	C11	C9	114.23(18)	C9A C11AC12A	113.1(4)
C13	C12	C11	111.30(18)	C13AC12AC11A	111.4(4)
C12	C13	C14	107.27(16)	C12AC13AC14A	107.9(4)
C12	C13	C17	116.20(18)	C12AC13AC17A	116.2(4)
C12	C13	C19	110.9(2)	C14AC13AC17A	99.9(4)
C14	C13	C17	99.76(16)	C19AC13AC12A	110.4(6)
C19	C13	C14	113.5(2)	C19AC13AC14A	112.5(6)
C19	C13	C17	108.9(2)	C19AC13AC17A	109.5(6)
C8	C14	C13	114.58(16)	C8A C14AC13A	113.9(4)
C8	C14	C15	119.34(18)	C8A C14AC15A	119.5(4)
C15	C14	C13	104.19(17)	C15AC14AC13A	104.3(4)
C14	C15	C16	104.00(18)	C14AC15AC16A	103.9(4)
C17	C16	C15	106.26(19)	C15AC16AC17A	107.0(4)
C16	C17	C13	104.87(18)	C16AC17AC13A	104.5(4)
C20	C17	C13	115.70(19)	C20AC17AC13A	114.1(4)
C20	C17	C16	114.5(2)	C20AC17AC16A	114.5(4)
O2	C20	C17	121.9(2)	O2A C20AC17A	121.2(6)

O2	C20	C21		120.1(3)	O2A	C20A	C21A		122.1(7)
C21	C20	C17		118.0(2)	C21A	C20A	C17A		116.6(5)
O1	C22	C23		109.2(3)	O1A	C22A	C23A		107.2(5)
C24	C23	C22		121.4(5)	C24A	C23A	C22A		121.8(8)
C24	C23	C28		118.9(5)	C28A	C23A	C22A		121.1(7)
C28	C23	C22		119.7(5)	C28A	C23A	C24A		116.7(7)
C23	C24	C25		121.0(3)	C25A	C24A	C23A		120.5(6)
C26	C25	C24		119.4(3)	C26A	C25A	C24A		120.2(5)
O3	C26	C27		123.1(5)	C25A	C26A	O3A		116.0(6)
C25	C26	O3		115.7(4)	C25A	C26A	C27A		122.7(6)
C25	C26	C27		121.2(5)	C27A	C26A	O3A		120.9(7)
C28	C27	C26		118.1(3)	C28A	C27A	C26A		116.6(6)
C23	C28	C27		121.4(3)	C27A	C28A	C23A		123.0(6)

Table S13. Torsion Angles for 3e.

A	B	C	D	Angle/ [°]	A	B	C	D	Angle/ [°]
O1	C3	C4	C5	-178.7(3)	O1A	C3A	C4A	C5A	-179.7(6)
O1	C22	C23	C24	116.9(4)	O1A	C22A	C23A	C24A	124.3(7)
O1	C22	C23	C28	-65.3(5)	O1A	C22A	C23A	C28A	-62.8(9)
O3	C26	C27	C28	179.4(4)	O3A	C26A	C27A	C28A	-176.3(6)
C1	C2	C3	O1	177.92(18)	C1A	C2A	C3A	O1A	179.4(4)
C1	C2	C3	C4	58.8(3)	C1A	C2A	C3A	C4A	58.3(6)
C2	C1	C10	C5	50.1(4)	C2A	C1A	C10A	C5A	51.4(8)
C2	C1	C10	C9	169.50(18)	C2A	C1A	C10A	C9A	168.7(4)
C2	C1	C10	C18	-68.4(2)	C2A	C1A	C10A	C18A	-68.8(5)
C2	C3	C4	C5	-56.7(3)	C2A	C3A	C4A	C5A	-56.1(7)
C3	O1	C22	C23	176.5(3)	C3A	O1A	C22A	C23A	176.5(6)
C3	C4	C5	C6	-125.8(4)	C3A	C4A	C5A	C6A	-126.9(10)
C3	C4	C5	C10	54.0(5)	C3A	C4A	C5A	C10A	53.1(11)
C4	C5	C6	C7	-179.7(3)	C4A	C5A	C6A	C7A	-179.5(7)
C4	C5	C10	C1	-48.2(5)	C4A	C5A	C10A	C1A	-48.7(11)
C4	C5	C10	C9	-166.2(3)	C4A	C5A	C10A	C9A	-165.7(7)
C4	C5	C10	C18	70.8(4)	C4A	C5A	C10A	C18A	71.9(9)
C5	C6	C7	C8	14.4(4)	C5A	C6A	C7A	C8A	14.6(10)
C6	C5	C10	C1	131.6(4)	C6A	C5A	C10A	C1A	131.4(11)
C6	C5	C10	C9	13.5(6)	C6A	C5A	C10A	C9A	14.3(14)

C6 C5 C10C18	-109.5(5)	C6A C5A C10AC18A	-108.1(13)
C6 C7 C8 C9	-42.2(3)	C6A C7A C8A C9A	-43.0(6)
C6 C7 C8 C14	-162.86(17)	C6A C7A C8A C14A	-162.1(4)
C7 C8 C9 C10	58.3(2)	C7A C8A C9A C10A	59.8(5)
C7 C8 C9 C11	-173.45(18)	C7A C8A C9A C11A	-173.4(4)
C7 C8 C14C13	-179.47(18)	C7A C8A C14AC13A	178.4(4)
C7 C8 C14C15	-55.0(2)	C7A C8A C14AC15A	-57.5(5)
C8 C9 C10C1	-160.98(17)	C8A C9A C10AC1A	-162.2(4)
C8 C9 C10C5	-42.7(3)	C8A C9A C10AC5A	-44.4(7)
C8 C9 C10C18	78.4(2)	C8A C9A C10AC18A	76.4(5)
C8 C9 C11C12	51.6(2)	C8A C9A C11AC12A	51.9(5)
C8 C14C15C16	-165.82(18)	C8A C14AC15AC16A	-164.5(4)
C9 C8 C14C13	59.1(2)	C9A C8A C14AC13A	59.1(5)
C9 C8 C14C15	-176.44(17)	C9A C8A C14AC15A	-176.8(4)
C9 C11C12C13	-54.2(2)	C9A C11AC12AC13A	-53.5(6)
C10C1 C2 C3	-57.6(3)	C10AC1A C2A C3A	-57.4(6)
C10C5 C6 C7	0.6(7)	C10AC5A C6A C7A	0.4(17)
C10C9 C11C12	-179.97(16)	C10AC9A C11AC12A	179.5(4)
C11C9 C10C1	71.9(2)	C11AC9A C10AC1A	70.7(5)
C11C9 C10C5	-169.8(3)	C11AC9A C10AC5A	-171.5(6)
C11C9 C10C18	-48.7(2)	C11AC9A C10AC18A	-50.7(5)
C11C12C13C14	55.1(2)	C11AC12AC13AC14A	55.5(5)
C11C12C13C17	165.69(17)	C11AC12AC13AC17A	166.6(4)
C11C12C13C19	-69.2(3)	C11AC12AC13AC19A	-67.9(7)
C12C13C14C8	-60.4(2)	C12AC13AC14AC8A	-60.7(5)
C12C13C14C15	167.41(19)	C12AC13AC14AC15A	167.3(4)
C12C13C17C16	-152.53(19)	C12AC13AC17AC16A	-153.3(4)
C12C13C17C20	80.3(2)	C12AC13AC17AC20A	81.0(6)
C13C14C15C16	-36.5(2)	C13AC14AC15AC16A	-35.9(5)
C13C17C20O2	113.9(3)	C13AC17AC20AO2A	110.0(9)
C13C17C20C21	-66.9(3)	C13AC17AC20AC21A	-70.6(7)
C14C8 C9 C10	179.97(15)	C14AC8A C9A C10A	-179.7(3)
C14C8 C9 C11	-51.8(2)	C14AC8A C9A C11A	-52.8(5)
C14C13C17C16	-37.7(2)	C14AC13AC17AC16A	-37.5(5)
C14C13C17C20	-164.88(18)	C14AC13AC17AC20A	-163.3(4)
C14C15C16C17	12.0(2)	C14AC15AC16AC17A	11.4(6)
C15C16C17C13	16.4(2)	C15AC16AC17AC13A	16.6(6)

C15 C16 C17 C20	144.3(2)	C15A C16A C17A C20A	142.1(5)
C16 C17 C20 O2	-8.3(4)	C16A C17A C20A O2A	-10.3(10)
C16 C17 C20 C21	170.9(2)	C16A C17A C20A C21A	169.1(5)
C17 C13 C14 C8	178.07(16)	C17A C13A C14A C8A	177.4(4)
C17 C13 C14 C15	45.9(2)	C17A C13A C14A C15A	45.5(4)
C19 C13 C14 C8	62.4(3)	C19A C13A C14A C8A	61.3(7)
C19 C13 C14 C15	-69.8(3)	C19A C13A C14A C15A	-70.6(7)
C19 C13 C17 C16	81.4(3)	C19A C13A C17A C16A	80.8(7)
C19 C13 C17 C20	-45.8(3)	C19A C13A C17A C20A	-45.0(7)
C22 O1 C3 C2	74.1(2)	C22A O1A C3A C2A	70.2(6)
C22 O1 C3 C4	-166.3(2)	C22A O1A C3A C4A	-167.9(5)
C22 C23 C24 C25	178.4(3)	C22A C23A C24A C25A	178.0(6)
C22 C23 C28 C27	-178.7(3)	C22A C23A C28A C27A	-177.8(6)
C23 C24 C25 C26	-0.8(5)	C23A C24A C25A C26A	-4.9(9)
C24 C23 C28 C27	-0.8(6)	C24A C23A C28A C27A	-4.5(10)
C24 C25 C26 O3	-179.5(3)	C24A C25A C26A O3A	177.2(5)
C24 C25 C26 C27	1.2(6)	C24A C25A C26A C27A	4.5(11)
C25 C26 C27 C28	-1.4(6)	C25A C26A C27A C28A	-3.9(10)
C26 C27 C28 C23	1.2(5)	C26A C27A C28A C23A	3.9(9)
C28 C23 C24 C25	0.6(6)	C28A C23A C24A C25A	4.8(9)
C29 O3 C26 C25	174.9(3)	C29A O3A C26A C25A	173.7(6)
C29 O3 C26 C27	-5.8(6)	C29A O3A C26A C27A	-13.4(9)

Table S14. Hydrogen Atom Coordinates ($\text{\AA} \times 10^4$) and Isotropic Displacement Parameters ($\text{\AA}^2 \times 10^3$) for 3e.

Atom	x	y	z	U(eq)
H1A	6401	7893	578	43
H1B	5410	6592	417	43
H2A	5358	7178	2303	45
H2B	6671	7529	2496	45
H3	4843	5214	2109	40
H4A	6251	4682	2396	39
H4B	7212	5991	2594	39
H6	6491	4072	670	40
H7A	6187	4345	-1388	41
H7B	7407	4465	-1128	41
H8	8347	6422	-1246	34

H9	6150	6275	-1145	35
H11A	7050	8266	-1238	40
H11B	8285	8375	-1278	40
H12A	6618	7473	-3081	41
H12B	7819	8645	-3135	41
H14	6575	5670	-2914	36
H15A	7268	4505	-3405	42
H15B	8579	5490	-3204	42
H16A	8605	5964	-5063	48
H16B	7237	5178	-5165	48
H17	6925	6603	-4741	42
H18A	8380	8452	632	56
H18B	8828	7570	422	56
H18C	8295	7605	1636	56
H19A	9606	8640	-3491	52
H19B	9640	7470	-3471	52
H19C	9455	7981	-2306	52
H21A	8620	9298	-4897	74
H21B	7419	8498	-5516	74
H21C	8561	9182	-6264	74
H22A	3739	5000	3698	54
H22B	4460	6354	3923	54
H24	4444	6915	5838	47
H25	4224	6556	7803	46
H27	3875	3430	7257	47
H28	4087	3811	5284	49
H29A	2901	3130	8972	72
H29B	3453	3727	10171	72
H29C	4227	3586	9218	72
H1AA	6874	8139	1442	48
H1AB	7863	7826	1586	48
H2AA	6600	7530	-482	51
H2AB	7915	8484	-285	51
H3A	8414	7041	-97	46
H4AA	7039	5101	-404	51
H4AB	6060	5425	-597	51
H6A	6787	4237	1285	47

H7AA	7088	4784	3353	49
H7AB	5873	3684	3083	49
H8A	4918	4699	3246	42
H9A	7141	6732	3155	42
H11C	5040	6762	3295	48
H11D	6293	7866	3259	48
H12C	6713	7470	5101	41
H12D	5526	7466	5174	41
H14A	6710	5681	4911	41
H15C	5978	3813	5404	48
H15D	4675	3513	5199	48
H16C	6011	4503	7156	57
H16D	4649	3956	7044	57
H17A	6372	6268	6771	44
H18D	4880	6700	1420	60
H18E	4449	5367	1585	60
H18F	4969	5973	381	60
H19D	3727	5676	5506	51
H19E	3679	4468	5423	51
H19F	3893	5223	4294	51
H21D	4688	7328	6969	83
H21E	5922	7673	7476	83
H21F	4854	7273	8321	83
H22C	9536	8019	-1669	63
H22D	8758	8591	-1909	63
H24A	8943	9247	-3851	49
H25A	9111	9022	-5804	56
H27A	9357	6213	-5218	55
H28A	9163	6415	-3261	51
H29D	9933	6973	-8090	76
H29E	9012	6014	-7255	76
H29F	10302	6816	-6830	76

Table S15. Atomic Occupancy for 3e.

Atom	<i>Occupancy</i>	Atom	<i>Occupancy</i>	Atom	<i>Occupancy</i>
O1	0.6759(13)	O2	0.6759(13)	O3	0.6759(13)

C1	0.6759(13)	H1A	0.6759(13)	H1B	0.6759(13)
C2	0.6759(13)	H2A	0.6759(13)	H2B	0.6759(13)
C3	0.6759(13)	H3	0.6759(13)	C4	0.6759(13)
H4A	0.6759(13)	H4B	0.6759(13)	C5	0.6759(13)
C6	0.6759(13)	H6	0.6759(13)	C7	0.6759(13)
H7A	0.6759(13)	H7B	0.6759(13)	C8	0.6759(13)
H8	0.6759(13)	C9	0.6759(13)	H9	0.6759(13)
C10	0.6759(13)	C11	0.6759(13)	H11A	0.6759(13)
H11B	0.6759(13)	C12	0.6759(13)	H12A	0.6759(13)
H12B	0.6759(13)	C13	0.6759(13)	C14	0.6759(13)
H14	0.6759(13)	C15	0.6759(13)	H15A	0.6759(13)
H15B	0.6759(13)	C16	0.6759(13)	H16A	0.6759(13)
H16B	0.6759(13)	C17	0.6759(13)	H17	0.6759(13)
C18	0.6759(13)	H18A	0.6759(13)	H18B	0.6759(13)
H18C	0.6759(13)	C19	0.6759(13)	H19A	0.6759(13)
H19B	0.6759(13)	H19C	0.6759(13)	C20	0.6759(13)
C21	0.6759(13)	H21A	0.6759(13)	H21B	0.6759(13)
H21C	0.6759(13)	C22	0.6759(13)	H22A	0.6759(13)
H22B	0.6759(13)	C23	0.6759(13)	C24	0.6759(13)
H24	0.6759(13)	C25	0.6759(13)	H25	0.6759(13)
C26	0.6759(13)	C27	0.6759(13)	H27	0.6759(13)
C28	0.6759(13)	H28	0.6759(13)	C29	0.6759(13)
H29A	0.6759(13)	H29B	0.6759(13)	H29C	0.6759(13)
O1A	0.3241(13)	O2A	0.3241(13)	O3A	0.3241(13)
C1A	0.3241(13)	H1AA	0.3241(13)	H1AB	0.3241(13)
C2A	0.3241(13)	H2AA	0.3241(13)	H2AB	0.3241(13)
C3A	0.3241(13)	H3A	0.3241(13)	C4A	0.3241(13)
H4AA	0.3241(13)	H4AB	0.3241(13)	C5A	0.3241(13)
C6A	0.3241(13)	H6A	0.3241(13)	C7A	0.3241(13)
H7AA	0.3241(13)	H7AB	0.3241(13)	C8A	0.3241(13)
H8A	0.3241(13)	C9A	0.3241(13)	H9A	0.3241(13)
C10A	0.3241(13)	C11A	0.3241(13)	H11C	0.3241(13)
H11D	0.3241(13)	C12A	0.3241(13)	H12C	0.3241(13)
H12D	0.3241(13)	C13A	0.3241(13)	C14A	0.3241(13)
H14A	0.3241(13)	C15A	0.3241(13)	H15C	0.3241(13)
H15D	0.3241(13)	C16A	0.3241(13)	H16C	0.3241(13)
H16D	0.3241(13)	C17A	0.3241(13)	H17A	0.3241(13)

C18A	0.3241(13)	H18D	0.3241(13)	H18E	0.3241(13)
H18F	0.3241(13)	C19A	0.3241(13)	H19D	0.3241(13)
H19E	0.3241(13)	H19F	0.3241(13)	C20A	0.3241(13)
C21A	0.3241(13)	H21D	0.3241(13)	H21E	0.3241(13)
H21F	0.3241(13)	C22A	0.3241(13)	H22C	0.3241(13)
H22D	0.3241(13)	C23A	0.3241(13)	C24A	0.3241(13)
H24A	0.3241(13)	C25A	0.3241(13)	H25A	0.3241(13)
C26A	0.3241(13)	C27A	0.3241(13)	H27A	0.3241(13)
C28A	0.3241(13)	H28A	0.3241(13)	C29A	0.3241(13)
H29D	0.3241(13)	H29E	0.3241(13)	H29F	0.3241(13)

Table S16. Crystal data and structure refinement for 4c.

Identification code	yi3c
Empirical formula	C ₂₇ H ₅₂ BO ₅ F ₄ PRu
Formula weight	675.54
Temperature/K	100.00(10)
Crystal system	monoclinic
Space group	I2/a
a/Å	16.7775(4)
b/Å	9.6540(2)
c/Å	39.1720(11)
α/°	90.00
β/°	93.260(2)
γ/°	90.00
Volume/Å ³	6334.4(3)
Z	8
ρ _{calc} g/cm ³	1.417
μ/mm ⁻¹	4.975
F(000)	2832.0
Crystal size/mm ³	0.3068 × 0.2254 × 0.0989
Radiation	CuKα (λ = 1.54184)
2Θ range for data collection/°	9.04 to 149.48
Index ranges	-20 ≤ h ≤ 20, -11 ≤ k ≤ 11, -48 ≤ l ≤ 48
Reflections collected	55980
Independent reflections	6382 [R _{int} = 0.0867, R _{sigma} = 0.0312]
Data/restraints/parameters	6382/0/372
Goodness-of-fit on F ²	1.320
Final R indexes [I>=2σ (I)]	R ₁ = 0.0927, wR ₂ = 0.2173
Final R indexes [all data]	R ₁ = 0.0933, wR ₂ = 0.2175
Largest diff. peak/hole / e Å ⁻³	2.01/-3.04

Table S17. Fractional Atomic Coordinates ($\times 10^4$) and Equivalent Isotropic Displacement Parameters ($\text{\AA}^2 \times 10^3$) for 4c. U_{eq} is defined as 1/3 of the trace of the orthogonalised U_{IJ} tensor.

Atom	x	y	z	U(eq)
Ru1	3527.7(4)	5291.1(7)	1498.09(16)	21.2(2)
P2	3581.5(11)	6073(2)	952.3(5)	17.1(4)
F1	2366(4)	-673(7)	1485.9(16)	49.2(17)
F2	2053(4)	791(8)	1907.3(16)	51.4(17)
F3	3199(4)	-462(9)	1948.8(18)	59(2)
F4	3058(4)	1312(8)	1568(2)	58(2)
O1	4920(4)	3516(8)	1366.2(18)	38.3(17)
O2	2568(4)	6649(8)	1623.1(16)	31.0(15)
O3	3455(4)	4666(9)	2027.7(17)	35.8(19)
O4	2453(4)	3865(8)	1455.3(16)	24.9(14)
C1	4390(4)	7310(10)	883(2)	21.5(18)
C2	4282(5)	8684(8)	1086(2)	17.6(16)
C3	4949(5)	9703(8)	1023(2)	20.3(17)
C4	5766(5)	9062(10)	1112(2)	25.7(19)
C5	5883(5)	7744(10)	907(2)	24.4(18)
C6	5231(5)	6689(9)	963(2)	20.3(17)
C7	3773(5)	4661(9)	645(2)	21.0(18)
C8	3821(5)	5037(9)	267(2)	21.2(17)
C9	4166(5)	3831(10)	67(2)	24.1(18)
C10	3697(5)	2507(10)	107(2)	27(2)
C11	3586(5)	2160(10)	479(2)	25.8(19)
C12	3245(5)	3365(10)	674(2)	25.5(19)
C13	2683(4)	7057(9)	806(2)	19.7(17)
C14	2734(4)	7961(9)	483(2)	20.1(17)
C15	1999(5)	8910(9)	438(2)	21.4(17)
C16	1222(5)	8059(10)	424(2)	23.0(18)
C17	1185(5)	7125(10)	735(2)	26.4(19)
C18	1919(5)	6180(10)	775(2)	25.1(19)

C19	4361(5)	4172(11)	1416(2)	29(2)
C20	2106(6)	6459(12)	1922(2)	36(2)
C21	2720(6)	4266(13)	2180(2)	37(3)
C22	1774(5)	4146(11)	1658(2)	28(2)
C23	1994(6)	4937(12)	1991(2)	32(2)
C24	1280(6)	4773(14)	2221(3)	47(3)
B1	2674(7)	256(13)	1738(3)	34(3)
O1S	4274(4)	6046(7)	2513.2(16)	32.7(15)
C1S	4616(5)	5456(11)	2757(2)	28(2)
C2S	4703(7)	3910(12)	2778(3)	42(3)
C3S	4949(7)	6291(14)	3052(3)	49(3)

Table S18. Anisotropic Displacement Parameters ($\text{\AA}^2 \times 10^3$) for 4c. The Anisotropic displacement factor exponent takes the form: $-2\pi^2[h^2a^{*2}\mathbf{U}_{11}+2hka^{*}\mathbf{b}^{*}\mathbf{U}_{12}+\dots]$.

Atom	\mathbf{U}_{11}	\mathbf{U}_{22}	\mathbf{U}_{33}	\mathbf{U}_{23}	\mathbf{U}_{13}	\mathbf{U}_{12}
Ru1	16.1(3)	30.6(4)	17.0(3)	0.7(3)	0.7(2)	-6.9(3)
P2	12.2(9)	21.0(11)	18.0(9)	1.6(8)	0.8(7)	0.2(8)
F1	61(4)	46(4)	39(3)	-8(3)	-11(3)	15(3)
F2	47(4)	65(5)	44(4)	-9(3)	14(3)	9(3)
F3	45(4)	70(5)	60(4)	14(4)	-16(3)	10(4)
F4	46(4)	45(4)	87(5)	16(4)	21(4)	8(3)
O1	26(3)	51(5)	39(4)	15(3)	7(3)	9(3)
O2	30(3)	39(4)	26(3)	-1(3)	11(3)	-3(3)
O3	30(3)	60(6)	17(3)	0(3)	-1(3)	-15(4)
O4	20(3)	31(4)	23(3)	-2(3)	3(2)	-2(3)
C1	11(3)	33(5)	21(4)	-3(4)	0(3)	0(3)
C2	23(4)	6(4)	24(4)	-3(3)	3(3)	2(3)
C3	23(4)	8(4)	30(4)	1(3)	2(3)	0(3)
C4	19(4)	29(5)	29(4)	-1(4)	-1(3)	-7(4)
C5	13(4)	30(5)	30(4)	-1(4)	4(3)	0(3)
C6	16(4)	18(4)	28(4)	4(3)	1(3)	-4(3)

C7	13(3)	30(5)	19(4)	5(3)	0(3)	1(3)
C8	21(4)	20(4)	23(4)	1(3)	2(3)	-6(3)
C9	21(4)	28(5)	24(4)	2(4)	3(3)	1(4)
C10	24(4)	28(5)	31(5)	-11(4)	2(3)	1(4)
C11	26(4)	19(5)	32(5)	1(4)	7(4)	4(4)
C12	22(4)	31(5)	25(4)	-3(4)	7(3)	-2(4)
C13	15(4)	26(5)	18(4)	0(3)	0(3)	-1(3)
C14	14(4)	24(5)	23(4)	0(3)	2(3)	0(3)
C15	17(4)	20(4)	28(4)	-3(3)	3(3)	7(3)
C16	19(4)	23(5)	26(4)	-2(4)	-1(3)	1(3)
C17	15(4)	32(5)	32(5)	5(4)	2(3)	0(4)
C18	16(4)	34(5)	26(4)	-7(4)	2(3)	-6(4)
C19	25(4)	39(6)	21(4)	11(4)	-5(3)	-9(4)
C20	41(6)	41(6)	28(5)	-7(4)	19(4)	-13(5)
C21	31(5)	60(7)	21(4)	9(5)	3(4)	-17(5)
C22	17(4)	39(6)	28(4)	-4(4)	4(3)	-7(4)
C23	30(5)	44(6)	22(4)	0(4)	9(4)	-8(5)
C24	42(6)	67(9)	34(5)	-10(5)	20(5)	-18(6)
B1	31(5)	34(7)	36(6)	4(5)	6(4)	4(5)
O1S	34(3)	34(4)	29(3)	6(3)	-3(3)	-5(3)
C1S	22(4)	36(6)	27(4)	0(4)	5(3)	-4(4)
C2S	40(6)	42(7)	46(6)	2(5)	11(5)	4(5)
C3S	53(7)	59(8)	35(6)	-9(6)	-10(5)	-12(6)

Table S19. Bond Lengths for 4c.

Atom	Atom	Length/ \AA	Atom	Atom	Length/ \AA
Ru1	P2	2.274(2)	C5	C6	1.521(11)
Ru1	O2	2.154(7)	C7	C8	1.532(11)
Ru1	O3	2.171(7)	C7	C12	1.542(12)
Ru1	O4	2.267(6)	C8	C9	1.534(12)
Ru1	C19	1.810(10)	C9	C10	1.514(13)

P2	C1	1.839(9)	C10	C11	1.519(12)
P2	C7	1.858(9)	C11	C12	1.521(12)
P2	C13	1.846(8)	C13	C14	1.543(11)
F1	B1	1.409(14)	C13	C18	1.534(11)
F2	B1	1.369(12)	C14	C15	1.539(11)
F3	B1	1.363(13)	C15	C16	1.540(11)
F4	B1	1.394(13)	C16	C17	1.518(12)
O1	C19	1.158(12)	C17	C18	1.534(12)
O2	C20	1.453(10)	C20	C23	1.507(15)
O3	C21	1.451(11)	C21	C23	1.531(14)
O4	C22	1.451(10)	C22	C23	1.539(13)
C1	C2	1.561(11)	C23	C24	1.548(12)
C1	C6	1.548(11)	O1S	C1S	1.228(11)
C2	C3	1.520(11)	C1S	C2S	1.501(15)
C3	C4	1.527(11)	C1S	C3S	1.490(14)
C4	C5	1.524(13)			

Table S20. Bond Angles for 4c.

Atom	Atom	Atom	Angle/ [°]	Atom	Atom	Atom	Angle/ [°]
O2	Ru1	P2	94.71(18)	C10	C9	C8	112.1(7)
O2	Ru1	O3	82.4(3)	C9	C10	C11	112.2(7)
O2	Ru1	O4	77.6(3)	C10	C11	C12	112.6(8)
O3	Ru1	P2	176.6(2)	C11	C12	C7	110.4(7)
O3	Ru1	O4	79.3(3)	C14	C13	P2	117.6(5)
O4	Ru1	P2	101.88(17)	C18	C13	P2	113.8(6)
C19	Ru1	P2	87.7(3)	C18	C13	C14	109.4(7)
C19	Ru1	O2	176.8(3)	C15	C14	C13	110.5(6)
C19	Ru1	O3	95.1(3)	C14	C15	C16	111.0(7)
C19	Ru1	O4	104.1(4)	C17	C16	C15	111.2(7)
C1	P2	Ru1	115.0(3)	C16	C17	C18	111.5(7)
C1	P2	C7	103.0(4)	C17	C18	C13	110.0(8)

C1	P2	C13	102.5(4)	O1	C19	Ru1	176.4(9)
C7	P2	Ru1	112.5(3)	O2	C20	C23	110.2(8)
C13	P2	Ru1	112.8(3)	O3	C21	C23	111.2(8)
C13	P2	C7	110.2(4)	O4	C22	C23	113.6(7)
C20	O2	Ru1	123.1(6)	C20	C23	C21	113.3(9)
C21	O3	Ru1	124.1(5)	C20	C23	C22	110.9(8)
C22	O4	Ru1	119.4(6)	C20	C23	C24	108.3(9)
C2	C1	P2	111.7(5)	C21	C23	C22	110.1(9)
C6	C1	P2	112.9(6)	C21	C23	C24	107.3(8)
C6	C1	C2	110.9(7)	C22	C23	C24	106.6(8)
C3	C2	C1	111.1(6)	F2	B1	F1	108.7(9)
C2	C3	C4	111.1(7)	F2	B1	F4	110.0(9)
C5	C4	C3	111.0(7)	F3	B1	F1	107.4(9)
C6	C5	C4	111.5(7)	F3	B1	F2	112.4(9)
C5	C6	C1	111.4(7)	F3	B1	F4	111.2(9)
C8	C7	P2	118.3(6)	F4	B1	F1	107.0(9)
C8	C7	C12	109.1(7)	O1S	C1S	C2S	122.9(9)
C12	C7	P2	115.2(5)	O1S	C1S	C3S	119.3(10)
C7	C8	C9	110.8(7)	C3S	C1S	C2S	117.8(10)

Table S21. Hydrogen Bonds for 4c.

D	H	A	d(D-H)/Å	d(H-A)/Å	d(D-A)/Å	D-H-A/°
O2H2F1 ¹			0.96(13)	1.74(13)	2.659(10)	161(10)
O3H3O1S			0.68(12)	1.97(12)	2.643(10)	168(15)
O4H4F4			0.68(10)	2.01(11)	2.692(11)	172(12)

Table S22. Torsion Angles for 4c.

A	B	C	D	Angle/°	A	B	C	D	Angle/°
Ru1P2	C1	C2		-64.4(6)	O4	Ru1	O3	C21	-28.1(9)
Ru1P2	C1	C6		61.4(6)	O4	Ru1	C19	O1	179(100)
Ru1P2	C7	C8		179.7(5)	O4	C22	C23	C20	78.6(11)

Ru1P2	C7	C12	48.3(6)	O4	C22C23C21	-47.6(11)
Ru1P2	C13C14		164.1(5)	O4	C22C23C24	-163.7(9)
Ru1P2	C13C18		-66.0(6)	C1	P2 C7 C8	-55.8(7)
Ru1O2	C20C23		-35.6(11)	C1	P2 C7 C12	172.7(6)
Ru1O3	C21C23		-26.0(13)	C1	P2 C13C14	39.9(7)
Ru1O4	C22C23		-26.9(11)	C1	P2 C13C18	169.7(6)
P2	Ru1O2	C20	165.2(7)	C1	C2 C3 C4	-56.0(9)
P2	Ru1O3	C21	82(4)	C2	C1 C6 C5	-53.2(9)
P2	Ru1O4	C22	-120.0(6)	C2	C3 C4 C5	57.7(9)
P2	Ru1C19O1		77(12)	C3	C4 C5 C6	-57.2(10)
P2	C1	C2 C3	-179.3(5)	C4	C5 C6 C1	55.2(9)
P2	C1	C6 C5	-179.5(6)	C6	C1 C2 C3	53.8(9)
P2	C7	C8 C9	167.1(5)	C7	P2 C1 C2	172.8(6)
P2	C7	C12C11	-165.6(6)	C7	P2 C1 C6	-61.4(6)
P2	C13C14C15		-169.3(6)	C7	P2 C13C14	-69.2(7)
P2	C13C18C17		166.9(6)	C7	P2 C13C18	60.6(7)
O2	Ru1P2	C1	100.9(4)	C7	C8 C9 C10	55.7(9)
O2	Ru1P2	C7	-141.6(3)	C8	C7 C12C11	58.7(9)
O2	Ru1P2	C13	-16.2(4)	C8	C9 C10C11C12	-51.5(10)
O2	Ru1O3	C21	50.6(9)	C9	C10C11C12	52.0(10)
O2	Ru1O4	C22	-27.8(6)	C10C11C12C7		-55.7(10)
O2	Ru1C19O1		-60(15)	C12C7	C8 C9	-58.7(8)
O2	C20C23C21		80.5(10)	C13P2	C1 C2	58.3(6)
O2	C20C23C22		-43.9(11)	C13P2	C1 C6	-175.8(6)
O2	C20C23C24		-160.5(8)	C13P2	C7 C8	52.9(7)
O3	Ru1P2	C1	69(3)	C13P2	C7 C12	-78.6(7)
O3	Ru1P2	C7	-173(3)	C13C14C15C16		-56.2(9)
O3	Ru1P2	C13	-48(3)	C14C13C18C17		-59.3(9)
O3	Ru1O2	C20	-16.6(7)	C14C15C16C17		54.3(9)
O3	Ru1O4	C22	56.8(7)	C15C16C17C18		-55.4(10)
O3	Ru1C19O1		-101(12)	C16C17C18C13		58.2(9)

O3	C21C23C20	-46.2(11)	C18C13C14C15	58.8(9)
O3	C21C23C22	78.7(11)	C19Ru1P2 C1	-76.9(4)
O3	C21C23C24	-165.6(9)	C19Ru1P2 C7	40.6(4)
O4	Ru1P2 C1	179.1(4)	C19Ru1P2 C13	166.0(4)
O4	Ru1P2 C7	-63.3(3)	C19Ru1O2 C20	-57(7)
O4	Ru1P2 C13	62.1(4)	C19Ru1O3 C21	-131.5(9)
O4	Ru1O2 C20	64.0(7)	C19Ru1O4 C22	149.4(7)

Table S23. Hydrogen Atom Coordinates ($\text{\AA} \times 10^4$) and Isotropic Displacement Parameters ($\text{\AA}^2 \times 10^3$) for 4c.

Atom	x	y	z	U(eq)
H	4140(50)	6460(100)	1570(20)	20(20)
H2	2610(70)	7630(130)	1590(30)	40(30)
H3	3650(70)	5110(140)	2140(30)	40(40)
H4	2630(60)	3250(110)	1500(30)	20(30)
H1	4354	7554	635	26
H2A	3762	9107	1014	21
H2B	4281	8477	1333	21
H3A	4882	10543	1163	24
H3B	4916	9985	779	24
H4A	6189	9737	1063	31
H4B	5815	8844	1359	31
H5A	5880	7977	660	29
H5B	6409	7334	975	29
H6A	5275	6371	1204	24
H6B	5304	5875	815	24
H7	4323	4331	716	25
H8A	4163	5865	246	25
H8B	3281	5266	168	25
H9A	4162	4079	-178	29
H9B	4728	3675	150	29
H10A	3980	1734	0	33

H10B	3167	2605	-15	33
H11A	4108	1892	591	31
H11B	3223	1355	491	31
H12A	3215	3109	918	31
H12B	2697	3570	581	31
H13	2594	7728	995	24
H14A	3225	8533	504	24
H14B	2765	7359	280	24
H15A	2028	9447	223	26
H15B	1998	9573	630	26
H16A	758	8695	415	28
H16B	1190	7486	214	28
H17A	697	6549	712	32
H17B	1153	7702	943	32
H18A	1936	5560	574	30
H18B	1884	5598	982	30
H20A	1578	6909	1884	43
H20B	2386	6901	2123	43
H21A	2744	4551	2423	45
H21B	2664	3246	2171	45
H22A	1521	3257	1716	33
H22B	1377	4694	1519	33
H24A	780	4940	2085	70
H24B	1330	5442	2409	70
H24C	1277	3831	2315	70
H2SA	4378	3552	2958	64
H2SB	5264	3672	2830	64
H2SC	4523	3497	2558	64
H3SA	5517	6078	3093	74
H3SB	4664	6065	3256	74
H3SC	4885	7279	3000	74

